AD NUMBER: AD0825297

LIMITATION CHANGES

TO:

Approved for public release; distribution is unlimited.

FROM:

Distribution authorized to Us Government Agencies and their Contractors; Export Control; 1 Aug 1967. Other requests shall be referred to Air Force Materials Laboratory, Wright-Patterson AFB, OH, 45433.

AUTHORITY

AFML ltr dtd 26 May 1972

AFML-67-306

INVESTIGATION OF HOT CORROSION OF NICKEL BASE SUPERALLOYS USED IN GAS TURBINE ENGINES

K. H. Ryan, J. R. Kildsig, and P. E. Hamilton

Allison Division • General Motors

Indianapolis, Indiana

TECHNICAL REPORT AFML-TR-67-306

August 1967

Air Force Materials Laboratory
Research and Technology Division
Air Force Systems Command
Wright-Patterson Air Force Base, Ohio

100

NOTICE

When Government drawings, specifications, or other data are used for any purpose other than in connection with a definitely related Government procurement operation, the United States Government thereby incurs no responsibility nor any obligation whatsoever; and the fact that the Government may have formulated, furnished, or in any way supplied the said drawings, specifications, or other data, is not to be regarded by implication or otherwise as in any manner licensing the holder or any other person or corporation, or conveying any rights or permission to manufacture, use, or sell any patented invention that may in any way be related thereto.

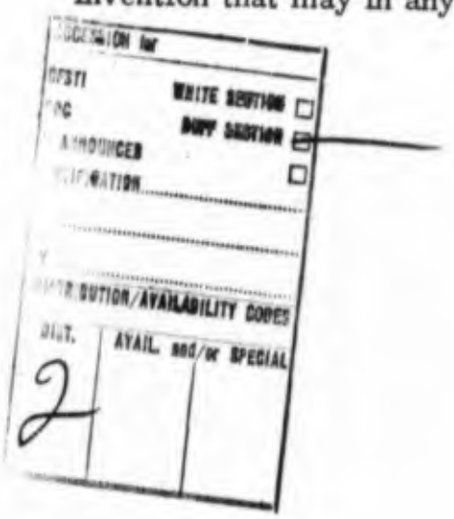

Copies of this report should not be returned unless return is required by security considerations, contractual obligations, or notice on a specific document.

AFML-67-306

INVESTIGATION OF HOT CORROSION OF NICKEL BASE SUPERALLOYS USED IN GAS TURBINE ENGINES

K. H. Ryan, J. R. Kildsig, and P. E. Hamilton

FOREWORD

This Summary Technical Report was prepared by the Materials Laboratories of Allison Division of General Motors Corporation. The work was initiated by the Systems Engineering Group, Air Force Materials Laboratories, Research and Technology Division under Contract AF33(615)-5211, Project No. 7381. Mr George Yoder, Research and Technology Division (MAAG), Wright Patterson Air Force Base, Ohio administered the program.

The work covers the period from 1 July 1966 through 31 August 1967. Mr P. E. Hamilton was the program manager and Mr. J. R. Kildsig the assistant program manager. C. O. Hill and P. L. Colcord were major contributors to the conduct of the program. Statistical analyses were provided by R. L. Finch and W. C. Smith of the Reliability Department. Electron microprobe studies were conducted by K. E. Muszar and the electron microscope analysis by D. R. Betner.

This technical report has been reviewed and is approved.

W. P. Conrardy

W. P. CONRARDY, Chief
Systems Support Branch
Materials Applications Div
AF Materials Laboratory

ABSTRACT

This is the Summary Technical Report of a program to investigate the hot corrosion of nickel base superalloys and covers the period 1 July 1966 through 31 August 1967. The most significant result obtained from the program was the derivation of a regression equation relating base metal volume loss to alloy chemistry and showing that chromium and aluminum were beneficial to hot corrosion resistance, whereas tungsten and molybdenum were detrimental. It was also established by electron microprobe study that hot corrosion resistance was related to alloy depletion in the surface layer of the corroded alloys. A high molybdenum content in the zone was detrimental and a high aluminum content beneficial to hot corrosion resistance. Hot corrosion severity increased with temperature in the range of 1700 to 2000°F in an approximate logarithmic fashion. The order of decreasing hot corrosion resistance of the ten alloys investigated was: PDRL 163, IN-728 NX, Alloy 713C + 2% Cr + Y, Alloy 713C + 2% Cr, Inco 717, Alloy 713C, Mar-M421*, IN-100, GMR-235, and Mar-M246. Heat treatment had a detrimental effect on the hot corrosion behavior of Mar M246 and GMR-235 and no observed effect on the other eight alloys.

*The Alloy Mar-M421 utilized in this investigation contained only 14.6% chromium in the airfoil test sections even though the master heat analysis indicated 15.1% chromium. This is below the 15.0 to 16.0% chromium content of the alloy recommended by Martin Metals Division of Martin Marietta Corporation; and the test results, therefore, may not accurately reflect the behavior of test airfoils with this recommended chromium content.

TABLE OF CONTENTS

SECTION TABLE OF CONTENTS (CONTD) PAGE

LIST OF ILLUSTRATIONS

FIGURE ILLUSTRATIONS (CONTD) PAGE

FIGURE ILLUSTRATIONS (CONTD) PAGE

TABLES

TABLE PAGE

TABLE | TABLES (CONTD) | PAGE

SECTION I

INTRODUCTION

This program consisted of an investigation of the hot corrosion problem experienced in turbine engine components fabricated from the nickel base superalloys. Corrosion of this nature is a serious operational problem in current gas turbine engines. Because components of advanced turbine engines will often operate at higher metal temperatures, hot corrosion behavior at temperatures to 1900°F is of particular interest. Allison experience with hot corrosion on uncoated Alloy 713C turbine blades and vanes is shown in Figure 1 which compares the extent of corrosion at airfoil midsections from turbine blades installed on the same rotor. The variation in the extent of attack on the macro sections illustrates the apparent variations in corrosion resistance which can occur on parts cast from the same alloy and exposed to the same environment. This variation suggests that a statistical approach is desirable in hot corrosion test programs.

PROGRAM OBJECTIVES

The program was designed to categorize the degree of hot corrosion attack that is suffered by representative nickel base turbine materials and to provide information on the following questions:

- How severe is the hot corrosion attack that occurs in superalloys between 1700 and 1900°F?
- How important are the influencing factors of chromium content, metallurgical structure, alloying elements used for strengthening purposes, and heat treatment?
- What are reliable temperature limits of usage in marine environments for the present superalloys?

TEST ALLOYS

Ten superalloys with varying chemical compositions and hot corrosion resistance were selected for the program. From a corrosion resistance viewpoint, the alloys fall into the following four groups.

- Group I—Alloy 713C, Alloy 713C with a 2% increase in chromium, and Alloy 713C with 2% chromium increase plus 0.25% yttrium

  Alloy 713C is widely used in gas turbine engines and is generally recognized as being susceptible to corrosion. This alloy serves as a baseline; the chromium and yttrium additions give an indication of the benefits to be derived from these alloy additions over a range of temperatures.

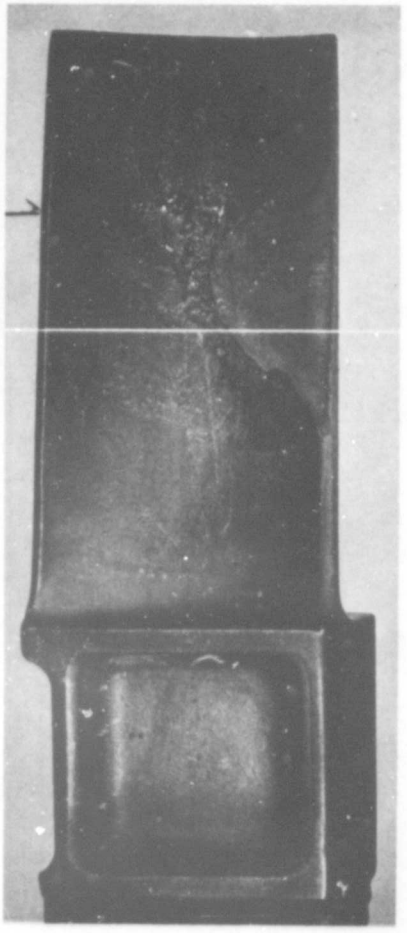

Figure 1. Typical hot corrosion of Alloy 713C turbine blades in service. Detail of concave airfoil surface of first stage turbine blade (Magn: 3x) and mid airfoil sections of five turbine blades from the same rotor (Magn: 6x).

- Group II—Mar-M421,* IN-728 NX, and PDRL 163
  These alloys were developed specifically to improve on the hot corrosion resistance of Alloy 713C while maintaining the same approximate strength level.

- Group III—IN-100 and Mar-M246
  These are alloys with compositions designed to provide creep-rupture strength significantly above that of Alloy 713C.

- Group IV—GMR-235 and Inco 717
  GMR-235 has been used several years with very few reports of sulfidation, possibly because the problem was not then recognized and because of lower temperature operating environments. Inco 717 has shown good sulfidation resistance on T56 engine tests with sea salt ingestion.

ALLOY PROCUREMENT

Nine of the test alloys were cast into T56 turbine blade configuration by the Stellite Division of Union Carbide. Alloy 713C test samples were obtained from the T56 production line. Wet chemical analyses were performed on airfoils of three test pieces to verify the composition of each casting lot under test for each selected alloy. Analysis of the individual castings also provided information on composition variation from casting-to-casting representing the same alloy heat.

Table I shows a comparison of nominal alloy compositions, the Stellite heat certifications, and the Allison airfoil analyses. Some variations did occur between the nominal chemistry, the heat analysis, and the three airfoil analyses. The three airfoil analyses, however, showed a relatively small amount of scatter and were generally in good agreement among themselves.

*Test blades of Alloy Mar-M421 showed an average airfoil analysis of 14.6% Cr which is below that of the 15.0 to 16.0% recommended by Martin Metals Division of Martin Marietta Corporation. Since chromium is critical to hot corrosion resistance, the corrosion resistance of the material tested in this program may not be typical of Mar-M421.

Table I.
Chemical analysis of nickel base alloys.

Alloy Heat No.	Analysis Source	Composition—weight percent C	Cr	W	Co	Ni	Ti	Al	Cb	Mo	Fe	Zr	B	Other
Alloy 713C	Nominal comp	0.14	14.0			Bal	0.85	6.0	2.3 (Cb+Ta)	4.5	*2.5	0.10	0.01	
	Allison[1] 1	0.12	13.20			Bal	0.80	6.39	2.18	4.66	0.10	0.096	0.0145	
	2	0.14	13.20			Bal	0.80	6.46	2.24	4.70	0.13	0.11	0.0135	
	3	0.13	13.30			Bal	0.76	6.25	2.10	4.75	0.10	0.11	0.0155	
Alloy 713C (Modified Cr)	Nominal comp	0.14	16.0			Bal	0.85	6.0	2.3 (Cb+Ta)	4.5	*2.5	0.10	0.01	
	Stellite Ht 216-2	0.12	15.91			Bal	0.81	6.14	2.02	4.50	0.26	0.09	0.01	
	Allison 1	0.11	15.70			Bal	0.80	5.84	2.24	4.66	0.23	0.10	0.015	
	2	0.10	15.55			Bal	0.80	5.88	2.06	4.70	0.23	0.096	0.007	
Alloy 713C (Modified Cr Yttrium)	Nominal comp	0.14	16.0			Bal	0.85	6.0	2.3 (Cb+Ta)	4.5	*2.5	0.10	0.01	0.25 yttrium
	Stellite Ht 217-2	0.12	15.87			Bal	0.81	6.14	2.02	4.5	0.26	0.09	0.01	0.38 yttrium
	Allison 1	0.17	15.70			Bal	0.85	6.35	1.65	4.66	0.20	0.10	0.0065	0.38 yttrium[2]
	2	0.12	15.70			Bal	0.85	6.08	1.68	4.66	0.20	0.096	0.0065	0.38 yttrium[2]
	3	0.14	15.55			Bal	0.89	6.48	1.81	4.66	0.20	0.10	0.0150	0.39 yttrium[2]
IN-100	Nominal comp	0.18	10.3		14.0	Bal	4.8	5.5		3.0		0.06	0.015	0.85 V
	Stellite	0.15	9.80		15.11	Bal	5.28	5.5		3.08		0.08	0.016	1.09
	Allison 1	0.17	10.25		14.80	Bal	5.17	6.03		3.04		0.030	0.010	1.00
	2	0.17	10.25		15.00	Bal	5.17	6.01		3.14		0.030	0.014	1.00
	3	0.16	10.20		14.80	Bal	5.22	6.78		3.18		0.030	0.010	1.00
GMR 235	Nominal comp	0.15	15.5			Bal	2.0	3.0		5.3	10.0		0.05	*1.0 Mn
	Stellite Ht 1598	0.13	15.26			Bal	1.79	2.71		5.86	9.44		0.04	0.18
	Allison 1	0.16	15.55			Bal	1.96	2.64		6.13	10.20		0.0295	0.16
	2	0.16	15.55			Bal	1.96	2.59		6.27	10.40		0.0320	0.21
	3	0.17	15.10			Bal	1.96	2.50		6.27	10.60		0.037	0.21
PDRL 163	Nominal comp	0.03	17.0	2.0		Bal		6.3	1.0	1.5		0.10	0.20	Ta 2.0
	Stellite OM543	0.06	16.95	2.00		Bal		6.25	1.05	1.50		0.10	0.019	1.83
	Allison[1] 1	0.07	16.50	2.00		Bal		6.57	1.43	1.38		0.158	0.0165	2.02
	2	0.07	16.60	1.82		Bal		6.62	1.51	1.42		0.131	0.0145	1.96
	3	0.07	16.60	1.96		Bal		6.57	1.51	1.42		0.131	0.0165	1.87
IN-728NX	Nominal comp	0.03	17.0	2.0	10.0	Bal		6.3	1.0	1.5		0.10	0.020	Ta 2.0
	Stellite OM542	0.07	16.62	1.99		Bal	0.48	6.16	1.83	2.02		0.15	0.024	2.29

		0.15	16.20		14.80	Bal	5.22	6.78		3.18		0.030	0.010	1.00
GMR 235	Nominal comp	0.15	15.5			Bal	2.0	3.0		5.3	10.0		0.05	*1.0 Mn
	Stellite Ht 1598	0.13	15.26			Bal	1.79	2.71		5.86	9.44		0.04	0.18
	Allison 1	0.16	15.55			Bal	1.96	2.64		6.13	10.20		0.0295	0.16
	2	0.16	15.55			Bal	1.96	2.59		6.27	10.40		0.0320	0.21
	3	0.17	15.10			Bal	1.96	2.50		6.27	10.60		0.037	0.21
PDRL 163	Nominal comp	0.03	17.0	2.0		Bal		6.3	1.0	1.5		0.10	0.20	Ta 2.0
	Stellite OM543	0.06	16.95	2.00		Bal		6.25	1.05	1.50		0.10	0.019	1.83
	Allison[1] 1	0.07	16.50	2.00		Bal		6.57	1.43	1.38		0.158	0.0165	2.02
	2	0.07	16.60	1.82		Bal		6.62	1.51	1.42		0.131	0.0145	1.96
	3	0.07	16.60	1.96		Bal		6.57	1.51	1.42		0.131	0.0165	1.87
IN-728NX	Nominal comp	0.03	17.0	2.0	10.0	Bal		6.3	1.0	1.5		0.10	0.020	Ta 2.0
	Stellite OM542	0.07	16.62	1.99		Bal	0.48	6.16	1.83	2.02		0.15	0.024	2.29
	Allison 1	0.07	16.00	1.82	9.35	Bal	0.45	6.40	1.30	1.84		0.19	0.018	2.56
	2	0.06	16.00	1.90	9.55	Bal	0.53	6.35	1.30	1.93		0.25	0.017	2.56
	3	0.07	16.10	1.95	9.77	Bal	0.53	6.40	1.16	1.89		0.22	0.016	2.72
**Mar M421	Nominal comp	0.15	15.5	3.5	10.0	Bal	1.8	4.3	1.8	1.8		0.06	0.015	
	Stellite	0.15	15.1	3.50	10.2	Bal	1.76	4.36	1.83	1.76		0.05	0.015	
	Allison 1	0.15	14.60	3.65	9.77	Bal	1.51	4.50	1.81	1.66		0.034	0.0055	
	2	0.11	14.60	3.52	10.45	Bal	1.56	4.50	2.00	1.56		0.034	0.0065	
	3	0.15	14.60	3.60	10.70	Bal	1.60	4.45	1.76	1.66		0.041	0.0055	
Mar M246	Nominal comp	0.15	9.0	10.0	10.0	Bal	1.5	5.5		2.5		0.08	0.015	Ta 1.5
	Stellite	0.13	9.22	10.4	10.1	Bal	1.49	5.55		2.38		0.06	0.014	1.48
	Allison 1	0.12	8.87	9.77	10.7	Bal	1.25	5.66		2.88		0.030	0.0135	2.50
	2	0.14	8.87	10.00	10.7	Bal	1.29	5.61		2.62		0.031	0.0150	2.50
	3	0.13	8.72	9.77	10.7	Bal	1.25	5.51		2.75		0.030	0.0160	2.46
Inco 717	Nominal comp	0.10	11.0		9.5	Bal	1.0	7.7	2.4	3.5		0.10	0.013	
	Stellite	0.12	12.16		10.19	Bal	1.06	6.84	2.70	4.16		0.16	0.02	
	Allison 1	0.11	12.00		11.00	Bal	1.07	7.40	2.94	4.43		0.14	0.0135	

[1] Wet chemical analysis performed on airfoils of 3 test specimens
[2] Obtained by X-ray fluoresence
* Denotes less than

**Airfoil analysis shows chromium content to be below the recommended minimum of 15.0%.chromium.

SECTION II

DESIGNED EXPERIMENTAL PROGRAM

A statistically designed experimental plan was devised using the weight change during testing and based on the standard deviation associated with the 500-cycle test. This standard deviation was developed from previous testing of nickel base alloys and reflects the normal variation which occurred within a given alloy. Eight tests per alloy were run, cycling to temperatures of 1700, 1750, 1800, 1850, and 1900°F, making a total of 40 tests per alloy. One-half of the test blades of each alloy were tested in the heat treated condition and the remainder tested as-cast.

Heat treatments used were those selected based on Allison experience and/or recommended by the alloy developers. Heat treatments are listed in Table II and the experimental plan is shown in Table III. Test blades were cathodically cleaned before weighing, and a predetermined cleaning correction factor was applied. Density determinations were made on each alloy and the weight losses converted to volume losses for analysis.

To investigate hot corrosion behavior at higher temperatures, one additional 500-cycle run was made cycling to 2000°F. Since it was a single run, it was treated separately and was not a part of the statistical volume loss analysis. The additional test run was made with a sample of each alloy in the as-cast condition only.

All tests were of 500 cycles duration.

Table II.
Alloy heat treatments.

Alloy	Heat treatments
Alloy 713C	2100°F/2 hr (hydrogen)
Alloy 713C + modified chromium	2100°F/2 hr (hydrogen)
Alloy 713C + modified chromium and yttrium	2100°F/2 hr (hydrogen)
Inco 717	2100°F/2 hr (hydrogen)
IN-100	2100°F/2 hr (hydrogen)
PDRL 163	2100°F/2 hr (vacuum-rapid cool) + 1950°F/4 hr (vacuum-rapid cool) + 1400°F/16 hr AC
IN-728 NX	2100°F/2 hr (vacuum-rapid cool) + 1950°F/4 hr (vacuum-rapid cool) + 1400°F/16 hr AC
Mar-M421	2100°F/2 hr (vacuum-rapid cool) + 1950°F/4 hr (vacuum-rapid cool) + 1400°F/16 hr AC
GMR-235	1800°F/5 hr (argon)
Mar-M246	1500°F/50 hr AC

Table III.

Basic experimental plan.

Sulfidation rig tests with heat treated and non-heat treated alloys.

Load Sequence*	Rig position 1 - 5	Rig position 6 - 10	Rig position 11 - 15	Rig position 16**
A	Alloys 1-5	HT alloys 1-5	Alloys 6-10	---
B	HT alloys 6-10	Alloys 1-5	HT alloys 1-5	---
C	Alloys 6-10	HT alloys 6-10	Alloys 1-5	---
D	HT alloys 1-5	Alloys 6-10	HT alloys 6-10	---
E	Alloys 1-5	HT alloys 1-5	Alloys 6-10	---
F	HT alloys 6-10	(Alloys 1-10 microexamination)		

*Load Sequence A was repeated cycling to 1700, 1750, 1800, 1850, and 1900°F followed by B, C, etc.

**Position 16 was filled with dummy blades and was not part of the weight loss analysis.

SECTION III

TEST RIG AND ENVIRONMENT

The program was conducted on a laboratory test rig which has been used for high temperature alloy and coating evaluation and has shown correlation with sea salt ingestion engine tests conducted at Allison. The laboratory rig is capable of producing sulfidation-oxidation corrosion basically the same as that found on turbine components returned from service or subjected to the accelerated turboprop engine test. Standard T56 turbine blades were used as test specimens (Figure 2). Each test cycle consists of heating 16 rotating (1800 rpm) turbine blades in a furnace to a preselected temperature after which the entire unit is retracted into a cooling chamber. Here it is sprayed with an aspirated solution of deionized water and 1% sulfate ion supplied as water-soluble sodium sulfate (Na_2SO_4). A cycle consists of 1.5 minutes heating time and 0.5 minutes cooling by the sodium sulfate solution. The test has been standardized at 500 cycles.

TEST RIG ATMOSPHERE CONTROLS

A sampling station was built into the fire chamber and a gas analyzer was employed for periodic evaluation of the combustion products.

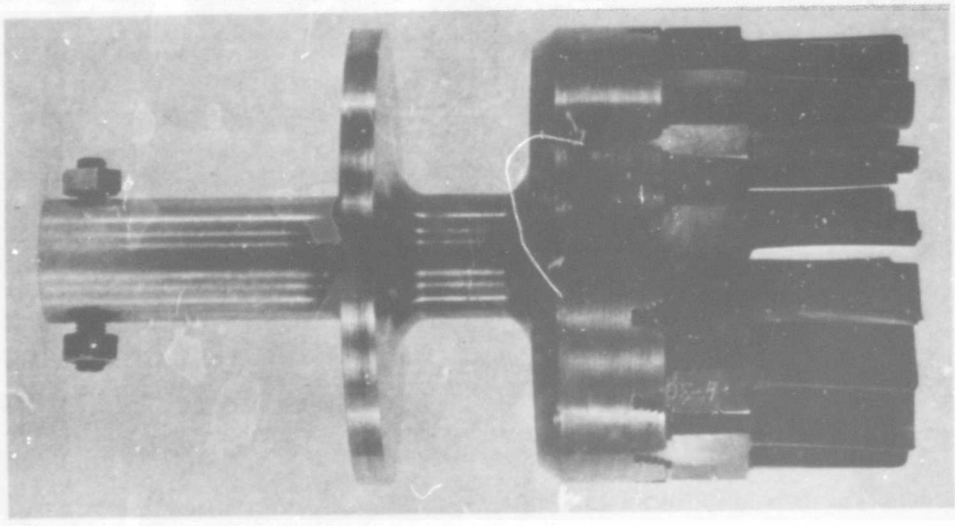

Sixteen-position test fixture and T56 turbine blade test specimens for the Allison sulfidation test rig. (magn 1X)

Figure 2. Hot corrosion rig test fixture and test blades.

PRECEDING PAGE BLANK

Based on exhaust gas analysis, the following operating controls were exercised.

- Limits were established for the fuel-air mixture at each temperature.
- The fire chamber was kept either oxidizing or neutral by adjustment of the air and fuel pressures.

Atmosphere conditions maintained in the fire chamber are shown in Table IV.

Table IV.
Fire chamber atmosphere conditions.

Test temperature, °F	1700	1750	1800	1850	1900	2000
Exhaust gas constituents, %						
CO_2	8-12	8-12	8-12	8-10	8-10	6-8
O_2	6-10	6-10	4-6	2-4	0-2	0-1
H	0.0	0.0	0.0	0.0	0-0.2	0-0.4
CO	0.0	0.0	0.0	0.0	0-0.2	0-0.4

THERMAL HISTORY OF TEST SPECIMENS

During the heating cycle, the temperature pattern on the test pieces was continually changing. In obtaining the thermal history of the test blades it was necessary to determine the temperature profile on the test pieces at intervals during the heating cycle. Several methods were used including infrared photography, optical pyrometer readings, and temperature sensitive paint. Infrared methods were satisfactory at the lower cyclic temperatures; however, the Templac paints gave the best results over the range of temperatures. Each paint melts at a specific temperature. Sample blades were coated with paints having melting points at 50°F intervals from 1400 to 2100°F. The painted blades were tested via a standard 1.5-minute heating cycle and results of the individual paints were used to form the temperature gradient at the end of the heating cycle. Figures 3 and 4 show the gradients at the end of the 1700, 1800, 1900, and 2000°F cyclic tests. Optical pyrometer readings were taken at several locations on the test blades at intervals during the heating cycle. These were combined with the temperature paint patterns to develop the thermal history for specific locations on the test specimens. Table V shows the thermal history of airfoil sections D'-D', C-C, and A-A. Areas of corrosion were measured at section D'-D'.

Table V.

Thermal history of airfoil sections.

(During heating cycle*)

Cyclic test temperature (°F)	Airfoil section	Percentage of test time in each temperature interval						
		Below 1500°F	1500 to 1600°F	1600 to 1700°F	1700 to 1800°F	1800 to 1900°F	1900 to 2000°F	2000°F
1700	D'-D'	27	20	34	19			
1750	D'-D'	26	16	24	34			
1800	D'-D'	19	11	16	39	15		
1850	D'-D'	16	9	9	15	51		
1900	D'-D'	15	7	6	11	50	11	
2000	D'-D'	—	14 —	6	5	13	49	13
1700	C-C	39	22	34	5			
1750	C-C	37	19	27	17			
1800	C-C	25	18	21	36			
1850	C-C	22	15	12	22	29		
1900	C-C	17	14	12	15	42		
2000	C-C	—	14 —	12	14	26	30	4
1700	A-A	53	38	9				
1750	A-A	53	29	18				
1800	A-A	37	36	27				
1850	A-A	37	21	42				
1900	A-A	35	19	25	21			
2000	A-A	—	46 —	18	27	9		

*Total time in furnace chamber during 500 cycles = 12.5 hours

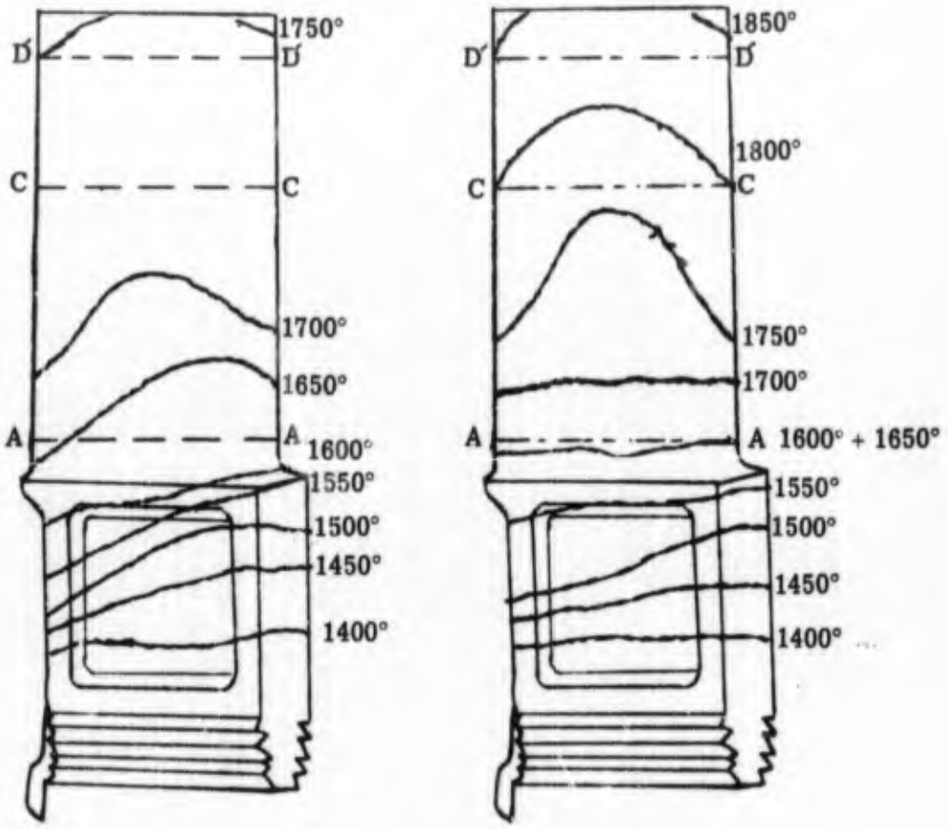

Cyclic test temperature 1700°F

Cyclic test temperature 1800°F

Temperature patterns on the test specimens at the end of the 1 1/2 minute heating cycle.

5370-3

Figure 3. Temperature profile for 1700 and 1800°F cyclic tests.

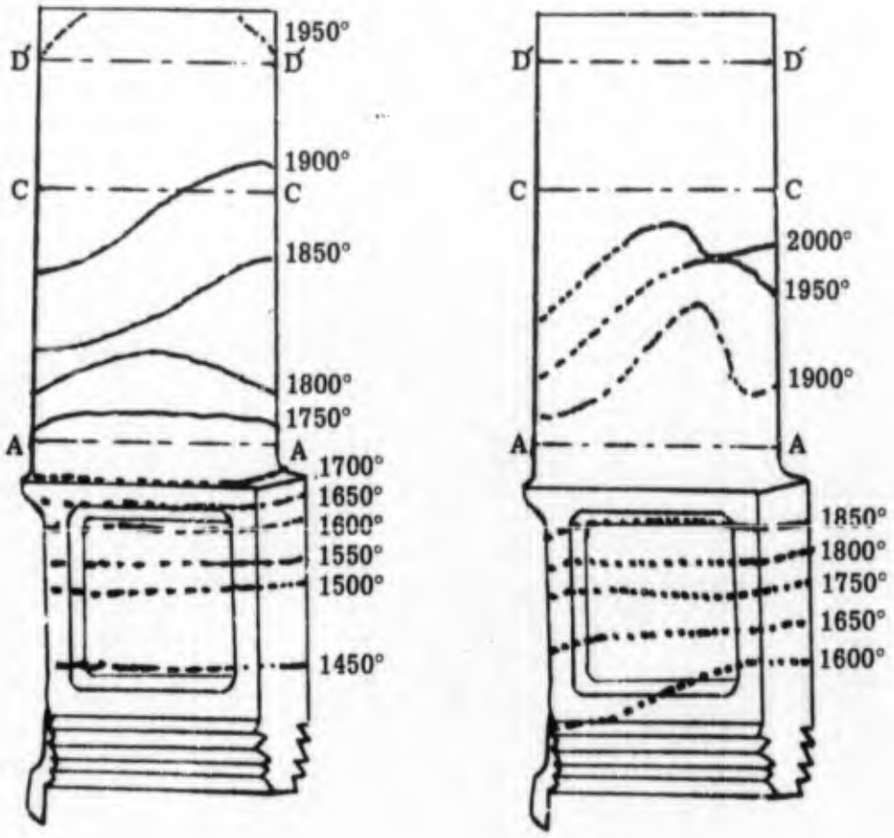

Cyclic test temperature
1900°F

Cyclic test temperature
2000°F

Temperature patterns on the test specimen at the end of the 1 1/2 minute heating cycle

5370-4

Figure 4. Temperature profile for 1900 and 2000°F cyclic tests.

BLANK PAGE

SECTION IV

TEST EVALUATIONS

To extract the maximum information from the test program, the test pieces were analyzed by several methods. These included volume loss during testing, areas of corrosion measured at an airfoil cross section, and binocular examination.

VOLUME LOSS EVALUATION

Test blades were weighed prior to testing and cathodically cleaned and reweighed after testing. Density determinations were made on each alloy and the weight losses were converted to volume losses. The primary objectives were to:

1. Correlate volume loss with test temperature
2. Compare volume loss due to hot corrosion among the ten alloys evaluated
3. Determine the effect of heat treatment on each alloy

The test schedule was designed to permit valid comparisons and evaluations of ten alloys: two treatment conditions (as-cast and heat treated) and five temperatures plus interactions among the three test variables. The ten alloys (as-cast and heat treated) composed 20 unique materials to be evaluated; however, the fixture had 15 positions available per test. The test procedure devised is shown in Table III in Section II of this report.

The test schedule was repeated over five temperatures before the loading configuration was changed. This procedure minimized the effect of extraneous variables which are time dependent. Differences among loadings were adjusted using the following technique. At each test temperature a bias or difference between loadings was computed using volume loss data for alloys common to both loadings; data generated in the second loading were adjusted using the computed bias. For example, loadings A and C had ten as-cast alloys in common. A miltiplicative factor was obtained by averaging the logs of the differences of the alloys appearing in both loadings. All material volume losses tested in loading C were then adjusted to loading A using the multiplicative factor computed. This adjusting technique was the same for all subsequent loadings.

The "run-to-run" differences were effectively controlled through the planned testing procedures and the adjusting techniques described in the preceding paragraph. Corrosion data are, in general, normally distributed in a logarithmic manner. Therefore, logs (Base 10) of volume loss (rather than observed data) were analyzed.

Analysis of Variance

The Analysis of Variance technique was used to analyze the test data. This method of analysis provided the mechanism to make tests of significance regarding the effect of the test variables upon volume loss. The results of analysis and tests of significance plus appropriate tables and charts illustrating significant results are presented in this section.

An interpretation of the Analysis of Variance (Table VI) follows.

- Alloys, treatments, and temperatures all produced significant changes in volume loss. The volume loss associated with any one of the three test variables is averaged over all values assigned to the remaining two variables. If temperature alone is evaluated, the volume losses associated with each of five temperatures are averaged over ten alloys, both in the as-cast and heat treated conditions.

Table VI.

Analysis of variance and tests of significance.

Factors tested	Degrees freedom	Mean square	F ratio
Alloys	9	6.041	324.4 **
Treatments	1	0.391	21.0 **
Temperatures	4	39.128	2100.0 **
Alloy by treatment interaction	9	0.134	7.2 **
Alloy by temperature interaction	36	0.070	3.8 **
Treatment by temperature interaction	4	0.040	2.1 **
Alloy by treatment by temperature interaction	36	0.014	0.7 **
Pooled error	300	0.019	

**Denotes significance at $\alpha \leq 0.01$

F ratios are computed by dividing the mean square for each factor by the mean square for pooled error. Significance is determined by comparing computed F ratios with tabular F values for the appropriate degrees of freedom; a factor is significant if the computed F exceeds the tabular F for some preselected value of α. The quantity $(1 - \alpha)$ is the probability that a change in volume loss is caused by a change in the independent test variables. The significance of an "interaction" indicates that the volume loss caused by changing one independent variable is dependent upon a specific value assigned to the interacting variable; e.g., the relationship between test temperatures and volume loss is not uniformly the same for all alloys. A comparative measure of change in volume loss caused by changing values assigned to the test variables is provided by the F ratios listed; larger ratios are associated with larger changes in volume loss caused by the test variables or their interactions.

- The significant interactions are of more practical consequence than are significant single variables. Interactions provide information to select combinations of factor levels which minimize volume loss.
  - The significance of the alloy X treatment interaction implies there is a change in hot corrosion resistance associated with heat treatments which was not the same for all alloys tested.
  - The materials X temperature interaction indicates that the relationship between volume loss and test temperatures is not the same for all materials tested. If volume losses versus temperatures were plotted for the alloys tested, the lines would not all be parallel.

Effect of Temperature on Volume Loss

Figures 5, 6, and 7 show volume loss averages associated with the independent test variables and their interactions. The volume losses presented are averages over all other factors not specifically shown in any particular table.

Figure 5 shows the relationship between volume loss and cyclic test temperature. The average volume loss per alloy increases in an approximately logarithmic fashion as test temperature increases.

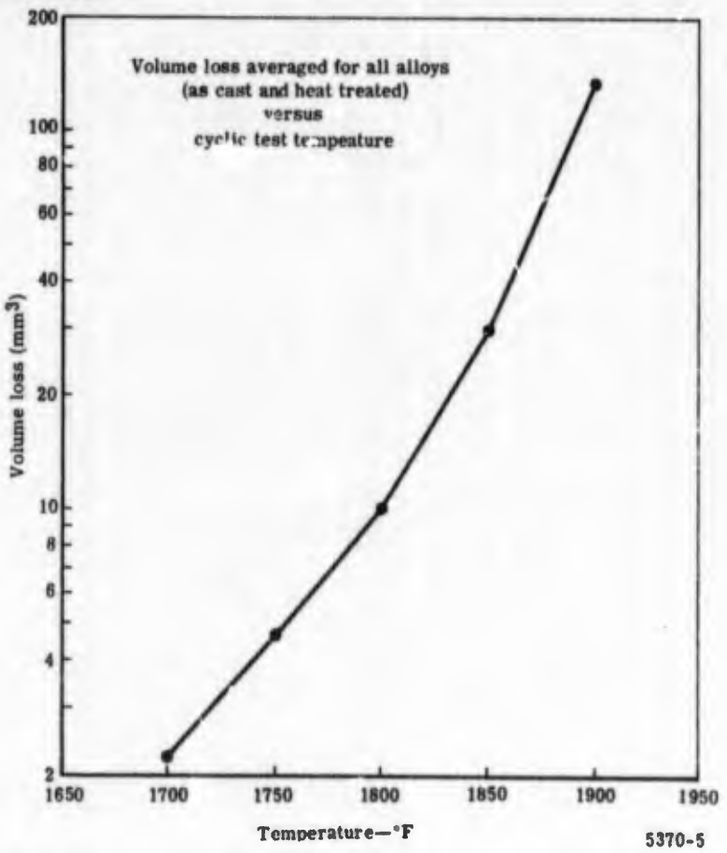

Figure 5. Alloy volume loss as a function of test temperature.

Hot Corrosion Resistance of Individual Alloys

Figure 6 shows the individual alloy volume losses averaged over all test temperatures and heat treatments. Materials are presented in order of decreasing hot corrosion resistance. Two of the alloys designed for sulfidation resistance, PDRL 163 and IN728NX, exhibited the least volume loss followed by the two high chromium versions of Alloy 713C. Note that the Allison chemical analysis of airfoil sections showed Mar M421 to have a chromium content of 14.60% which is below the specification of 15 to 16.0% chromium. This very likely contributed to the relatively poor showing of Mar M421 which was designed for hot corrosion resistance.

Individual alloy volume losses versus cyclic test temperatures are shown in Figure 7. The alloy temperature interactions were significant and further tests of significance are required to compare corrosion resistance among alloys at each of the five test temperatures. Tables VII through XI show differences in corrosion resistance among alloys as a function of test temperatures. In all tables the presence of an asterisk (*) denotes significance at $\alpha = 0.05$ (95% confidence level). The basic data analysis was performed using logarithms (Base 10) of observed volume losses. Averages were computed with logarithms and then reconverted to actual volume losses. Comparative volume losses for the designated materials are included in the tables. For example, in Table VII the average volume loss averaged over as-cast and heat treated for Mar M246 is 11.11 mm^3; the average volume loss for PDRL 163 is 0.42 mm^3; the ratio of the two numbers is 26.4 and is significant at $\alpha = 0.05$. Note that the alloys are ranked in descending order of volume loss for rows and ascending order for columns. Based on the significance tests, the following statements can be made concerning the relative hot corrosion resistance of the alloys:

- PDRL 163 and IN728NX showed significantly better resistance to hot corrosion than all other alloys at cyclic temperatures through 1850°F.

Table VII.

Significant differences between individual alloys at 1700°F cyclic temperature.

Material	Vol loss (mm^3)	Mar M246	GMR 235	Inco 717	IN 100	713C	Mar M421	713C +Cr+Y	713C +Cr	IN 728NX	PDRL 163
		11.11	4.50	2.67	2.34	2.30	2.06	1.99	1.98	1.11	0.42
PDRL 163	0.42	*26.452	*10.714	*6.357	*5.571	*5.476	*4.904	*4.738	*4.714	*2.642	
IN728NX	1.11	*10.009	* 4.045	*2.405	*2.108	*2.072	*1.855	*1.792	*1.783		
713C+Cr	1.98	* 5.611	* 2.272	1.348	1.181	1.161	1.040	1.005			
713C+Cr+Y	1.99	* 5.582	* 2.261	1.341	1.175	1.155	1.035				
Mar M421	2.06	* 5.393	* 2.184	1.296	1.135	1.116					
713C	2.30	* 4.830	* 1.956	1.160	1.017						
IN100	2.34	* 4.747	* 1.923	1.141							
Inco 717	2.67	* 4.161	* 1.685								
GMR 235	4.50	* 2.468									
Mar M246	11.11										

*Denotes a significant difference at $\alpha = 0.05$

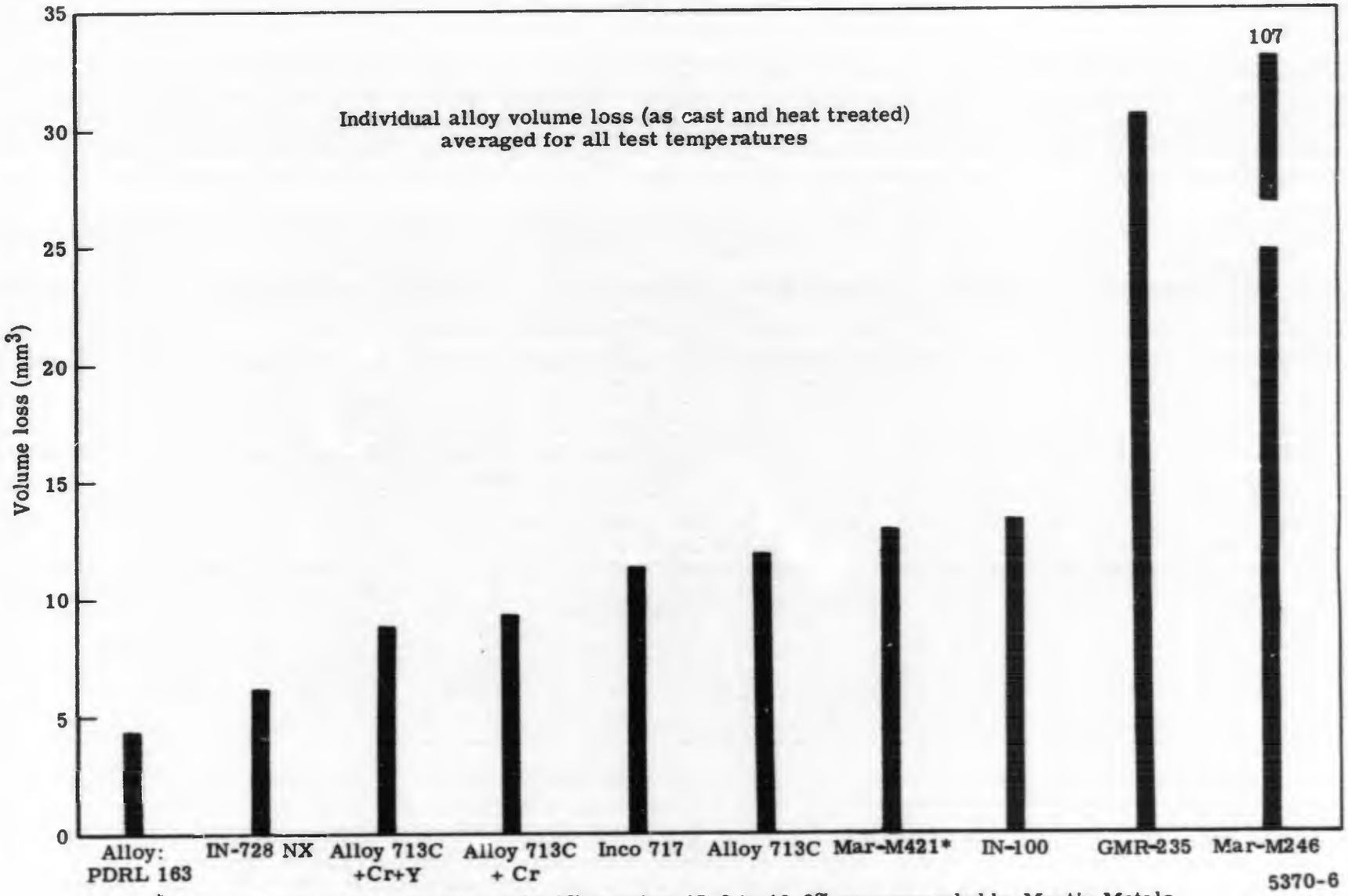

*Test airfoil chromium content of 14.6% is below 15.0 to 16.0% recommended by Martin Metals Division of Martin Marietta Corporation for this alloy designation.

Figure 6. Bar graph of individual alloy volume losses averaged over all test temperatures.

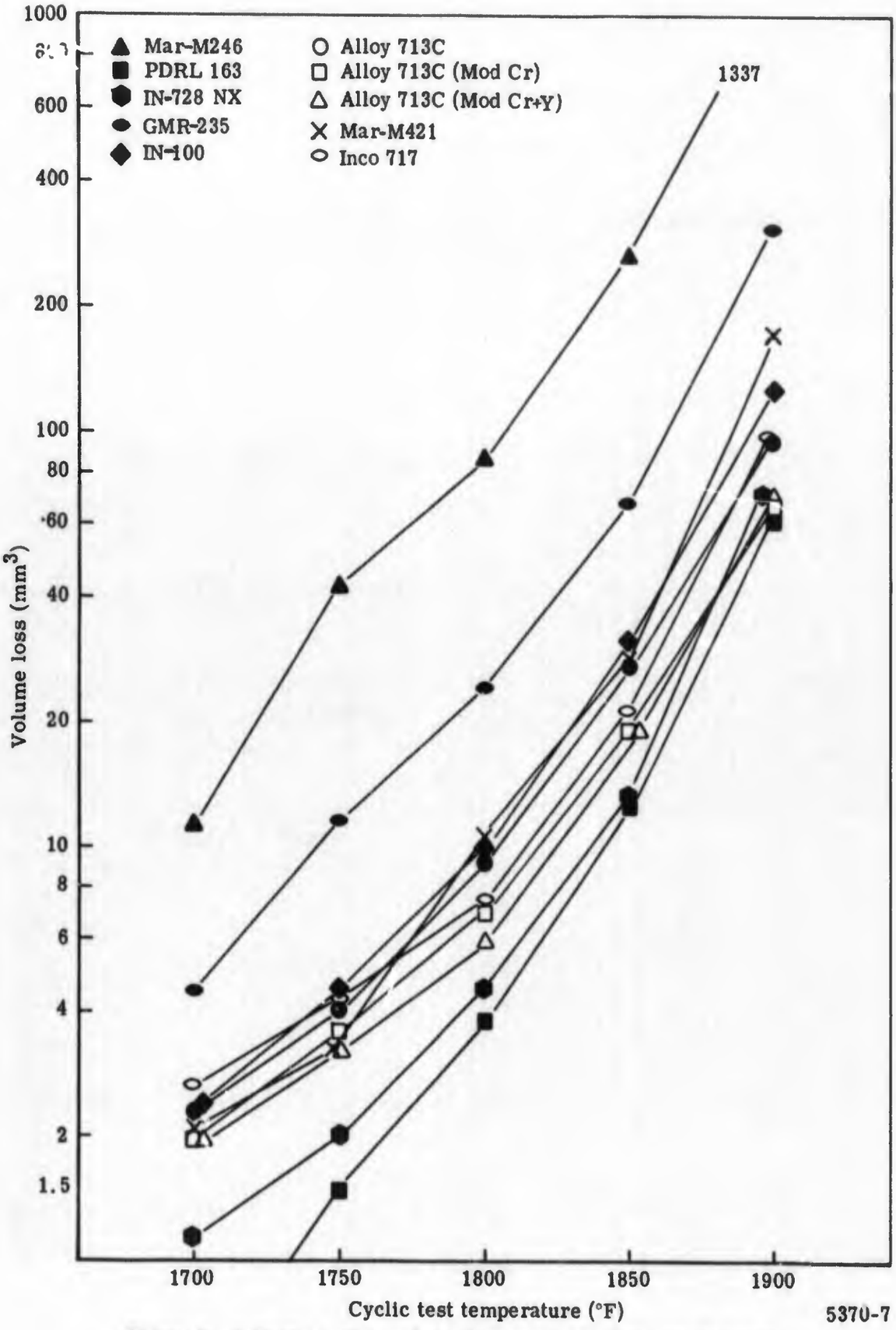

Figure 7. Individual alloy volume losses at each test temperature.

Table VIII.

Significant differences between individual alloys at 1750°F cyclic temperature.

Material	Vol. loss (mm^3)	Mar-M246 42.53	GMR-235 11.72	IN-100 4.46	Inco 717 4.37	713C 4.02	713C +Cr 3.67	713C +Cr+Y 3.23	Mar-M421 3.23	IN-728 NX 2.00	PDRL 163 1.48
PDRL 163	1.48	*28.736	*7.918	*3.013	*2.952	*2.716	*2.479	*2.182	*2.182	1.351	
IN728NX	2.00	*21.265	*5.860	*2.230	*2.185	*2.010	*1.835	*1.615	*1.615		
Mar M421	3.23	*13.167	*3.628	1.380	1.352	1.244	1.136	1.000			
713C+Cr+Y	3.23	*13.167	*3.628	1.380	1.352	1.244	1.136				
713C+Cr	3.67	*11.588	*3.193	1.215	1.190	1.095					
713C	4.02	*10.579	*2.915	1.109	1.087						
Inco 717	4.37	* 9.732	*2.681	1.020							
IN 100	4.46	* 9.535	*2.627								
GMR 235	11.72	* 3.628									
Mar M246	42.53										

*Denotes a significant difference at $\alpha = 0.05$

Table IX.

Significant differences between individual alloys at 1800°F cyclic temperature.

Material	Vol. loss (mm^3)	Mar-M246 85.59	GMR-235 24.53	Mar-M421 10.87	IN-100 10.17	713C 9.27	Inco 717 7.52	713C +Cr 7.02	713C +Cr+Y 5.98	IN-728 NX 4.30	PDRL 163 3.79
PDRL 163	3.79	*22.583	* 6.472	* 2.868	* 2.683	*2.445	*1.984	*1.852	*1.577	1.134	
IN728NX	4.30	*19.904	* 5.704	* 2.527	* 2.365	*2.155	*1.748	*1.632	*1.390		
713C+Cr+Y	5.98	*14.312	* 4.102	* 1.817	* 1.700	*1.550	1.257	1.173			
713C+Cr	7.02	*12.192	* 3.494	* 1.548	1.448	1.320	1.071				
Inco 717	7.52	*11.381	* 3.261	1.445	1.352	1.232					
713C	9.27	* 9.233	* 2.646	1.172	1.097						
IN 100	10.17	* 8.415	* 2.411	1.068							
Mar M421	10.87	* 7.873	* 2.256								
GMR 235	24.53	* 3.489									
Mar M246	85.59										

* Denotes a significant difference at $\alpha = 0.05$

Table X.

Significant differences between individual alloys at 1850°F cyclic temperature.

Material	Vol. loss (mm^3)	Mar-M246	GMR-235	IN-100	Mar-M421	713C	Inco 717	713C +Cr	713C +Cr+Y	IN-728 NX	PDRL 163
		265.3	68.47	31.61	28.44	27.65	21.70	19.53	19.09	13.46	12.17
PDRL 163	12.17	*21.799	* 5.626	* 2.597	* 2.336	* 2.271	* 1.782	* 1.604	* 1.568	1.105	
IN728NX	13.46	*19.710	* 5.086	* 2.348	* 2.112	* 2.054	* 1.612	* 1.450	* 1.418		
713C+Cr+Y	19.09	*13.897	* 3.586	* 1.655	* 1.489	* 1.448	1.136	1.023			
713C+Cr	19.53	*13.584	* 3.505	* 1.618	* 1.456	* 1.415	1.111				
Inco 717	21.70	*12.225	* 3.155	* 1.456	* 1.310	* 1.274					
713C	27.65	* 9.594	* 2.476	1.143	1.028						
Mar M421	28.44	* 9.328	* 2.407	1.111							
IN 100	31.61	* 8.392	* 2.166								
GMR 235	68.47	* 3.874									
Mar M246	265.3										

*Denotes a significant difference at $\alpha = 0.05$

Table XI.

Significant differences between individual alloys at 1900°F cyclic temperature.

Material	Vol. loss (mm^3)	Mar-M246	GMR-235	Mar-M421	IN-100	Inco 717	713C	IN-728 NX	713C +Cr+Y	713C +Cr	PDRL 163
		1337.25	302.6	170.9	128.4	96.66	95.61	70.63	69.01	68.54	60.16
PDRL 163	60.16	*22.228	*5.029	*2.840	*2.134	*1.606	*1.589	1.174	1.147	1.139	
713C+Cr	68.54	*19.510	*4.414	*2.493	*1.873	1.410	1.394	1.030	1.006		
713C+Cr+Y	69.01	*19.377	*4.384	*2.476	*1.860	1.400	1.385	1.023			
IN728NX	70.63	*18.933	*4.284	*2.419	*1.817	1.368	1.353				
713C	95.61	*13.986	*3.164	*1.787	1.342	1.010					
Inco 717	96.66	*13.834	*3.130	*1.768	1.328						
IN 100	128.4	*10.414	*2.356	1.330							
Mar M421	170.9	* 7.824	*1.770								
GMR 235	302.6	* 4.419									
Mar M246	1337.25										

*Denotes a significant difference at $\alpha = 0.05$

- There was no significant difference between PDRL 163 and IN-728 NX at any test temperature except 1700°F although numerically, PDRL 163 exhibited less volume loss at all test temperatures.
- The two high chromium versions of Alloy 713C showed improvement over Alloy 713C at all test temperatures; however, the difference was significant only at the 1800 and 1850°F temperatures.
- There was no significant difference at any test temperature between Alloy 713C + Cr and Alloy 713C + Cr + Y. The high chromium version showed lower volume loss at 1700 and 1900°F and the high chromium plus yttrium alloy showed lower volume loss at 1750, 1800 and 1850°F.
- Mar-M421, Alloy 713C, IN-100, and Inco 717 fell into one group with no significant difference between them at the 1700, 1750, and 1800°F cyclic test temperatures. At 1850°F, Inco 717 was significantly better than the other three and at 1900°F Inco 717 and Alloy 713C were significantly better than Mar-M421.
- GMR-235 and Mar-M246 showed significantly poorer corrosion resistance than the other eight alloys at all test temperatures.
- Mar-M246 showed significantly poorer corrosion resistance than the other nine alloys at all test temperatures.

Figures 8 through 11 show corrosion patterns on the test blades after 500 cycles of testing at the respective temperatures. Although not part of the statistical volume loss analysis, blades from the 2000°F cyclic test are included for comparison purposes. Note the steady increase in corrosion severity with increasing test temperature. The corrosion pattern on the lower airfoil and base of the blade is apparently related to the blade geometry. The sodium sulfate sprayed on during the cooling portion of the cycle is retained in greater quantities in the base section resulting in a higher concentration of contaminant in the lower region of the blade. Corrosion at the base of the blade occurred at lower temperatures because of the higher concentration of sodium sulfate.

Effect of Heat Treatments

Figure 12 shows the effect of heat treating on each alloy. Volume losses have been averaged over all test temperatures. The effect of heat treatment appears to be small on all alloys except GMR-235 and Mar-M246 where heat treatment has a large detrimental effect. This is confirmed by the significance tests as shown in Table XII.

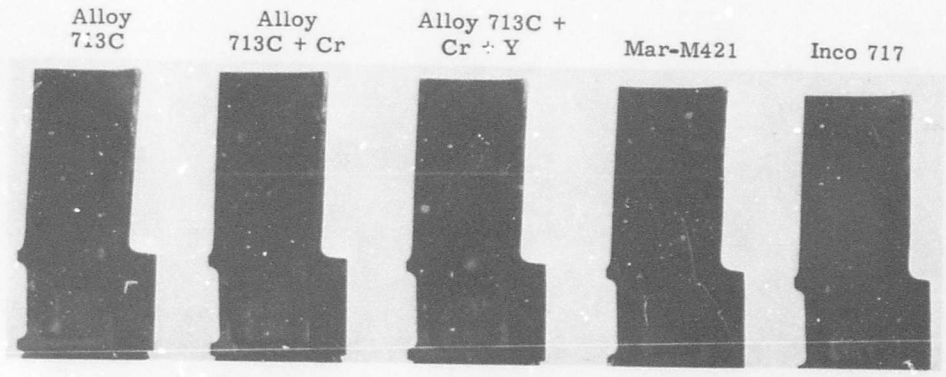

As cast condition

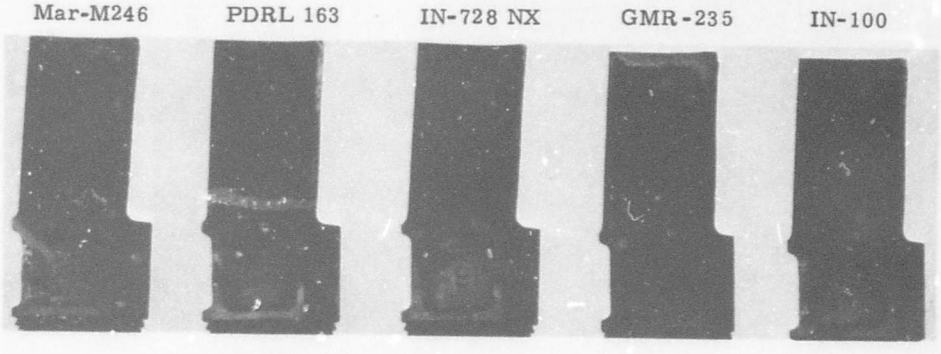

As cast condition

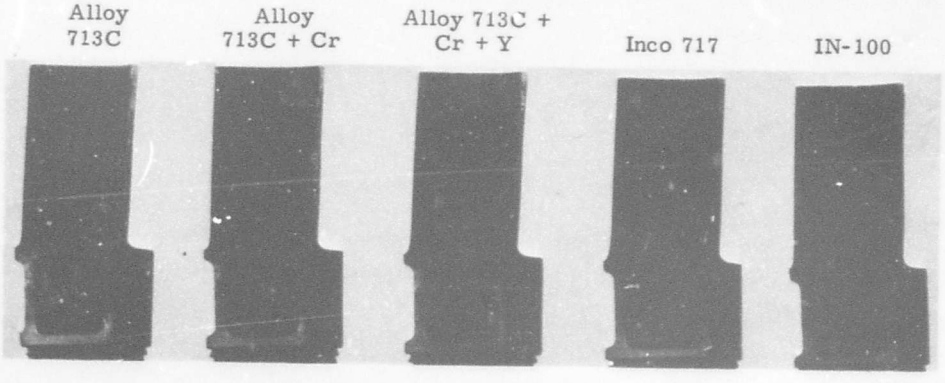

Heat treated condition

Surface conditions (concave side) of test specimens after exposure in the sulfidation-oxidation test rig. (Test No. S-2) (Magn 1X)

Figure 8. Test blades after 500-cycle test--1700°F cyclic temperature.

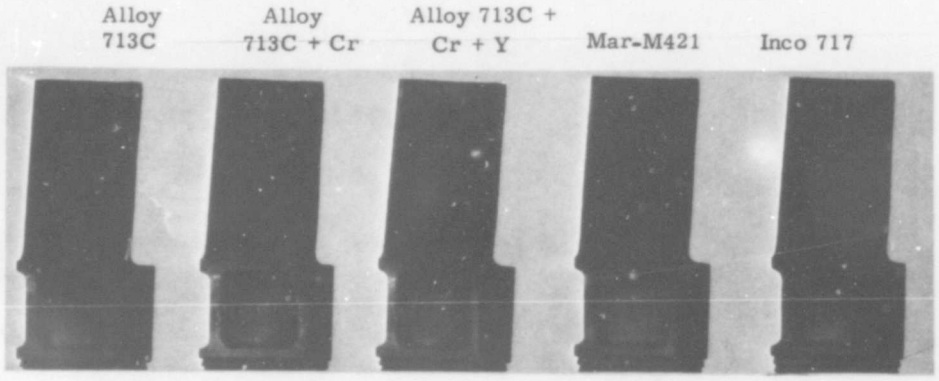

As cast condition

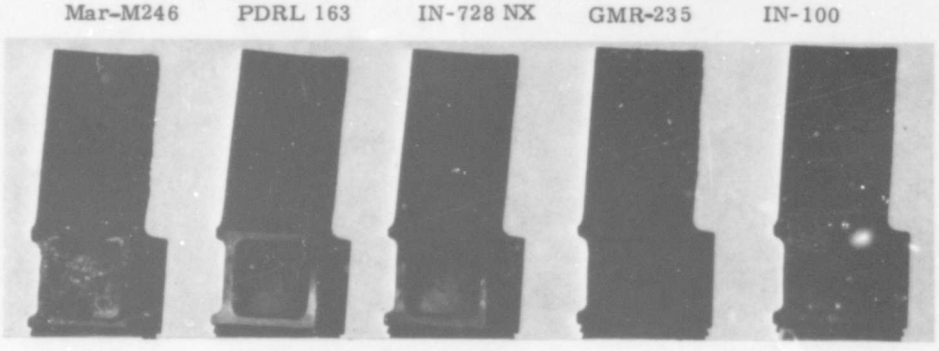

As cast condition

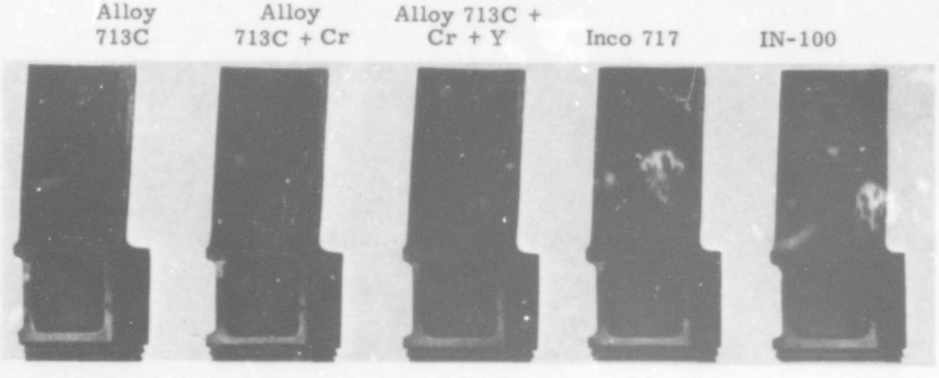

Heat treated condition

Surface conditions (concave side) of test specimens after exposure in the sulfidation-oxidation test rig. Test No. S-21 (Magn 1X)

Figure 9. Test blades after 500-cycle test—1800°F cyclic temperature.

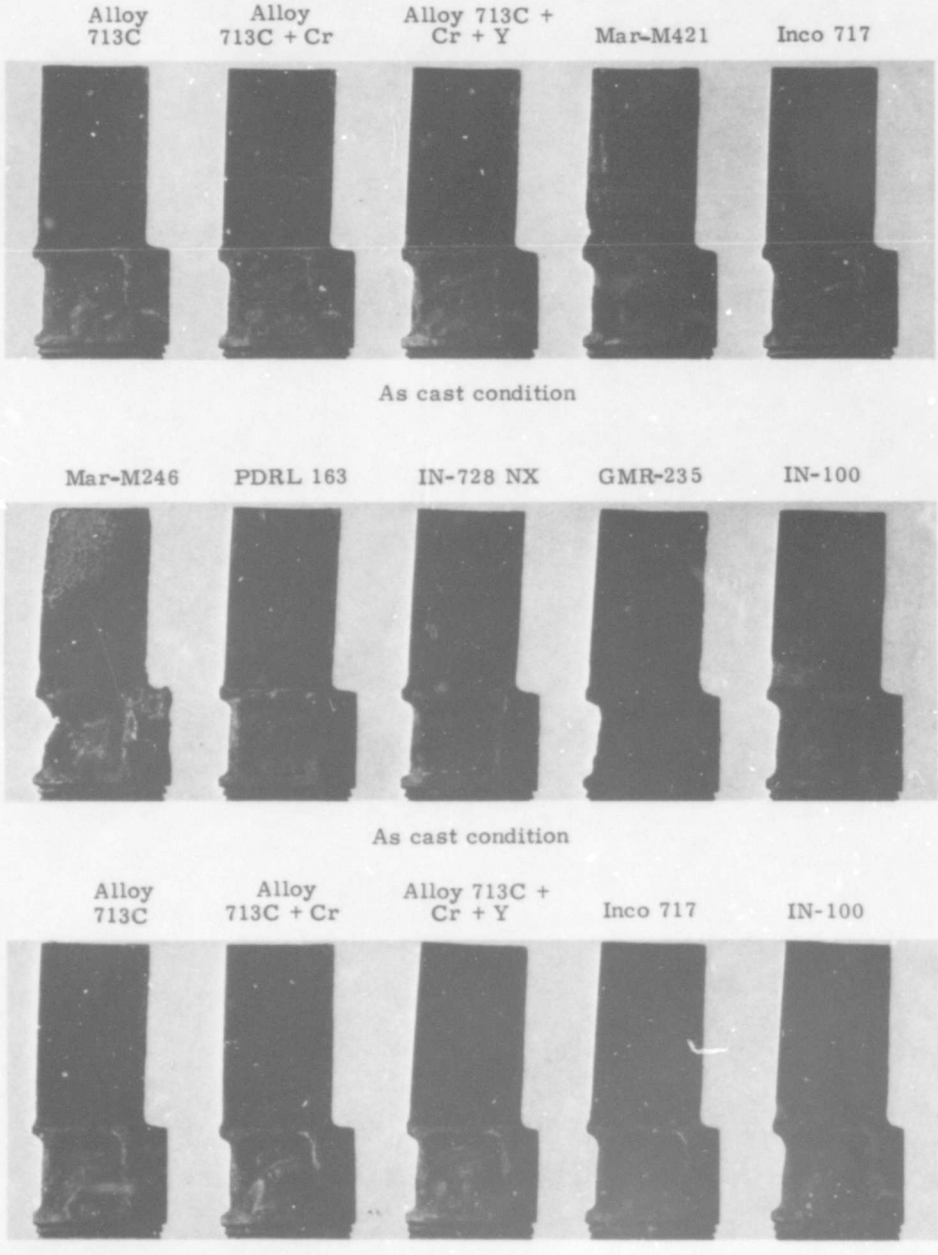

Surface conditions (concave side) of test specimens after exposure in the sulfidation-oxidation test rig. Test No. S-41 (Magn 1X)

Figure 10. Test blades after 500-cycle test—1900°F cyclic temperature.

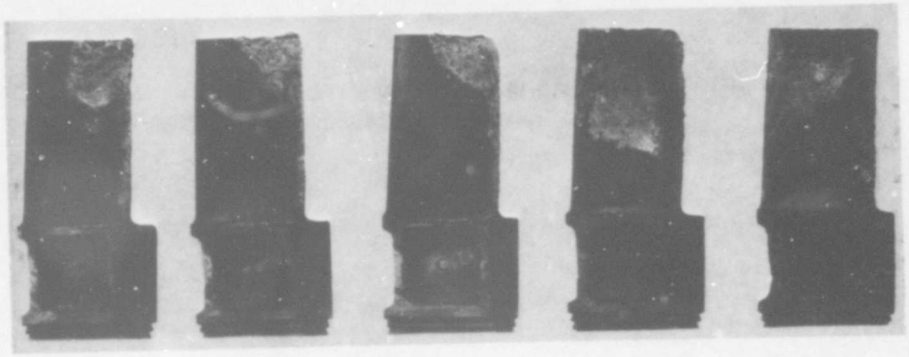

Figure 11. Test blades after 500-cycle test—2000°F cyclic temperature.

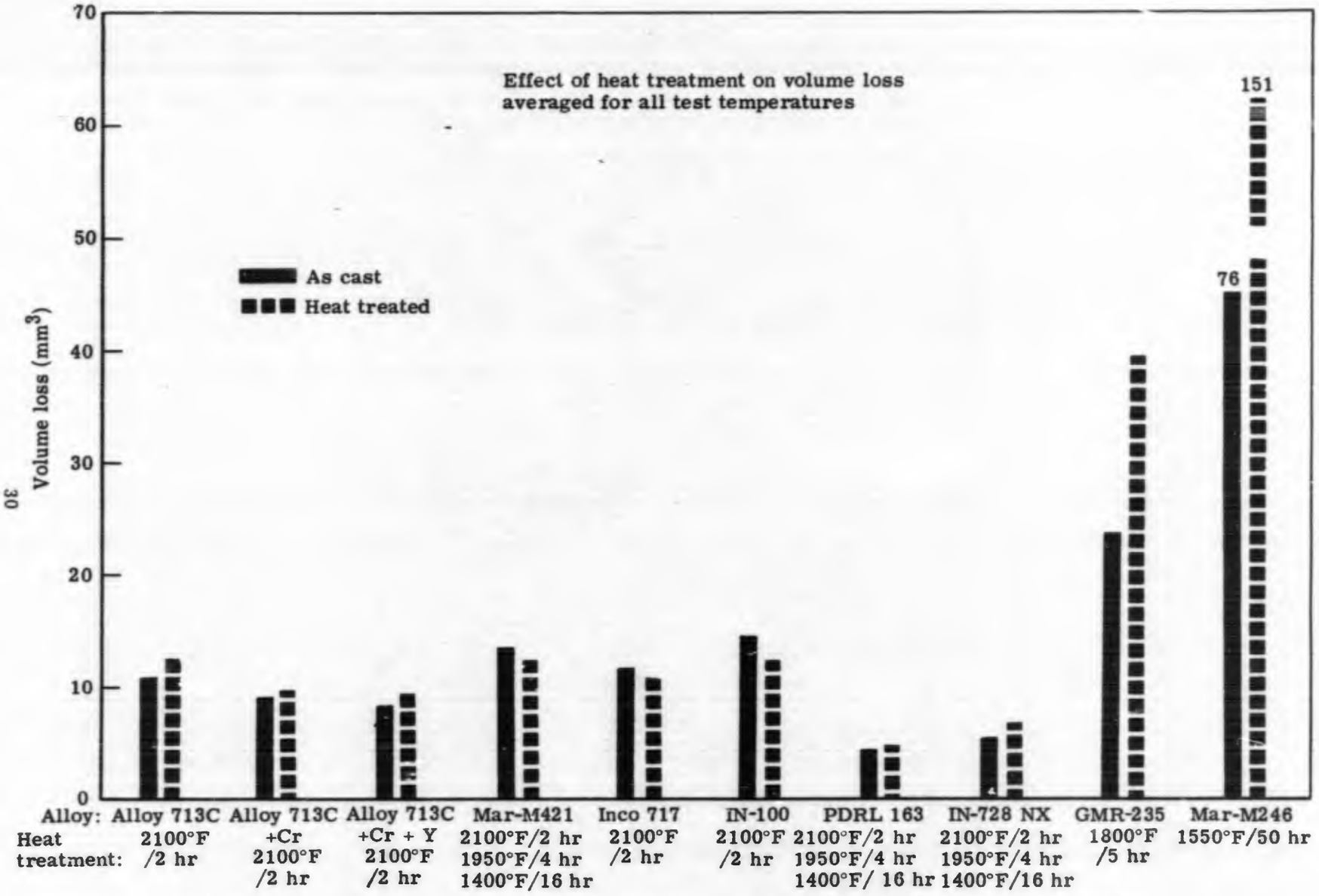

Figure 12. Bar graph showing the effect of heat treatment on individual alloy volume losses.

Table XII.

Significance tests of effects of heat treatment on individual alloys.

Alloy	Volume losses (mm^3) averaged over all test temp		
	As-cast	Heat treated	Difference ratio (heat treated/as-cast)
Alloy 713C	10.91	12.72	1.165
Alloy 713C + Cr	8.91	9.62	1.079
Alloy 713C + Cr + Y	8.20	9.30	1.134
Mar-M421	13.46	12.28	0.912
Inco 717	11.77	10.85	0.921
Mar-M246	76.24	151.50	1.987*
PDRL 163	4.31	4.54	1.053
IN-728 NX	5.67	6.76	1.192
GMR-235	23.78	39.25	1.659*
IN-100	14.52	12.35	0.850

*Denotes a significant difference at $\alpha = 0.05$ (95% confidence level). Over all test temperatures heat treatment had no significant effect on Alloy 713C, Alloy 713C + Cr, Alloy 713C + Cr + Y, Mar-M421, PDRL 163, IN-728 NX, Inco 717, and IN-100. Heat treatment did have a significantly detrimental effect on Mar-M246 and GMR-235.

Figures 13 through 22 are plots of the as-cast and the heat treated volume losses for each alloy at each cyclic test temperature. Although overall differences between as-cast and heat treated volume losses were not significant, Alloy 713C, Alloy 713C + Cr, and IN728NX show some increase in volume loss in the heat treated condition at four of the five test temperatures. Alloy 713C + Cr + Y showed a similar increase at all five test temperatures. Mar M421 decreased in volume loss in the heat treated condition at 1750, 1800, and 1850°F and had a substantial increase in volume loss at 1900°F. Inco 717 exhibited some decrease in volume loss in the heat treated condition at the 1800 and 1900°F test temperatures. PDRL 163 showed a random variation between the as-cast and heat treated volume losses. IN100 had a decrease in volume loss in the heat treated condition at all test temperatures above 1700°F. Mar M246 and GMR-235 exhibited a substantial increase in heat treated volume loss at all five test temperatures.

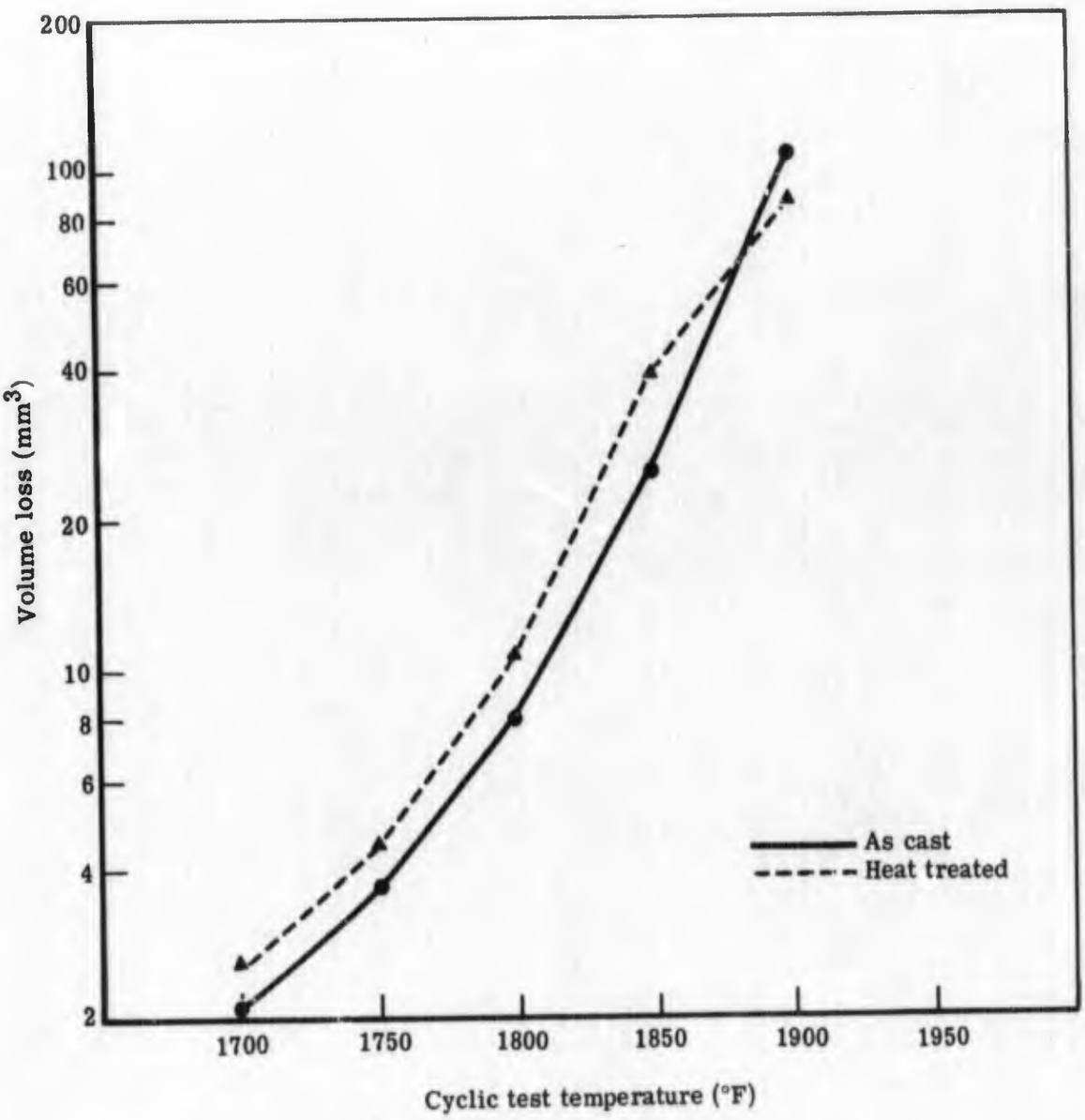

Figure 13. As-cast versus heat treated Alloy 713C at each cyclic test temperature.

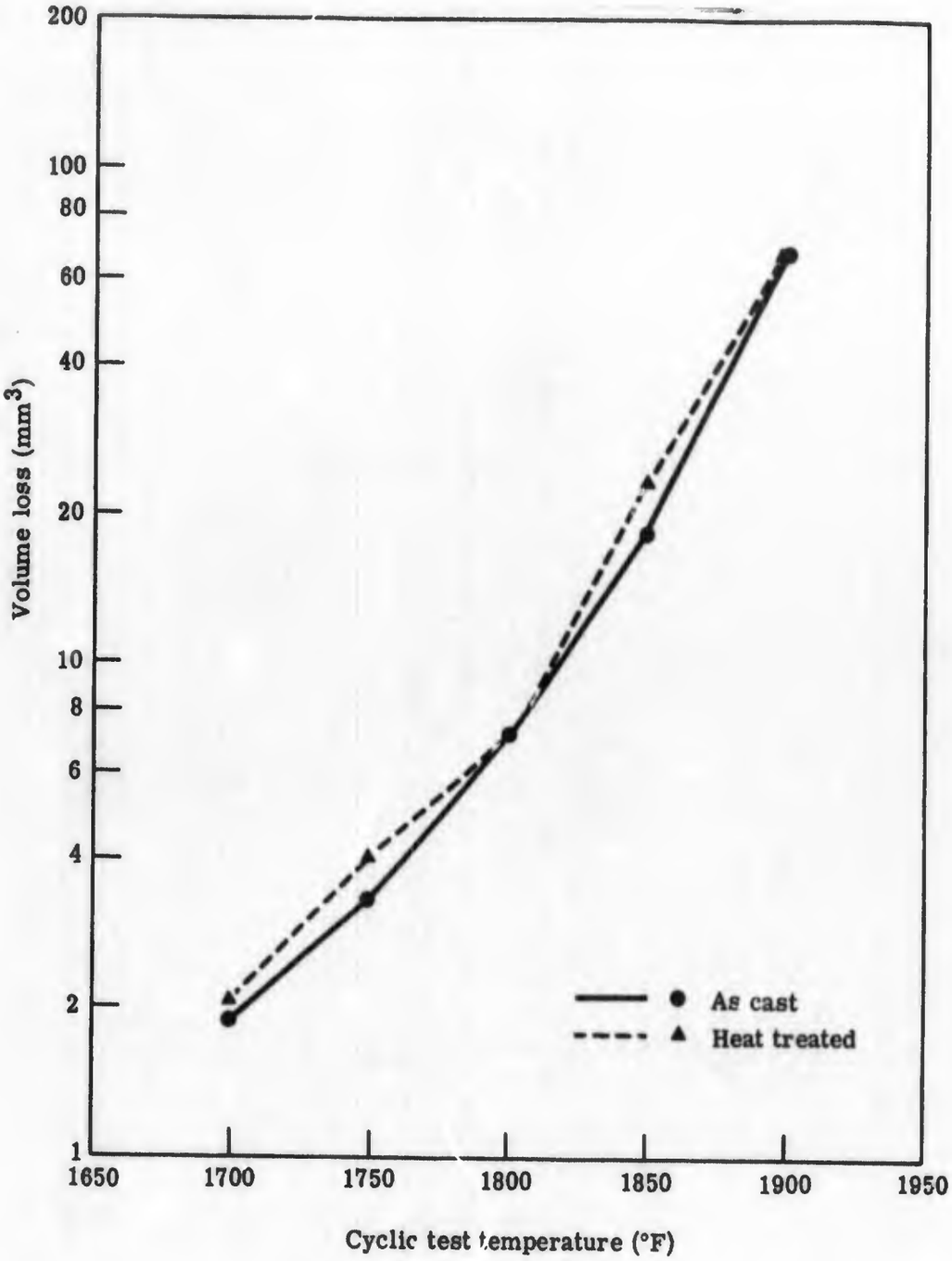

Figure 14. As-cast versus heat treated Alloy 713C + 2% Cr at each cyclic test temperature.

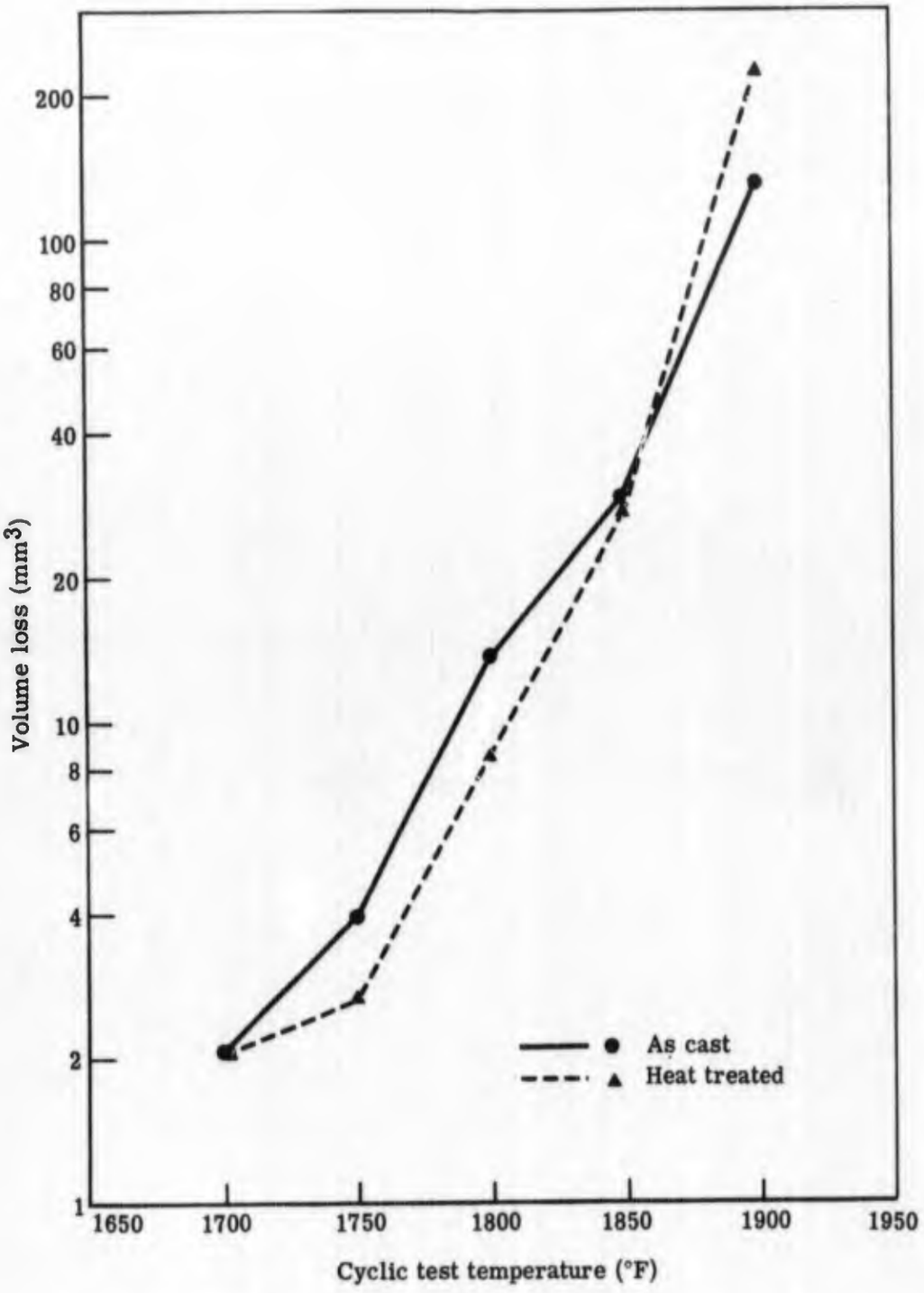

Figure 15. As-cast versus heat treated Alloy 713C + 2% Cr + Y at each cyclic test temperature.

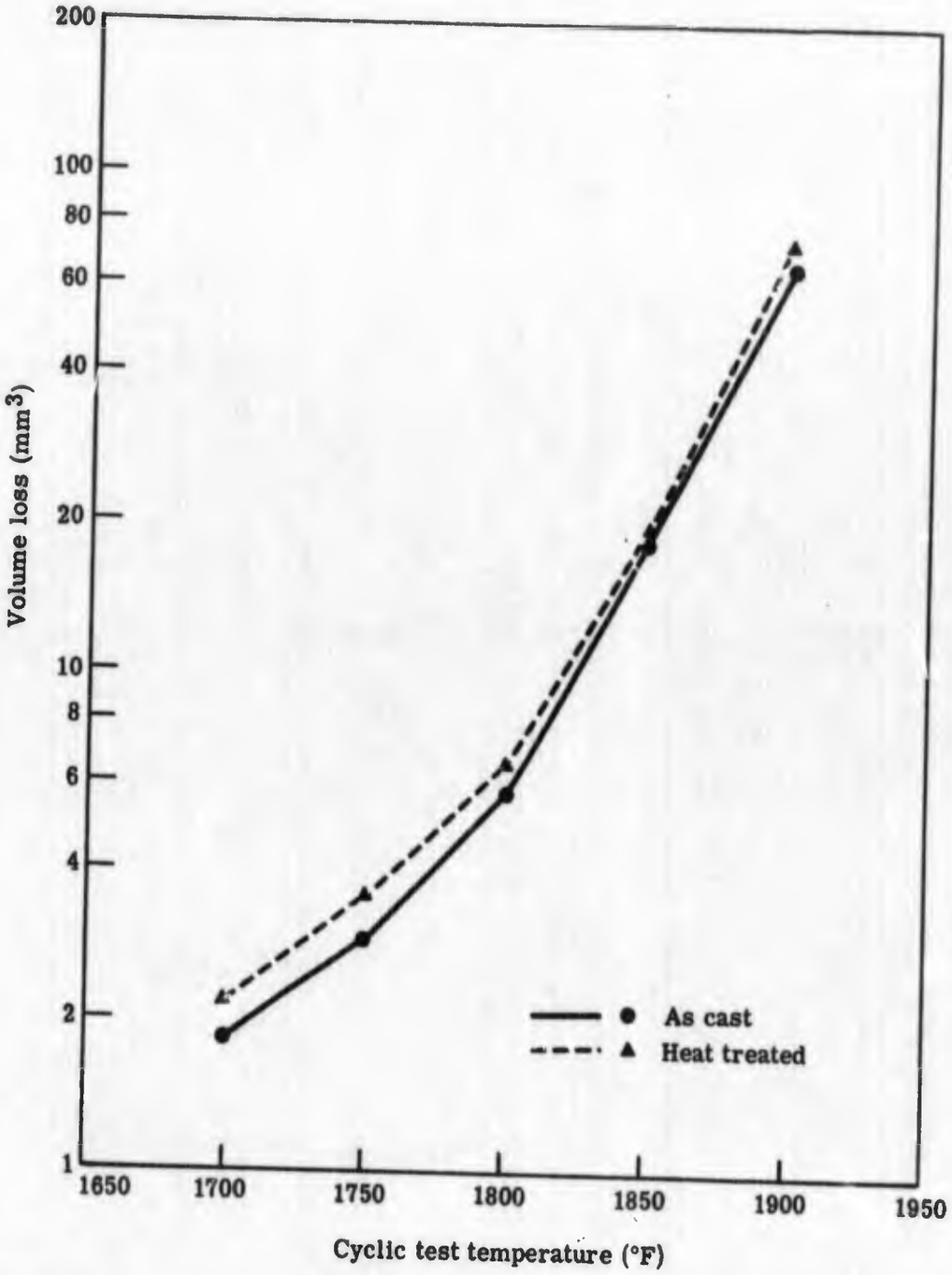

Figure 16. As-cast versus heat treated Mar-M421 at each cyclic test temperature.

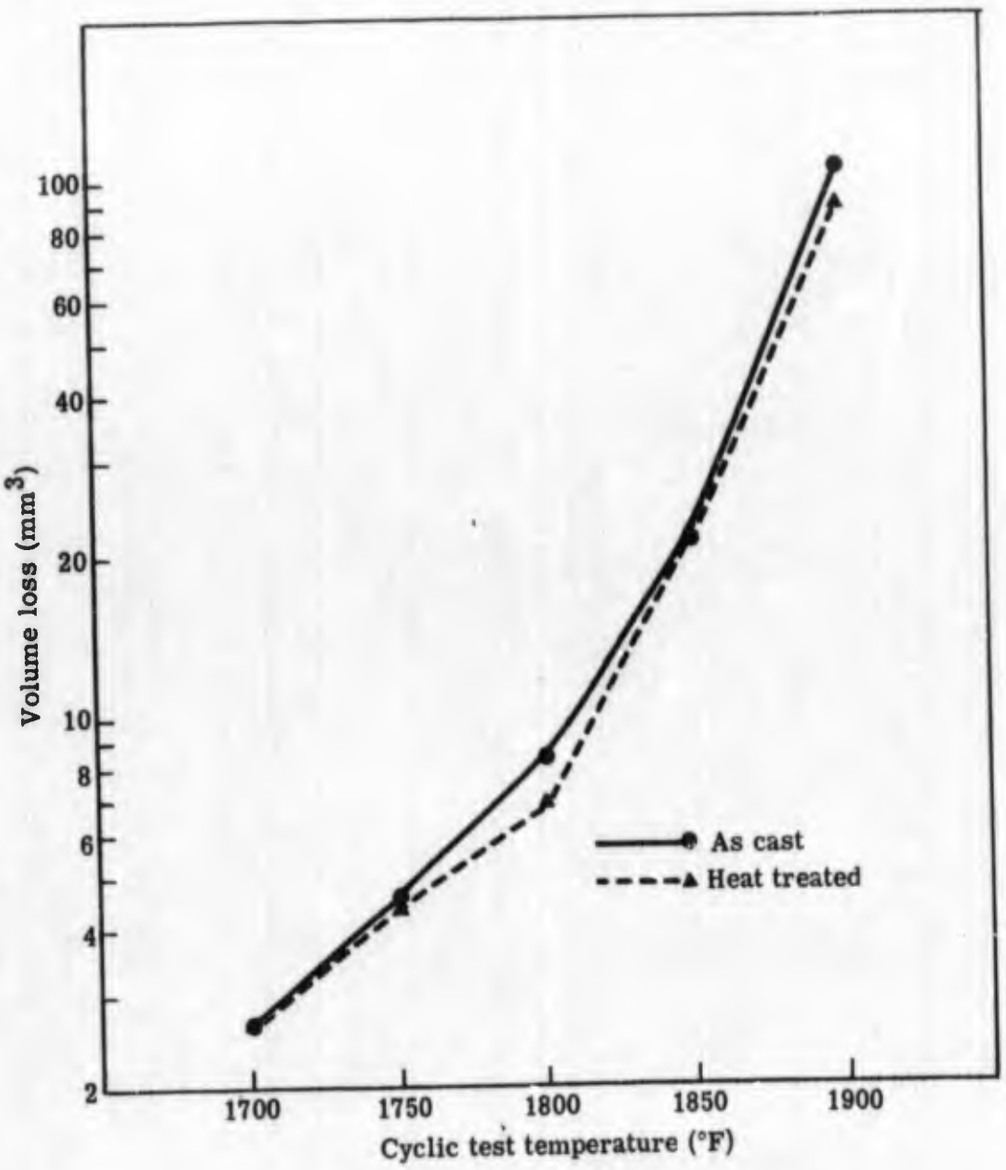

Figure 17. As-cast versus heat treated Inco 717 at each cyclic test temperature.

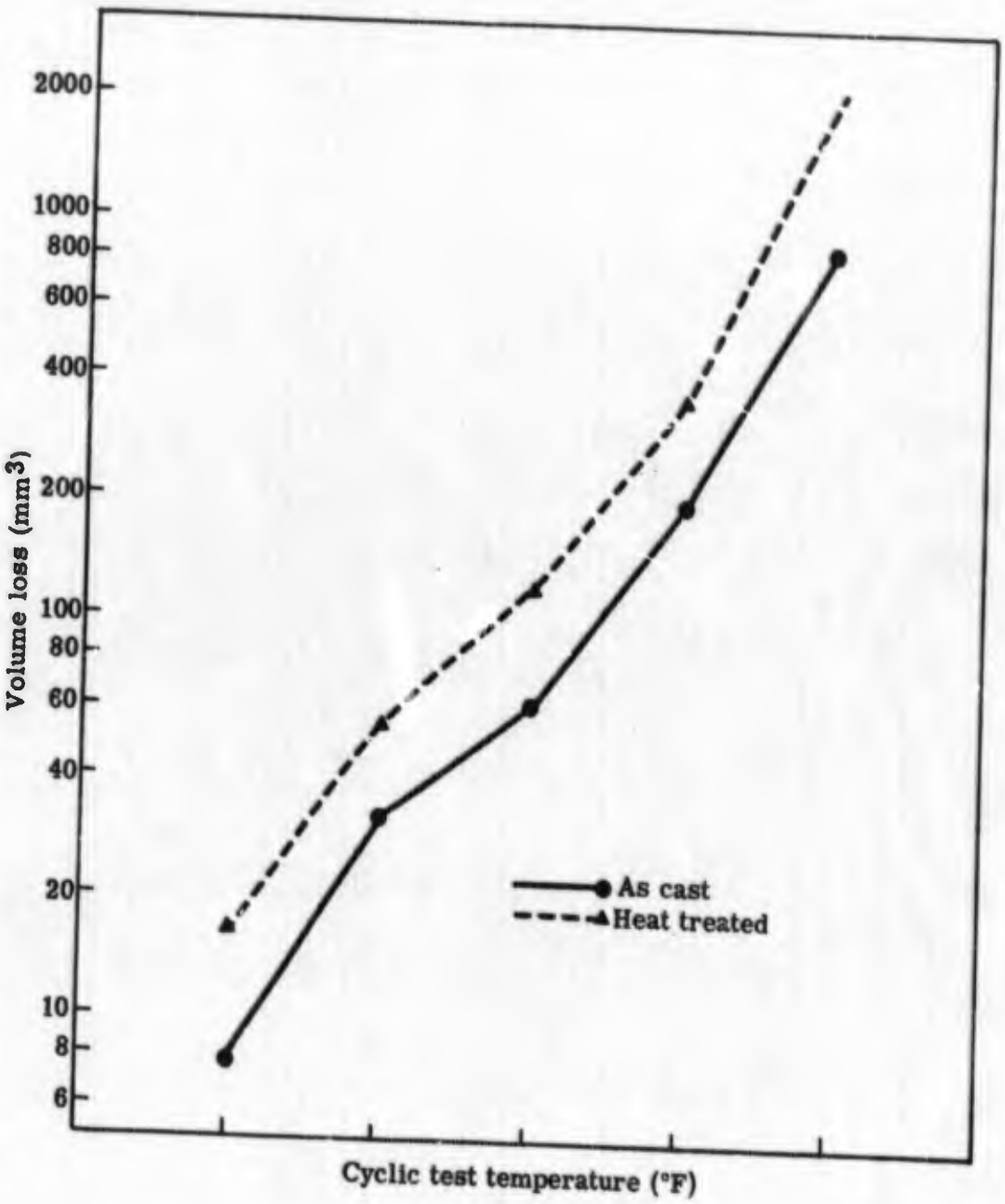

Figure 18. As-cast versus heat treated Mar-M246 at each cyclic test temperature.

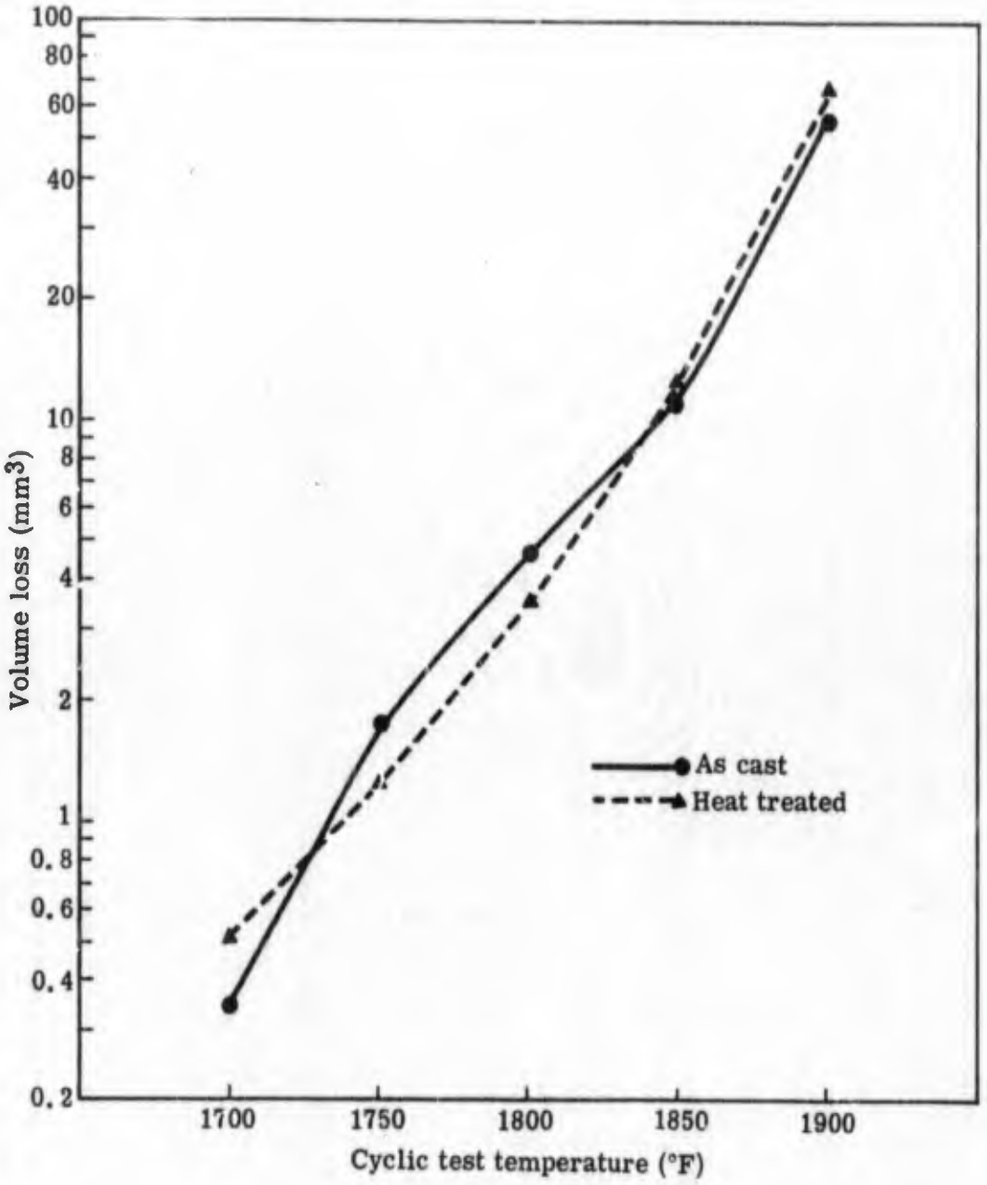

Figure 19. As-cast versus heat treated PDRL 163 at each cyclic test temperature.

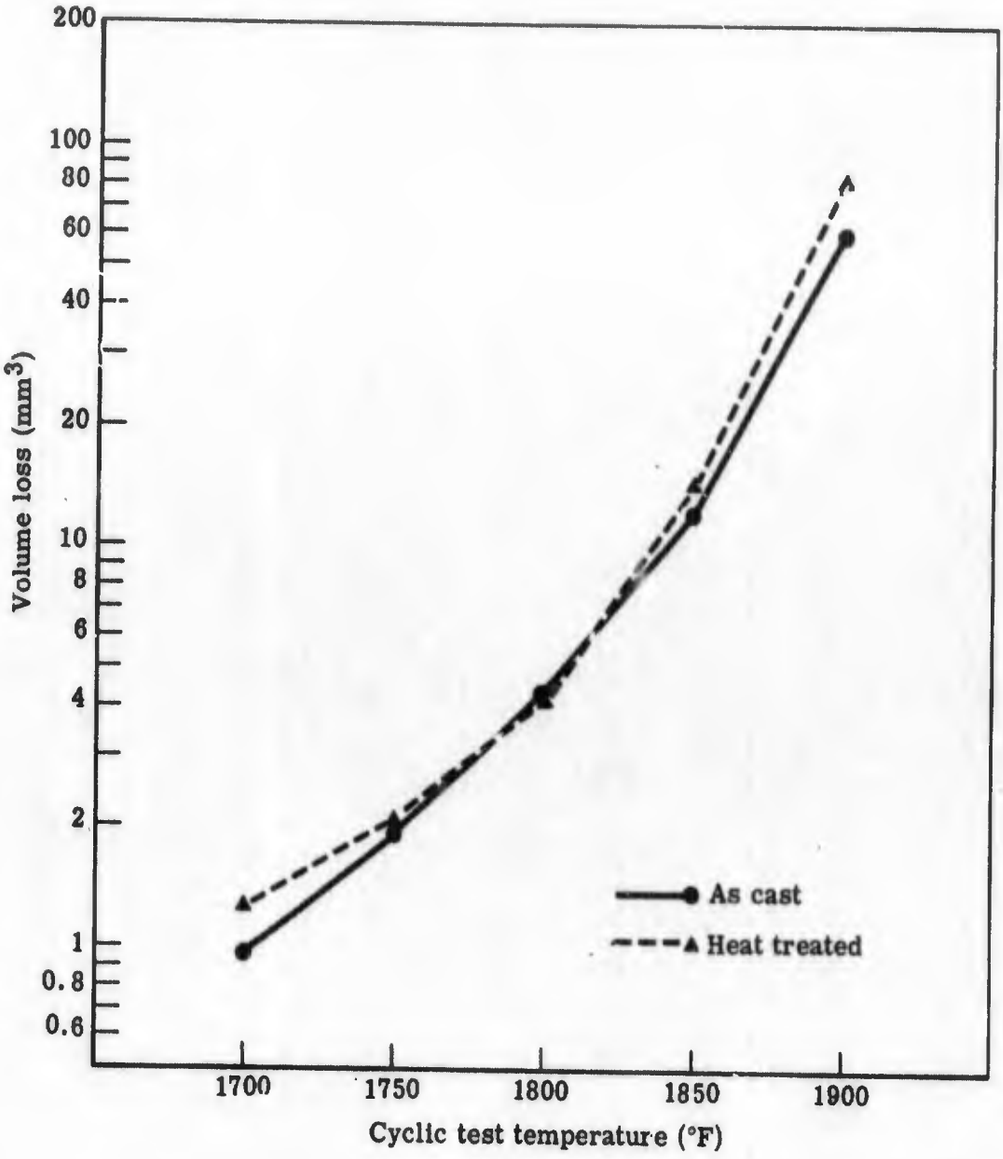

Figure 20. As-cast versus heat treated IN-728 NX at each cyclic test temperature.

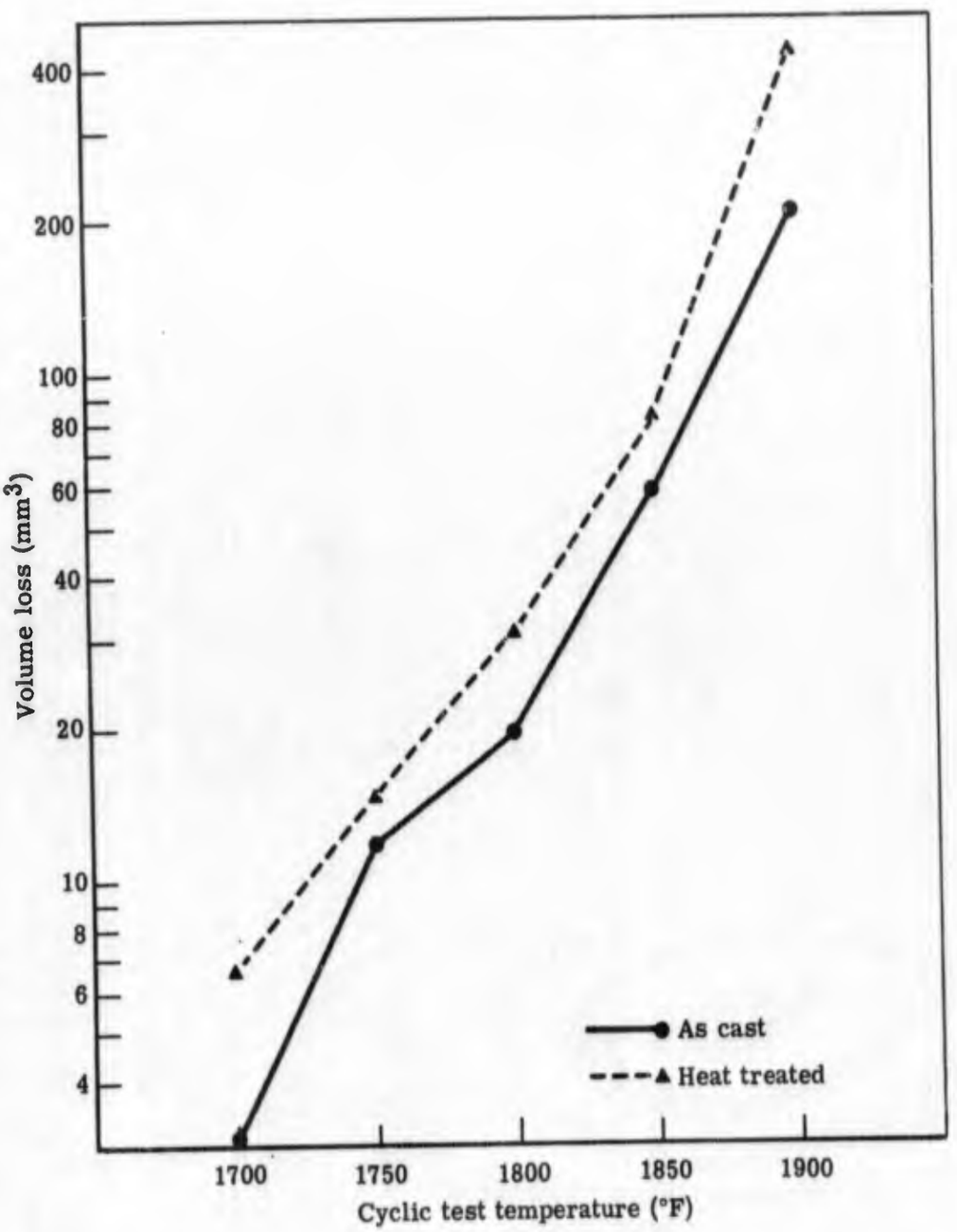

Figure 21. As-cast versus heat treated GMR-235 at each cyclic test temperature.

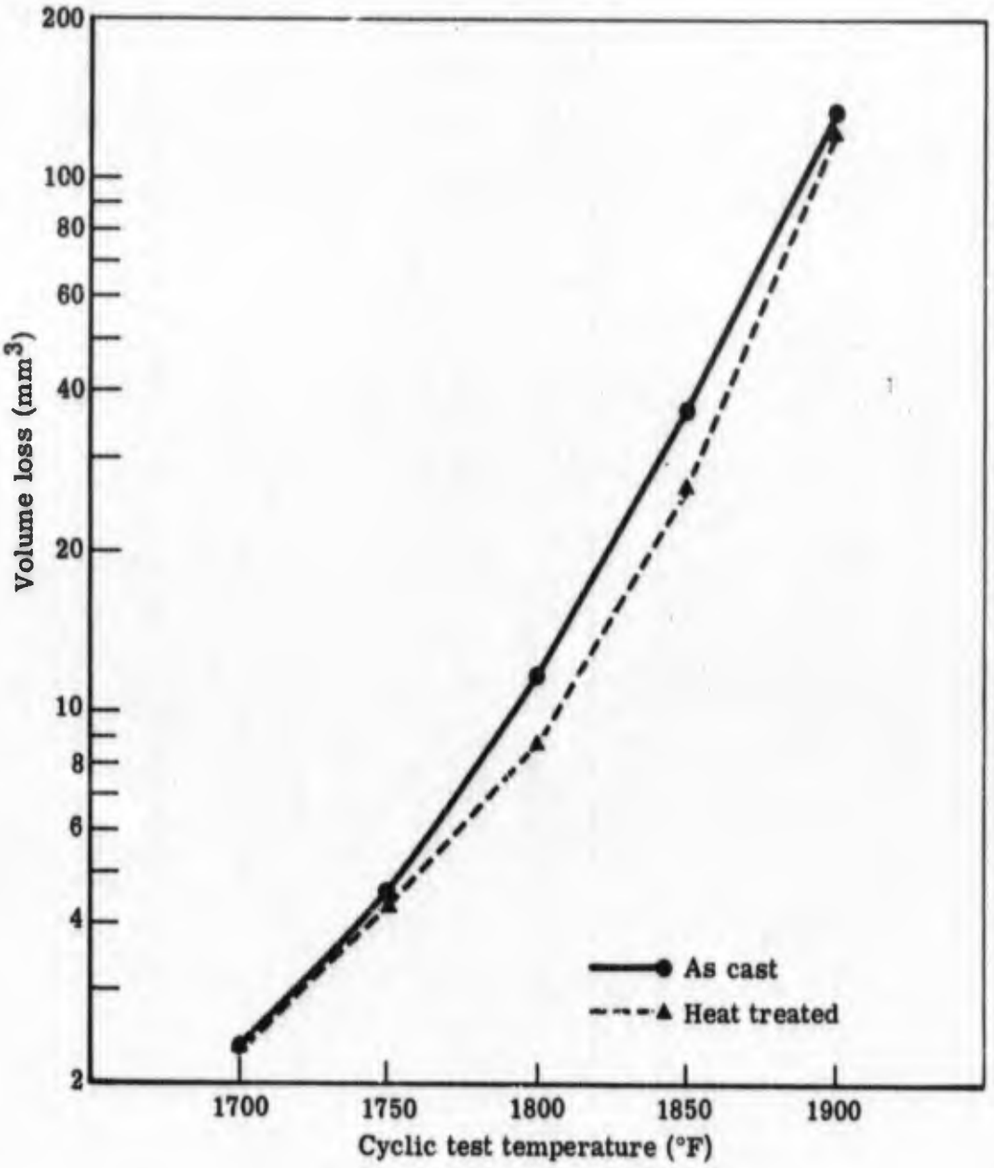

Figure 22. As-cast versus heat treated IN-100 at each cyclic test temperature.

2000°F Cyclic Test Run

Upon completion of the 1700 to 1900°F test run, a 500-cycle run was made on the ten as-cast alloys cycling to 2000°F. The purpose was to observe the hot corrosion rate at higher temperatures. After testing, the blades were cleaned and volume losses were obtained. Table XIII compares the average volume loss of the 2000°F cyclic test with the average as-cast volume losses at each of the lower test temperatures and shows a continuing increase in volume loss. This comparison can only be approximate since the average volume loss values at test temperatures from 1700 to 1900°F represent four runs each while the 2000°F volume loss is from a single run. Volume loss averages were calculated from logarithms and reconverted to numerical values.

Table XIII.
Volume loss of as-cast alloys averaged at each cyclic test temperature.

Cyclic test temperature (°F)	Average volume loss (mm^3)
1700	2.27(1)
1750	5.26(1)
1800	13.07(1)
1850	36.42(1)
1900	46.75(1)
2000	99.04(2)

(1) Average of ten as-cast alloys from four test runs
(2) Average of ten as-cast alloys from one test run

The volume losses from Table XIII cannot be directly compared with the statistical analysis of the 1700 to 1900°F data since the latter was adjusted to account for run-to-run variation.

The blades, after the 2000°F cyclic test, are shown in Figure 11. Note that the severest corrosion occurs near the tip of the blade where the temperature is highest. This is further illustrated by higher magnification photographs of the Alloy 713C and IN-100 test blades after testing and cleaning, Figures 23 and 24. Section D-D near the point of maximum attack had the following thermal history during the 2000°F cyclic test.

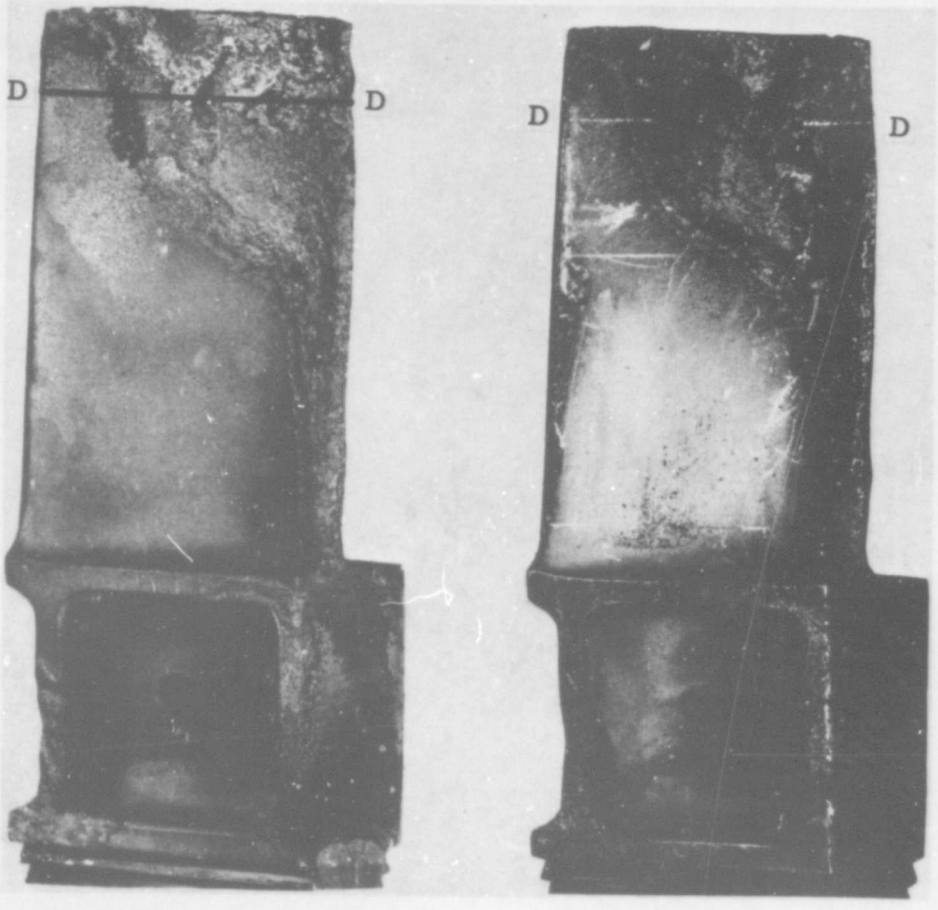

713C after testing (left) and after caustic cleaning (right) following 2000°F cyclic test (magn 3x)

Figure 23. Alloy 713C test blades from 2000°F test after testing and after cleaning.

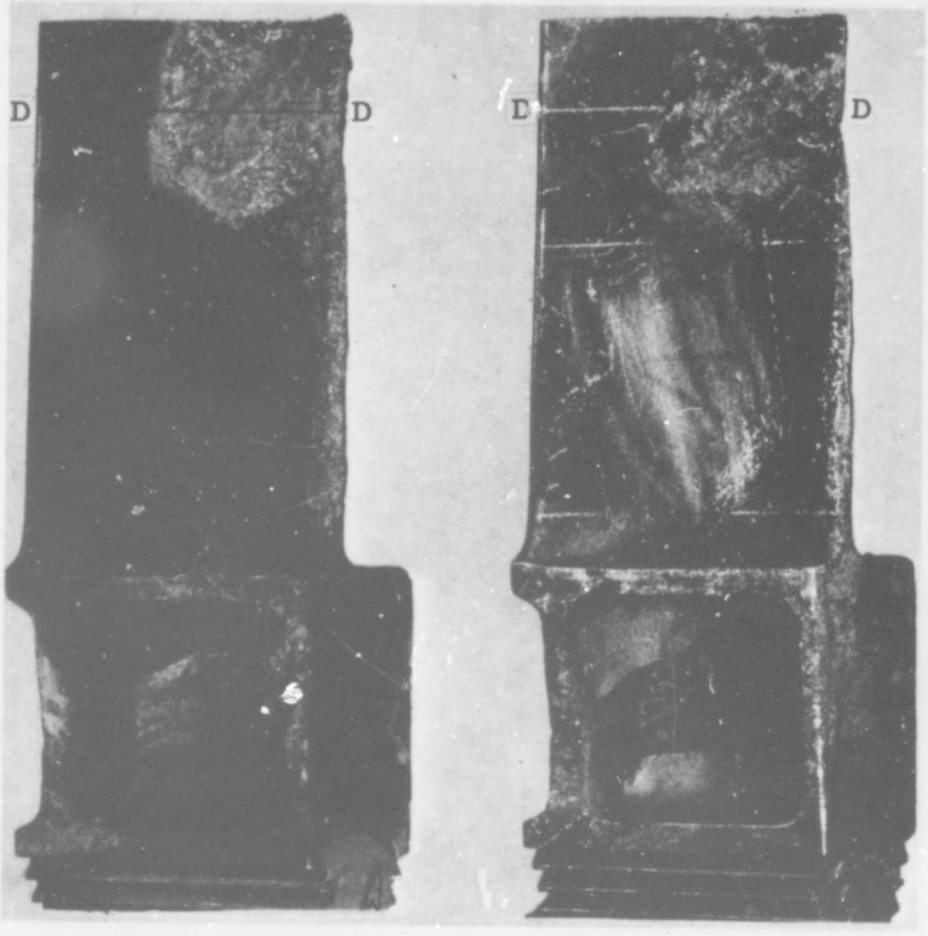

IN-100 after testing (left) and after caustic cleaning (right) following 2000°F cyclic test (magn 3x).

Figure 24. IN-100 test blade from 2000°F test after testing and after cleaning.

Temperature interval (°F)	Percentage of heating cycle in temperature interval	Cumulative percent
Above 1900	59	59
1800 to 1900	14	73
1600 to 1800	13	86
Below 1600	14	100

Since section D-D was above 1800°F, 73% of the heating cycle, and above 1900°F, 59% of the heating cycle, it appears that hot corrosion is severe in this temperature range.

Volume loss data for the 31 test runs are shown in Tables XIV through XIX.

AREA OF CORROSION EVALUATION AT AIRFOIL CROSS SECTION

To further investigate corrosion severity over the range of test temperatures, areas of corrosion were measured at an airfoil cross section. One as-cast turbine blade of each alloy from the 1700, 1800, 1900, and 2000°F cyclic tests was evaluated. Measurements were made at section D'-D' just above section D-D near the tip of the airfoil where the test temperatures were highest. Figure 25 shows the corrosion pattern at section D'-D' on IN-100 after the 1900°F cyclic test.

Temperature gradients at section D'-D' are shown in Figures 3 and 4 and the thermal history at this location is given in Table V in Section III of this report. Note that this section of the blade is above 1800°F for 61% of the heating cycle on the 1900°F test and 75% of the heating cycle during the 2000°F test. With few exceptions, corrosion severity at airfoil section D'-D' increased as the test temperature increased. This is in substantial agreement with the volume loss results reported previously. A plot of the average corrosion area for the ten alloys versus test temperature is shown in Figure 26. Similar to the corrosion measured by volume loss, the average corrosion area increased in an approximate logarithmic fashion. Figure 27 shows plots at each individual alloy corrosion area at each test temperature. Some reversal of alloy ranking occurs from temperature to temperature. Since only one sample of each alloy was evaluated at a test temperature, part of this may be due to the normal variation within each alloy. Table XX lists individual alloy area losses along with the method used in obtaining corrosion measurements.

Table XIV.

Volume losses during 500-cycle test—1700°F cyclic temperature.

Test Number	Volume loss in cubic millimeters					
	S-1	S-2	S-3	S-4	S-5	S-6
As cast						
Alloy						
713C	3.21	1.87	2.12		3.185	
713C (Mod Cr)	2.82	1.80	2.02		2.73	
713C (Mod Cr + Y)	2.90	1.54	2.14		2.59	
Mar-M421	3.04		2.23	1.69	2.63	
Inco 717	4.05	2.78	2.81		3.57	
Mar-M246	18.32		7.70	3.71	10.82	
PDRL 163	3.40		0.27	0.05	0.50	
IN-728 NX	1.40		1.03	0.68	1.53	
GMR-235	9.74		2.72	1.33	3.96	
IN-100	4.28	2.56	1.96		2.98	
Heat treated						
713C	4.34	2.47		1.83	3.68	
713C (Mod Cr)	3.04	2.19		1.50	3.05	
713C (Mod Cr + Y)	3.28	2.46		1.72	2.68	
Mar-M421		2.38	2.27	1.72		1.81
Inco 717	4.10	2.54		2.19	3.68	
Mar-M246		18.46	18.75	8.22		22.8
PDRL 163		0.46	0.41	0.38		0.84
IN-728 NX		1.08	1.00	1.49		1.64
GMR-235		7.49	5.20	3.92		12.37
IN-100	3.89	2.21		1.94	3.12	

Table XV.

Volume losses during 500-cycle test—1750°F cyclic temperature.

Test Number	Volume loss in cubic millimeters					
	S-11	S-12	S-13	S-14	S-15	S-16
As cast						
Alloy						
713C	3.24	3.83	5.65		4.42	
713C (Mod Cr)	2.83	3.54	5.79		3.82	
713C (Mod Cr + Y)	3.02	3.47	3.96		3.12	
Mar-M421	3.41		5.88	5.62	4.34	
Inco 717	4.31	4.06	9.00		4.53	
Mar-M246	54.71		70.31	26.13	23.06	
PDRL 163	0.79		5.21	2.59	1.79	
IN-728 NX	1.36		2.81	3.10	2.38	
GMR-235	8.56		34.41	9.21	8.31	
IN-100	4.53	3.88	9.89		4.67	
Heat treated						
713C	3.39	4.04		5.71	5.83	
713C (Mod Cr)	3.02	5.08		4.79	4.15	
713C (Mod Cr + Y)	2.99	3.65		4.44	3.92	
Mar-M421		4.73	7.07	0.69		1.87
Inco 717	3.84	3.80		5.59	4.77	
Mar-M246		61.32	124.78	91.25		21.21
PDRL 163		1.09	2.25	2.44		0.36
IN-728 NX		1.99	2.96	2.68		1.07
GMR-235		8.39	22.02	19.95		7.62
IN-100	4.39	4.04		4.63	4.53	

Table XVI.

Volume losses during 500-cycle test—1800°F cyclic temperature.

	Volume loss in cubic millimeters				
Test Number	S-21	S-22	S-23	S-24	S-25
As cast					
Alloy					
713C	8.46	14.16	9.26		12.9
713C (Mod Cr)	6.95	12.99	9.05		11.19
713C (Mod Cr + Y)	5.50	8.61	8.72		9.22
Mar-M421	7.81		9.99	11.03	108.45
Inco 717	7.37	21.30	9.43		11.38
Mar-M246	76.46		74.43	60.51	102.90
PDRL 163	3.08		4.96	5.88	7.48
IN-728 NX	4.72		5.15	5.32	6.93
GMR-235	20.21		23.77	19.73	40.88
IN-100	15.48	31.25	10.31		14.33
Heat treated					
713C	12.19	21.81		12.36	15.26
713C (Mod Cr)	7.71	10.24		9.43	11.34
713C (Mod Cr + Y)	5.71	9.97		9.17	10.85
Mar-M421		10.18	11.99	11.68	
Inco 717	7.67	9.32		8.60	12.88
Mar-M246		147.17	174.44	153.62	
PDRL 163		4.00	5.00	5.19	
IN-728 NX		4.85	5.46	6.71	
GMR-235		54.16	30.90	34.35	
IN-100	10.14	16.19		8.74	14.59

Table XVII.

Volume losses during 500-cycle test—1850°F cyclic temperature.

Test Number	Volume loss in cubic millimeters					
	S-31	S-32	S-33	S-34	S-35	S-36
As cast						
Alloy						
713C	25.79	39.39	46.59		33.36	
713C (Mod Cr)	17.53	27.75	36.06		27.93	
713C (Mod Cr + Y)	18.09	29.64	34.12		26.94	
Mar-M421	25.02		50.60	23.85	47.69	
Inco 717	17.32	42.77	39.34		31.15	
Mar-M246	229.06		287.29	168.70	206.21	
PDRL 163	8.60		22.59	9.29	18.01	
IN-728 NX	9.37		21.93	10.66	18.62	
GMR-235	88.95		79.31	55.89	56.39	
IN-100	45.49	83.14	62.13		36.30	
Heat treated						
713C	37.85	63.68		26.95	28.53	
713C (Mod Cr)	22.04	43.61		18.41	20.93	
713C (Mod Cr + Y)	17.52	47.46		16.00	23.01	
Mar-M421		51.35	42.71	22.42		12.34
Inco 717	19.61	52.70		17.54	25.60	
Mar-M246		516.11	498.43	359.40		183.83
PDRL 163		25.74	23.38	8.78		5.73
IN-728 NX		20.70	24.32	11.65		9.07
GMR-235		151.30	192.63	70.23		20.01
IN-100	31.70	46.16		24.08	28.38	

Table XVIII.

Volume losses during 500-cycle test—1900°F cyclic temperature.

Test Number	Volume loss in cubic millimeters					
	S-41	S-42	S-43	S-44	S-45	S-46
As cast						
Alloy						
713C	106.77	43.76	30.89		22.65	
713C (Mod Cr)	68.78	29.25	18.72		15.56	
713C (Mod Cr + Y)	72.24	28.91	19.35		12.53	
Mar-M421	117.65		32.31	59.64	30.27	
Inco 717	81.62	40.83	33.35		30.17	
Mar-M246	504.03		277.98	314.32	267.79	
PDRL 163	54.19		13.45	24.24	10.81	
IN-728 NX	66.27		16.51	18.86	14.81	
GMR-235	222.07		70.52	91.76	31.46	
IN-100	162.54	63.84	41.09		20.78	
Heat treated						
713C	114.84	39.72		18.62	20.90	
713C (Mod Cr)	81.94	27.25		22.87	13.52	
713C (Mod Cr + Y)	74.29	31.76		21.88	16.33	
Mar-M421		81.43	53.18	60.42		23.68
Inco 717	78.15	37.28		29.27	21.78	
Mar-M246		534.60	443.47	510.34		419.00
PDRL 163		26.20	14.33	20.49		6.83
IN-728 NX		27.76	17.82	23.24		10.38
GMR-235		143.03	120.12	154.95		341.20
IN-100	129.71	59.36		48.21	22.96	

Table XIX.

Volume losses during 500-cycle test—2000°F cyclic temperature.

As cast	Volume loss (mm^3)
Test No. S-61	
Alloy	
713C	101.2
713C (Mod Cr)	80.35
713C (Mod Cr + Y)	87.12
Mar-M421	109.7
Inco 717	131.2
Mar-M246	357.3
PDRL 163	27.08
IN-728 NX	49.61
GMR-235	162.4
IN-100	114.5

5370-25

Figure 25. Corrosion pattern on IN-100 at airfoil section D'-D'-1900°F cyclic test.

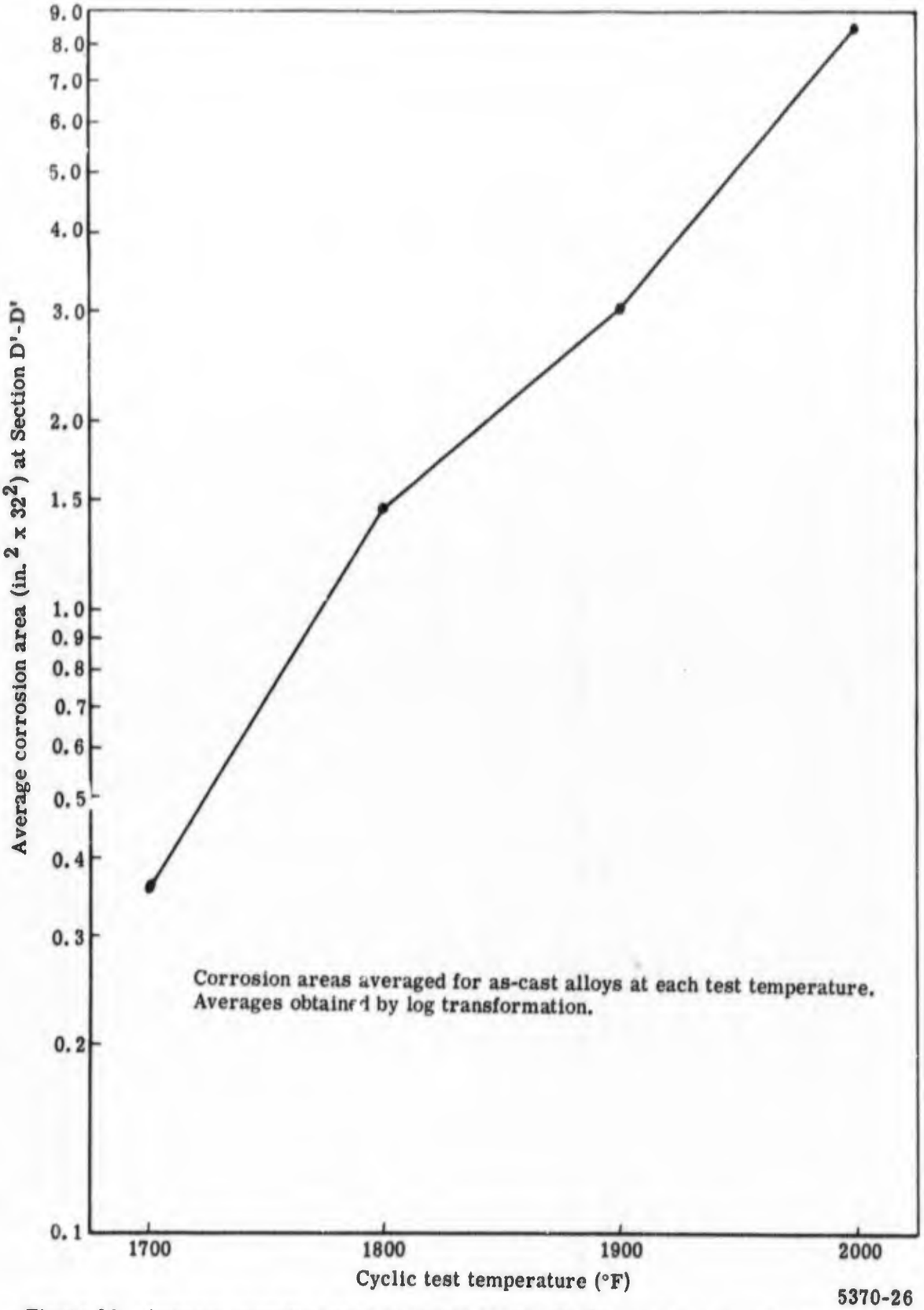

Figure 26. Average corrosion area at airfoil section D'-D' versus cyclic test temperature.

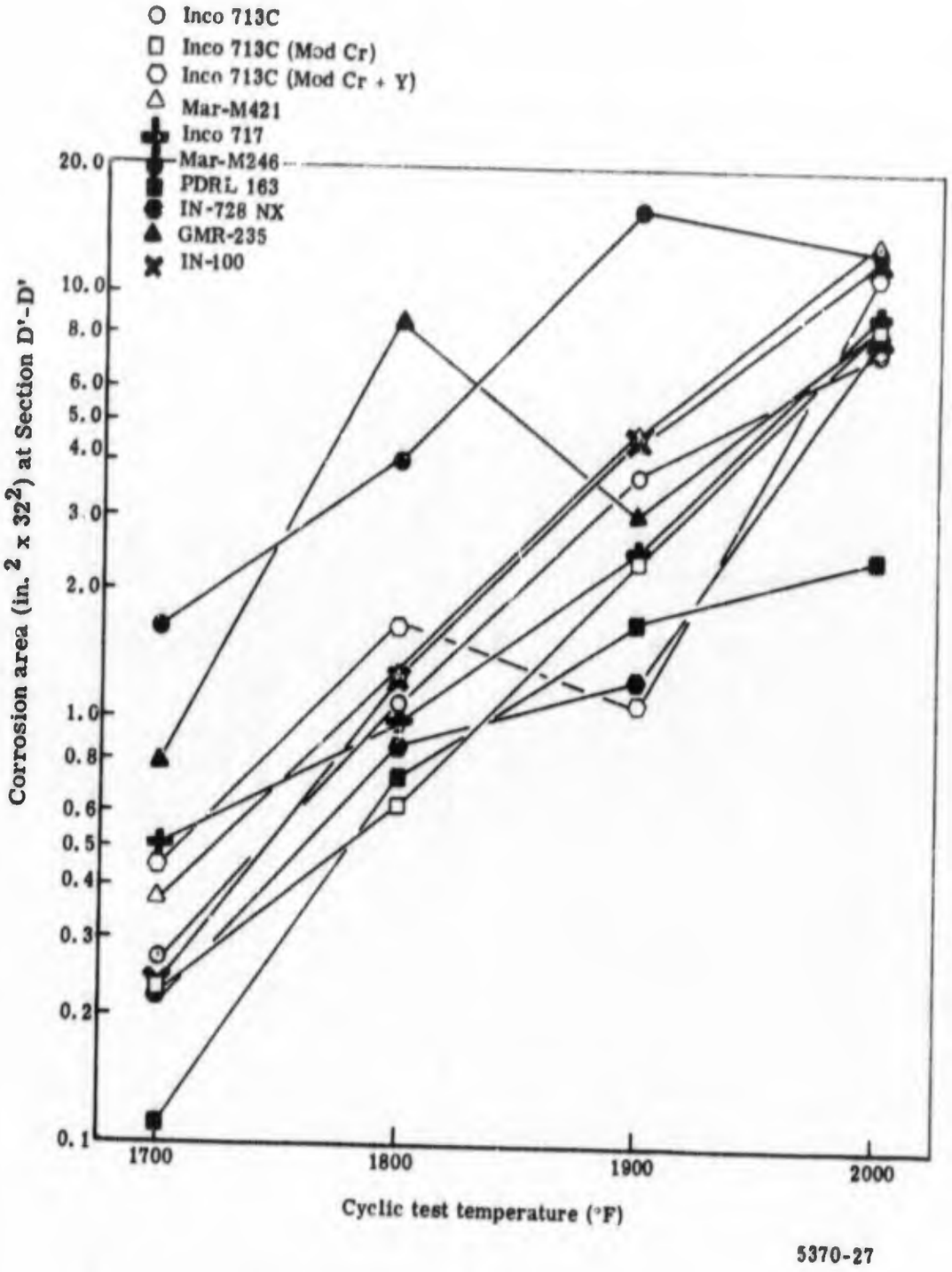

Figure 27. Alloy corrosion areas at airfoil section D'-D' versus cyclic test temperature.

Table XX.

Corrosion areas* at section D'-D' after 500-cycle test.

Cyclic test temperature (°F)	Corrosion area ($in.^2 \times 32^2$)			
Alloy—as-cast	1700	1800	1900	2000
Alloy 713C	0.27	1.10	3.79	7.60
Alloy 713C (Mod Cr)	0.23	0.63	2.40	8.78
Alloy 713C (Mod Cr + Y)	0.45	1.71	1.08	11.30
Mar-M421	0.38	1.30	4.77	13.70
Inco 717	0.50	1.00	2.59	9.09
Mar-M246	1.62	4.10	16.18	13.48
PDRL 163	0.11	0.74	1.72	2.49
IN-728 NX	0.22	0.83	1.28	7.92
GMR-235	0.78	2.80	3.08	8.73
IN-100	0.24	1.25	4.78	12.40

*Corrosion areas were determined by the following method:

1. Test blades were sectioned at airfoil section D'-D', mounted and polished.
2. Metallographic sections were projected on the scope of a Leitz Large Metallograph at 32X.
3. A transparency containing the original profile of section D'-D' was laid over the projected image and the corrosion areas were traced on the transparency.
4. Areas of corrosion were measured with a planimeter.

BINOCULAR EXAMINATION

As part of the preliminary evaluation of the test pieces, one blade of each alloy tested at each cyclic temperature from 1700 to 1900°F was given a detailed binocular examination at 7X magnification. The objective was to study the relative surface corrosion on each region of the blade as the test temperatures were increased. To make the examination as systematic as possible, transparent plastic templates subdivided into small areas were constructed for the concave and convex side of the blades. Individual areas were not of equal size but were constructed to best define the corrosion patterns which formed on the blades. A numerical system was used to rate the relative severity of the surface corrosion. Figure 28 shows the grid and the numerical system employed.

A = Dividing line between leading edge – upper airfoil region and lower airfoil – stalk region

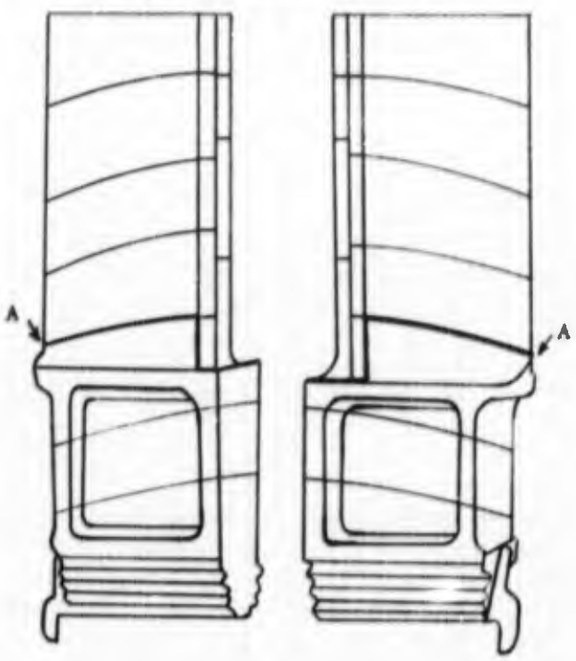

Numerical rating system applied to each subarea for binocular examination

Number	Relative corrosion severity (7 X magn)
0	No corrosion
1	Traces of oxide corrosion
2	Light corrosion over at least 1/3 of subarea
3	Medium corrosion over at least 1/3 of subarea
4	Heavy corrosion over at least 1/3 of subarea with some spalling of corrosion products
5	Severe spalling and splitting over at least 1/3 of subarea

5014-4

Figure 28. Grid system for binocular evaluation of test blades.

Corrosion appeared at two separate regions on the test blades. Figures 8 through 11 show the concave side of the test blades after completion of each of the 500 cycle tests. At the lower cyclic temperatures, corrosion first appeared at the tip of the leading edge gradually extended down the airfoil and then widened out with increasing test temperatures. Relatively light corrosion appeared on the stalk and lower airfoil sections of the blades at the lower cyclic temperatures. At the 1700°F cyclic temperature, the stalk area attained a maximum temperature of approximately 1550°F. Corrosion in this region gradually enlarged and increased in severity with increasing test temperatures. Corrosion at the base of the blade was apparently related to blade geometry. The sodium sulfate sprayed on during the cooling portion of the cycle is retained in greater quantities at the stalk section resulting in a higher concentration of contaminant in the lower region of the blade. Corrosion at the base of the blade apparently occurred at a lower temperature and with a higher concentration of sodium sulfate.

Summation of results of the binocular examination of the leading edge-upper airfoil corrosion are shown in Figure 29. Corrosion severity remains essentially constant for the 1700 and 1750°F cyclic tests; however, it shows a significant increase as maximum cyclic temperatures rise to 1800, 1850, and 1900°F. Differences in alloy susceptibility to surface corrosion are apparent with PDRL 163 and IN-728 NX showing the best corrosion resistance and Mar-M246 the poorest resistance. Figure 30 shows a plot of stalk-lower airfoil corrosion. For most of the alloys, corrosion was relatively constant up to the 1800°F test and then increases at 1850 and 1900°F.

The binocular examination provided a good preliminary method of systematically observing hot corrosion severity over a range of temperatures and was in general agreement with the other evaluation methods. The major deficiency of this method, of course, is that it measures surface corrosion only.

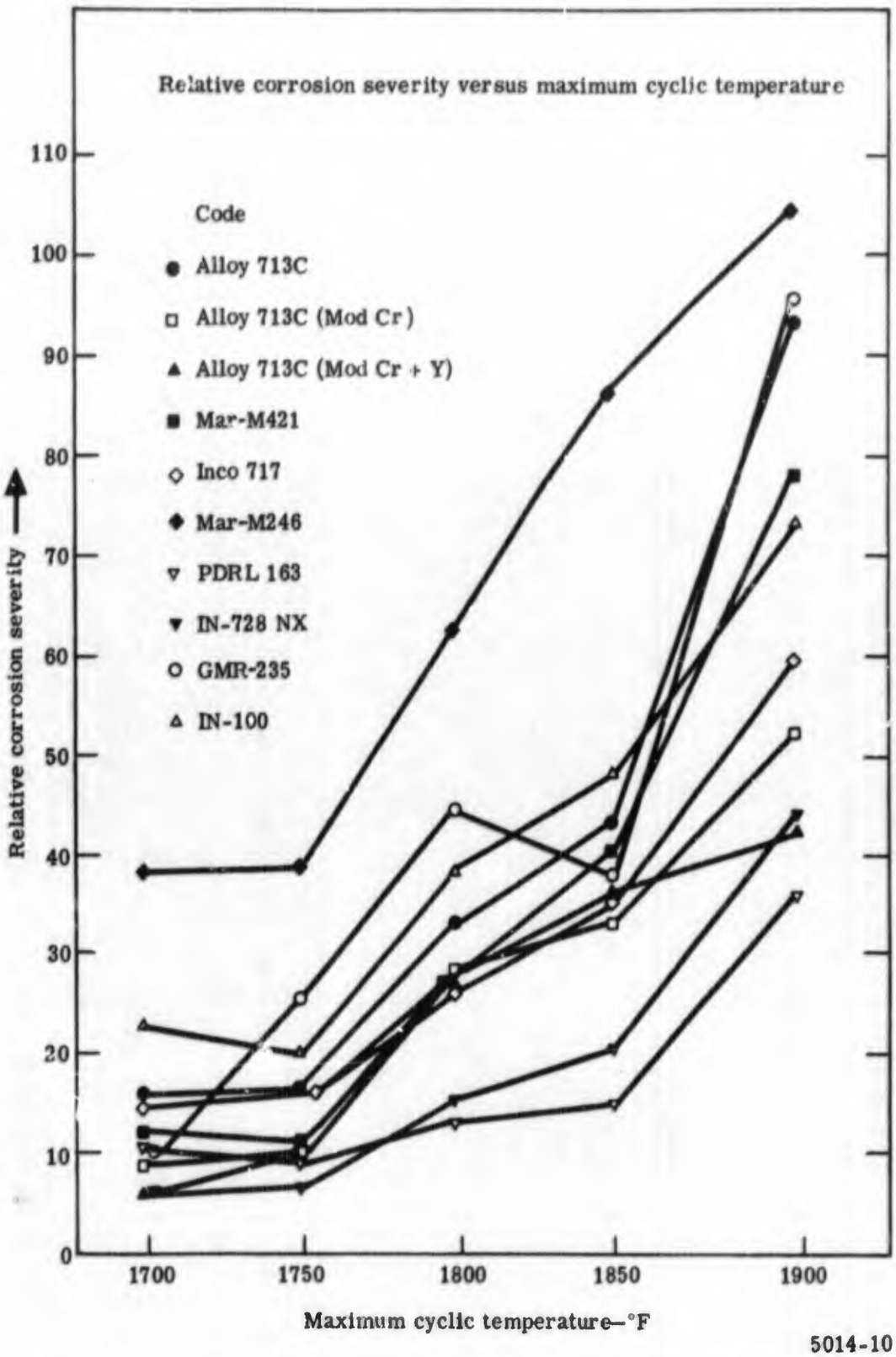

Figure 29. Binocular evaluation—leading edge and upper-middle airfoil.

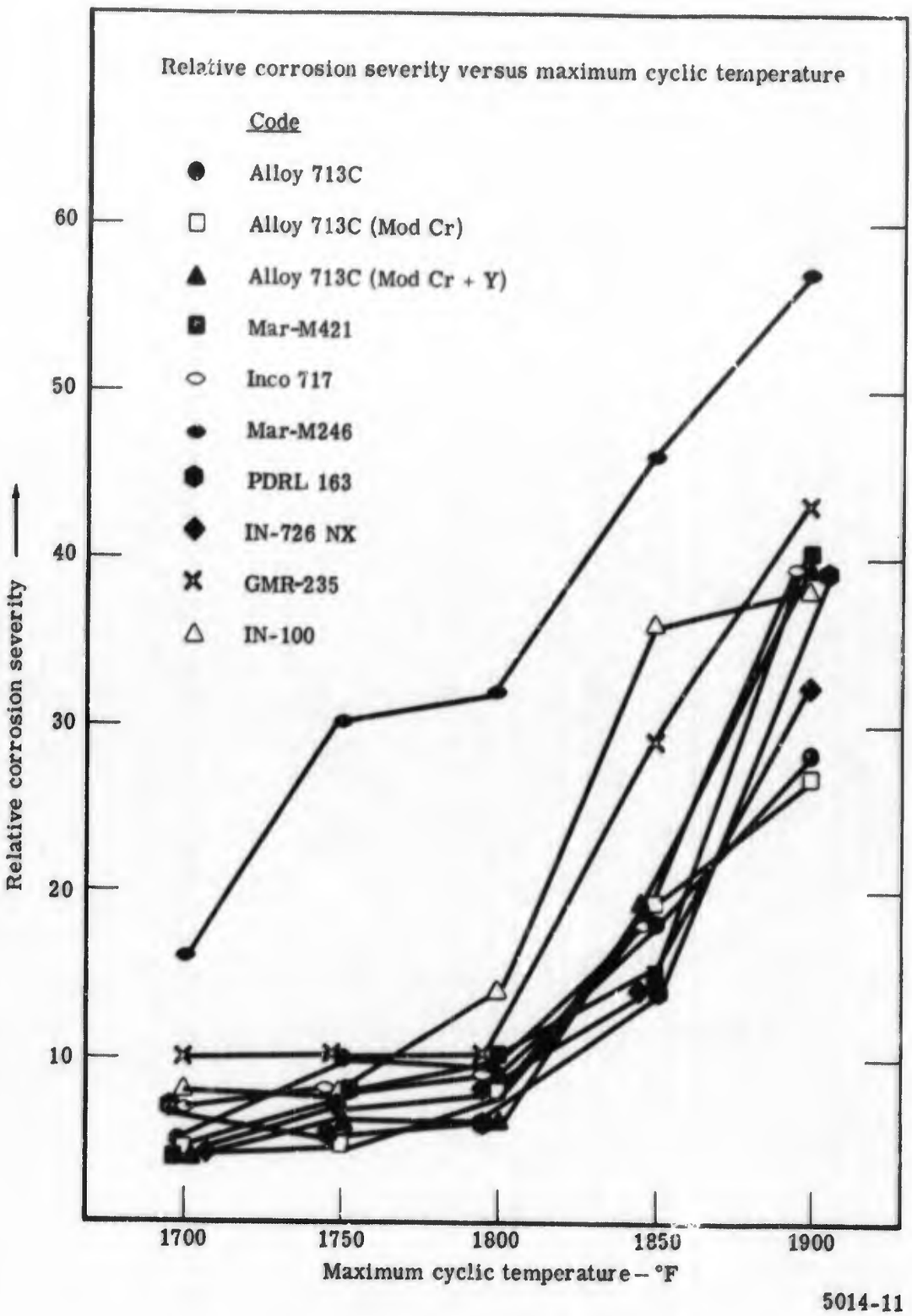

Figure 30. Binocular evaluation—stalk and lower airfoil.

SECTION V

REGRESSION ANALYSIS

As a follow-up to the analysis of variance, a regression analysis was made of the chemical compositions of the ten nickel base alloys. The purpose of the regression analysis was to obtain an association between the weight percents of the elements in an alloy and the corresponding loss of material during the corrosion tests.

In the analysis, a "Stepwise Regression Program", written for the IBM 7094, was used to arrive at a linear equation describing the relationship between the weight percent of the elements and the resulting volume losses of the as-cast alloys. The discussion of the analysis in the Appendix to this report contains a definition of a data point for this analysis; presents the mathematical model assumed to characterize the data; and describes how the program derives the regression equation.

RESULTS OF THE ANALYSIS

In the range of the analysis, it can be concluded for the as-cast alloys that:

- Increasing the weight percent of Cr or Al in an alloy will reduce volume loss due to hot corrosion
- Increasing the weight percent of W or Mo in an alloy will produce greater volume loss
- Raising the temperature will increase volume loss

The association between the aforementioned variables and volume loss is described by the following equation.

$$\log_{10}(\text{volume loss}) = (5.85238 \times 10^{-9})(\text{temperature}^3) - (1.33860 \times 10^{-5})(\text{temperature}^2) + (6.32837 \times 10^{-2})(\text{weight \% W}) + (8.63834 \times 10^{-2})(\text{weight \% Mo}) - (6.77702 \times 10^{-2})(\text{weight \% Cr}) - (8.982 \times 10^{-2})(\text{weight \% Al}) + 11.2807$$

This regression equation derived exclusively for the as-cast alloys cannot be extended to the heat treated alloys since volume loss changed significantly for certain alloys following the heat treatment. Inasmuch as no corresponding compositional changes were available, it was not possible to derive a regression equation for the heat treated alloys.

ACCURACY OF REGRESSION EQUATION

The multiple correlation coefficient measures the association between values of the independent variables in the regression equation and the dependent variable ($\log_{10}$ volume loss). If the equation exactly predicts volume loss, the coefficient is one and if there is no association between the equation and volume loss the coefficient is zero. The multiple correlation coefficient for the regression equation was calculated to be 0.9928 showing a high degree of correlation.

VOLUME LOSS PREDICTIONS WITH THE REGRESSION EQUATION

The effect of four elements on volume loss at a cyclic test temperature of 1800°F is interpreted graphically in Figure 31. The graphs were generated by fixing the test temperature and percentages of three elements in the equation and varying the fourth element. The graphs illustrate how the regression equation might be used in adjusting alloy compositions.

Figures 32 through 41 compare the average measured volume loss for each alloy at each test temperature with that predicted by the regression analysis equation.

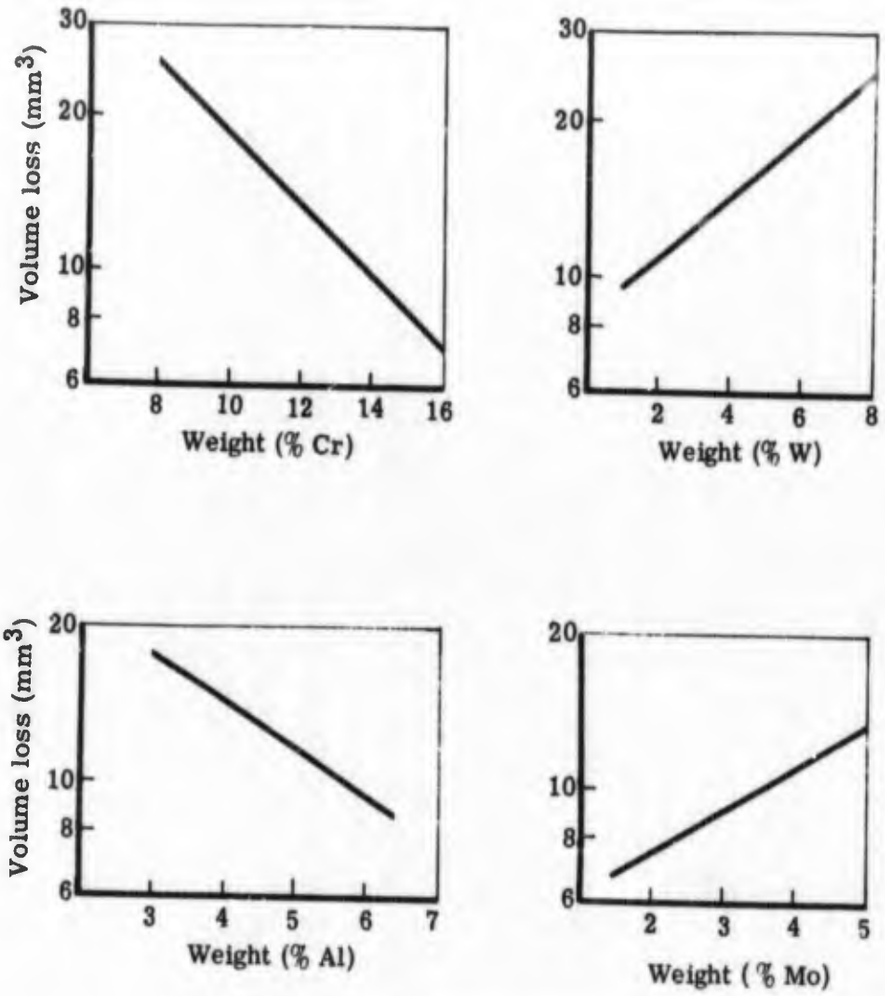

Notes:
Each graph was plotted using the mean values of the other three elements and a temperature of 1800°F.
Mean values: Cr=13.88%, W =1.74%, Mo =3.51%, Al =5.72%.

5370-31

Figure 31. The effects of Cr, W, Al, and Mo on volume loss as predicted by the regression equation.

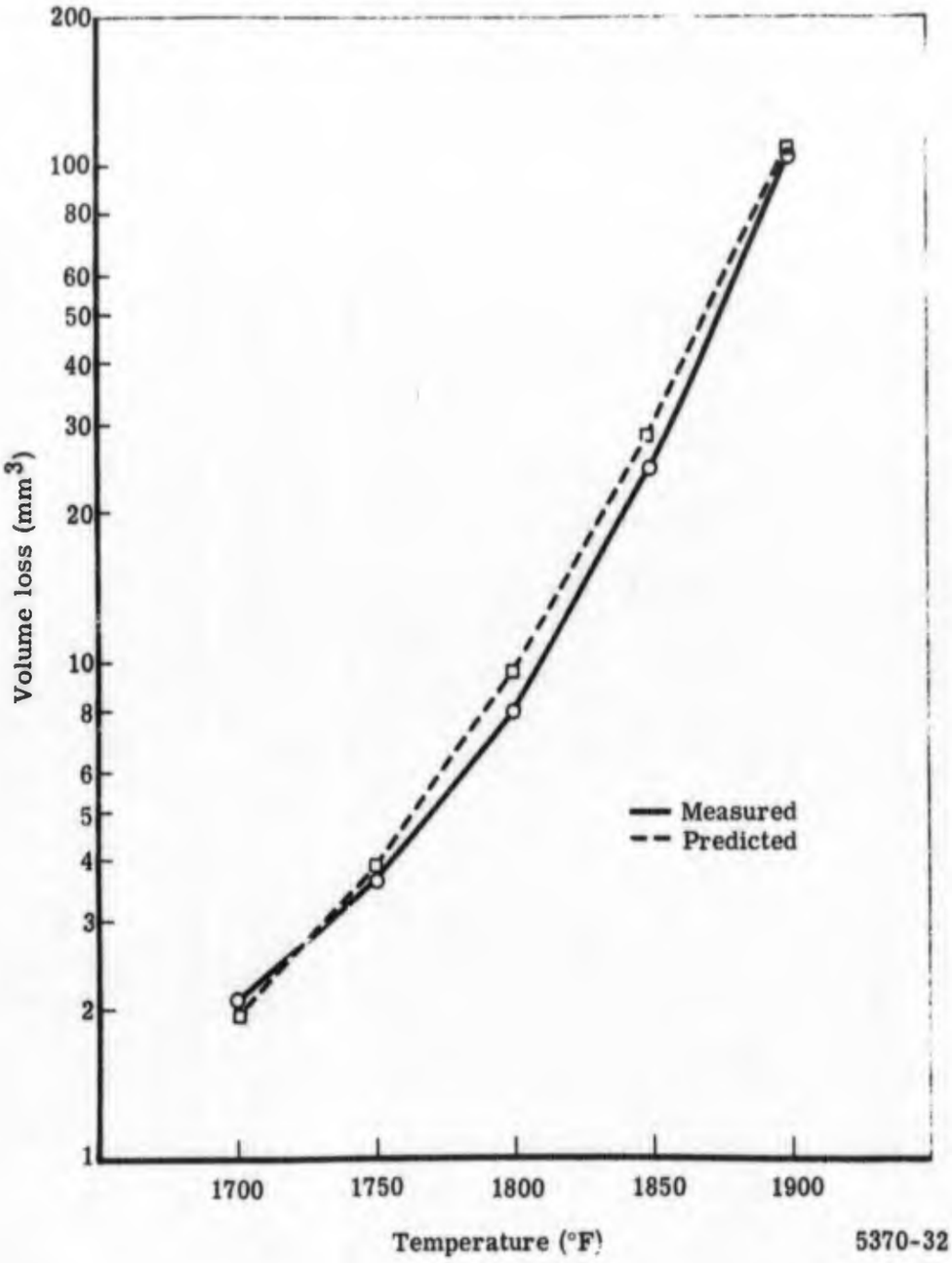

Figure 32. Comparison of the measured volume loss and the loss predicted by the regression equation for Alloy 713C.

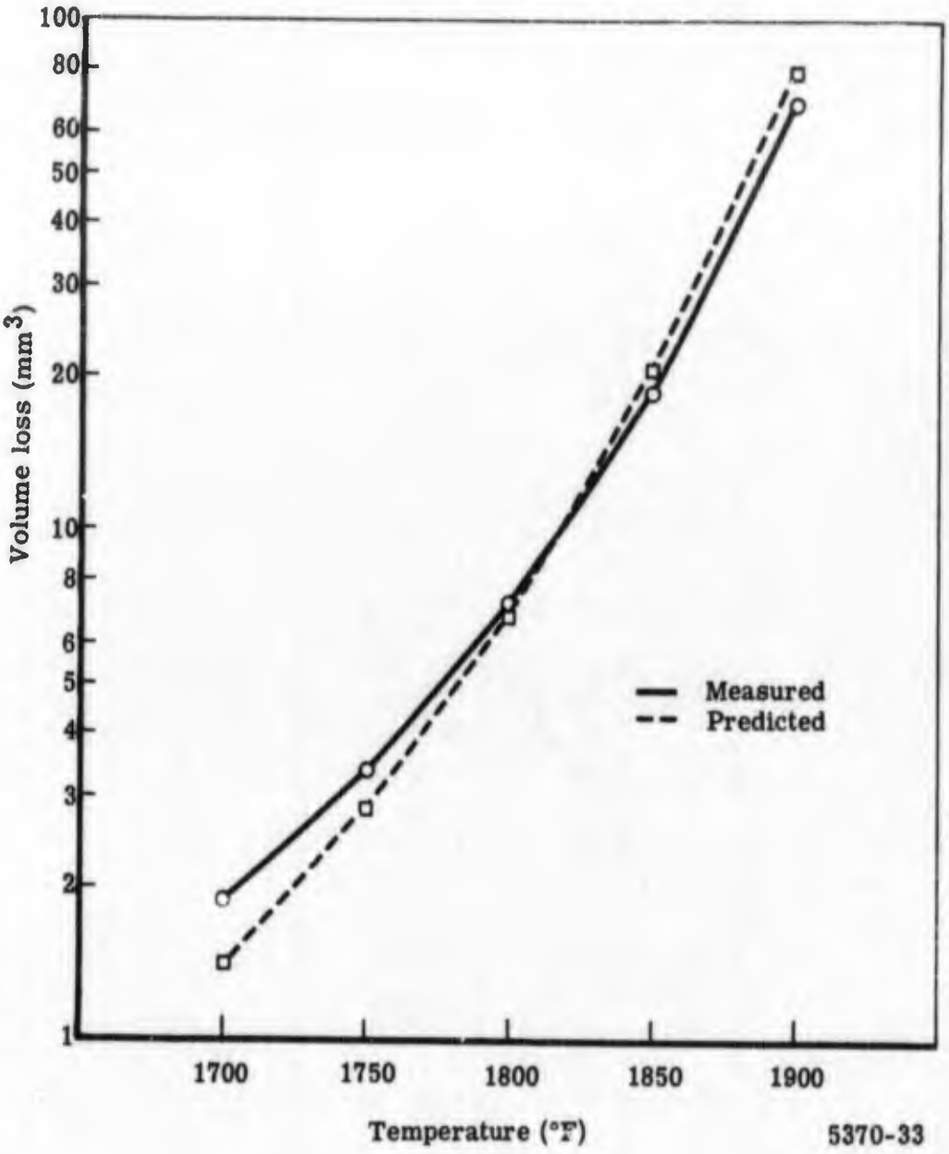

Figure 33. Comparison of the measured volume loss and the loss predicted by the regression equation for Alloy 713C + 2% Cr.

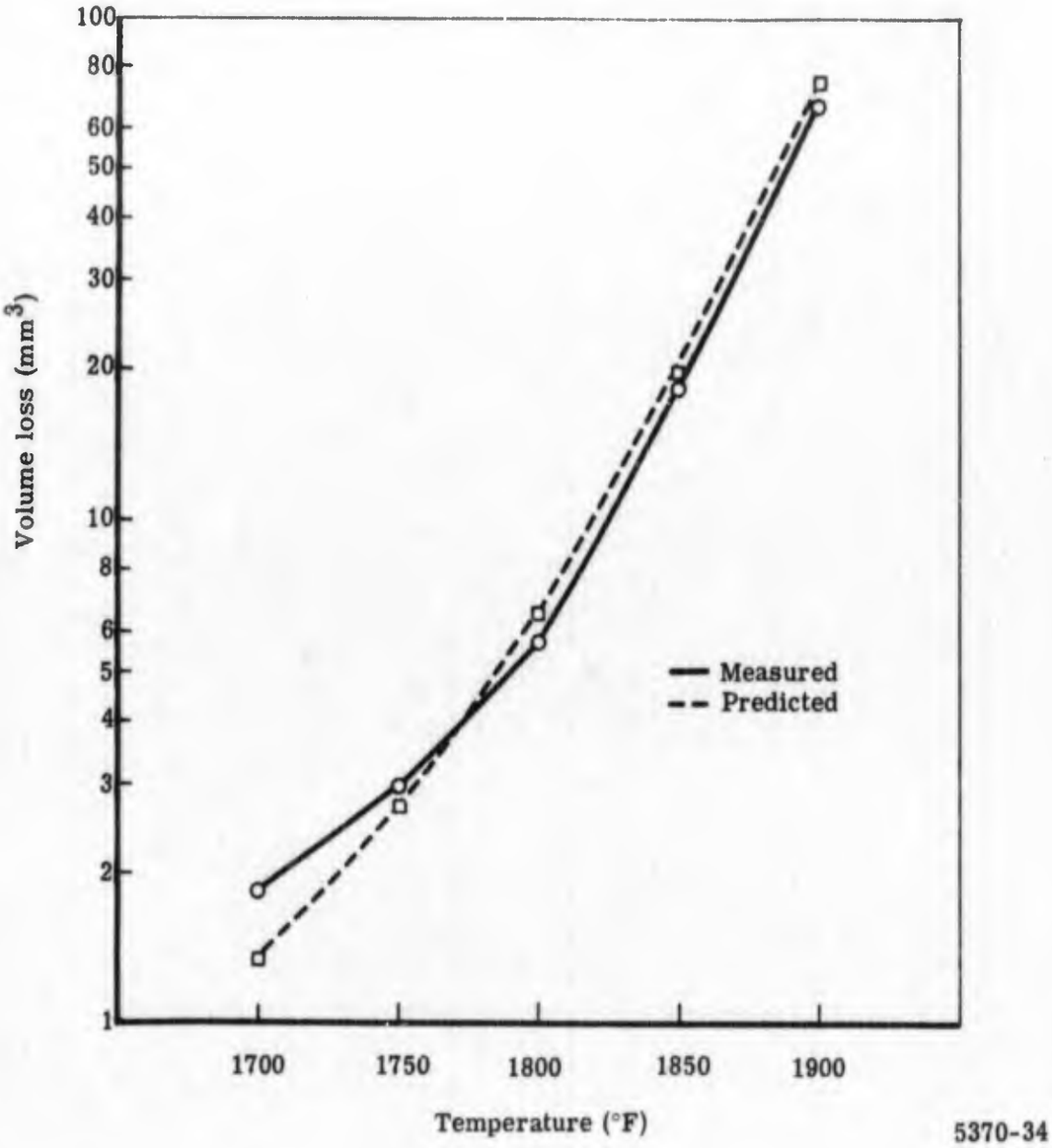

Figure 34. Comparison of the measured volume loss and the loss predicted by the regression equation for Alloy 713C + 2% Cr + Y.

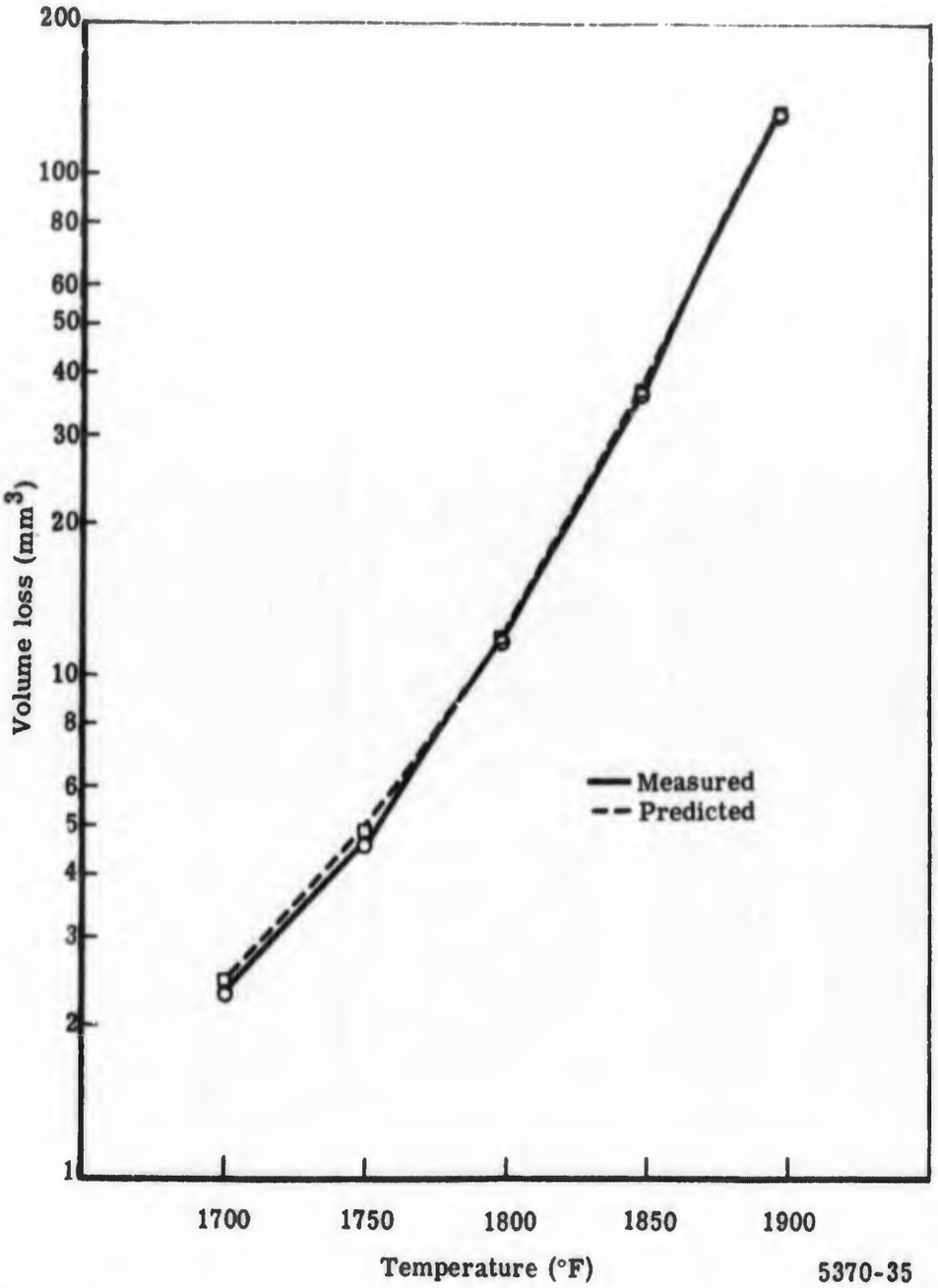

Figure 35. Comparison of the measured volume loss and the loss predicted by the regression equation for IN-100.

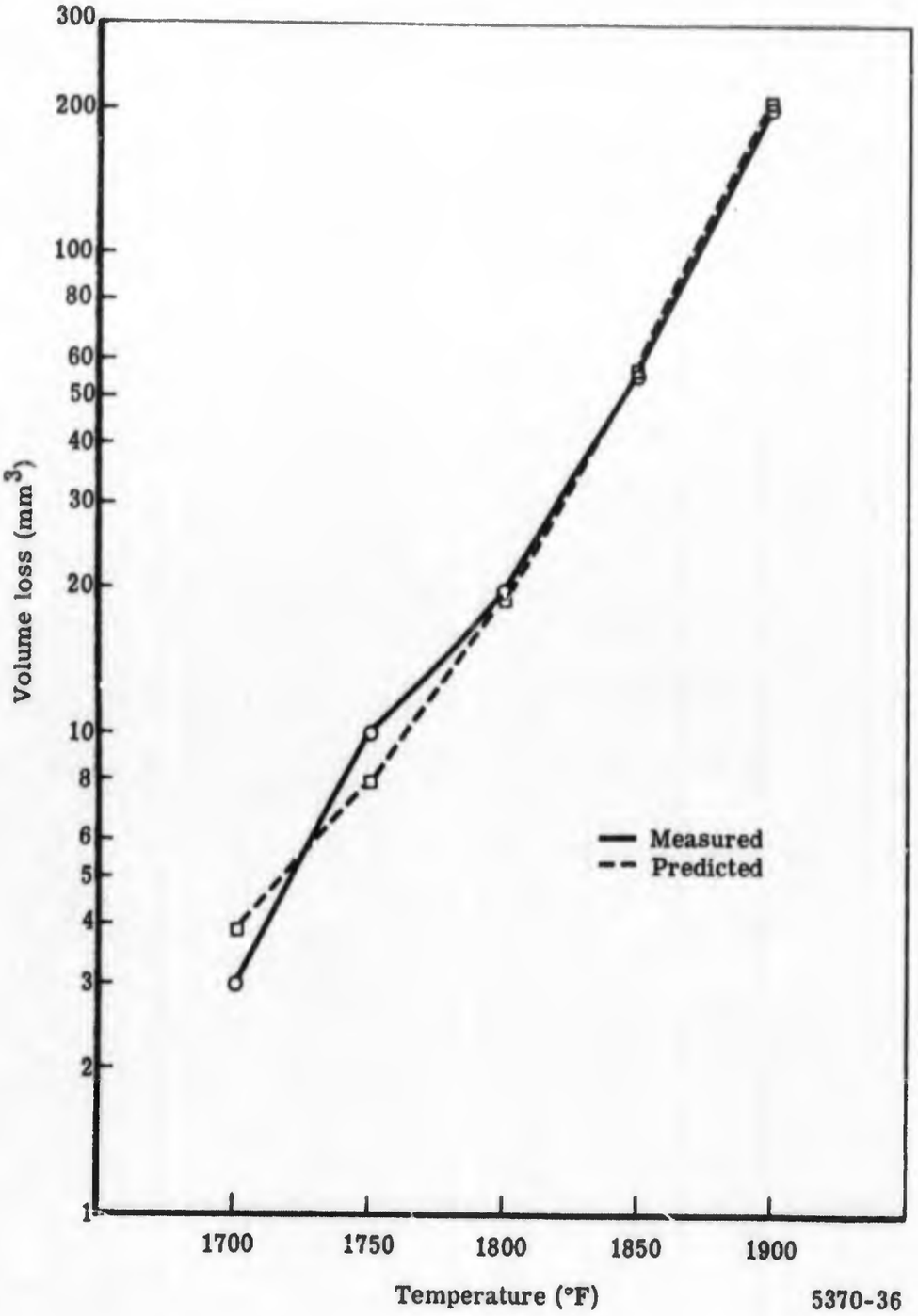

Figure 36. Comparison of the measured volume loss and the loss predicted by the regression equation for GMR-235.

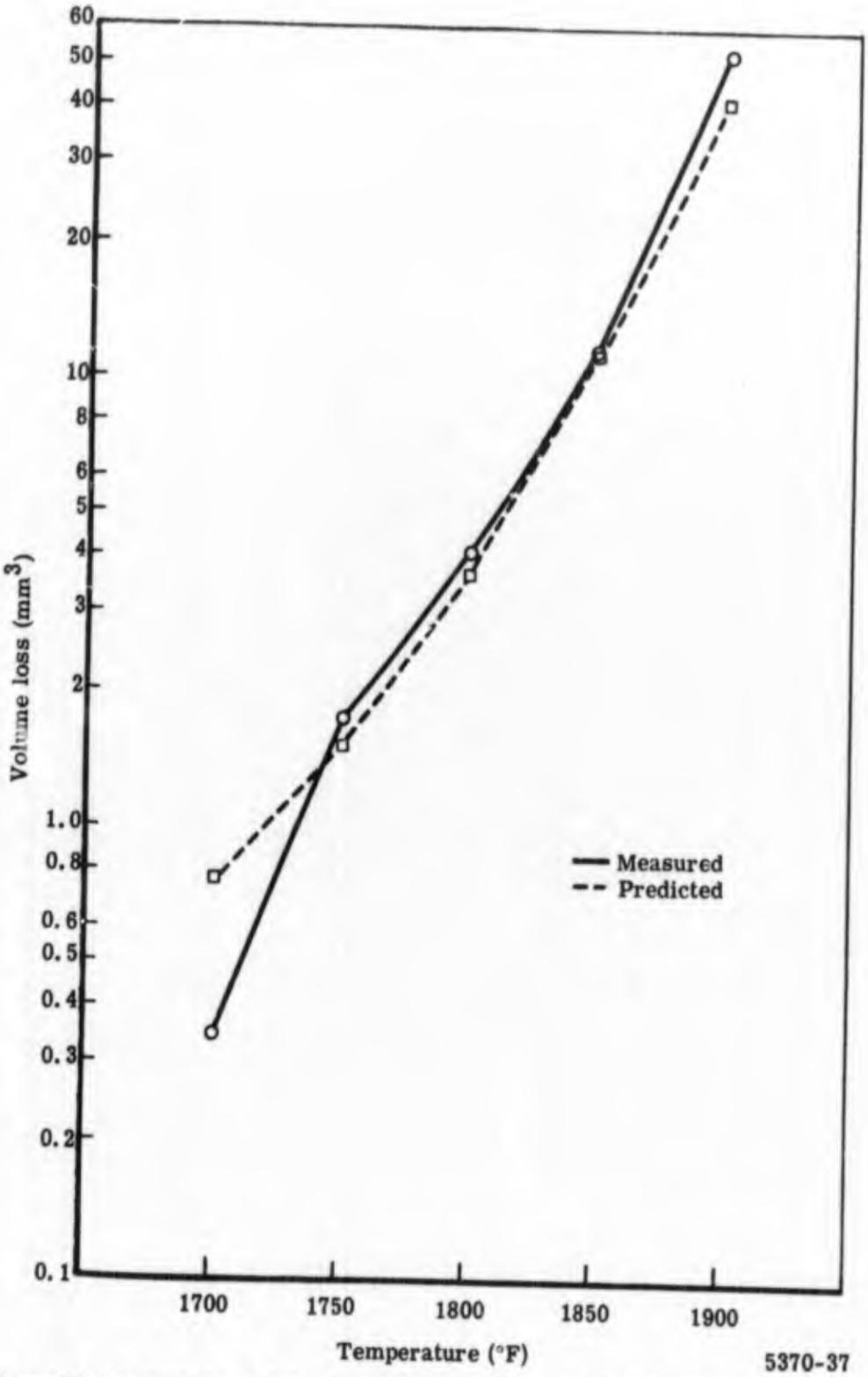

Figure 37. Comparison of the measured volume loss and the loss predicted by the regression equation for PDRL 163.

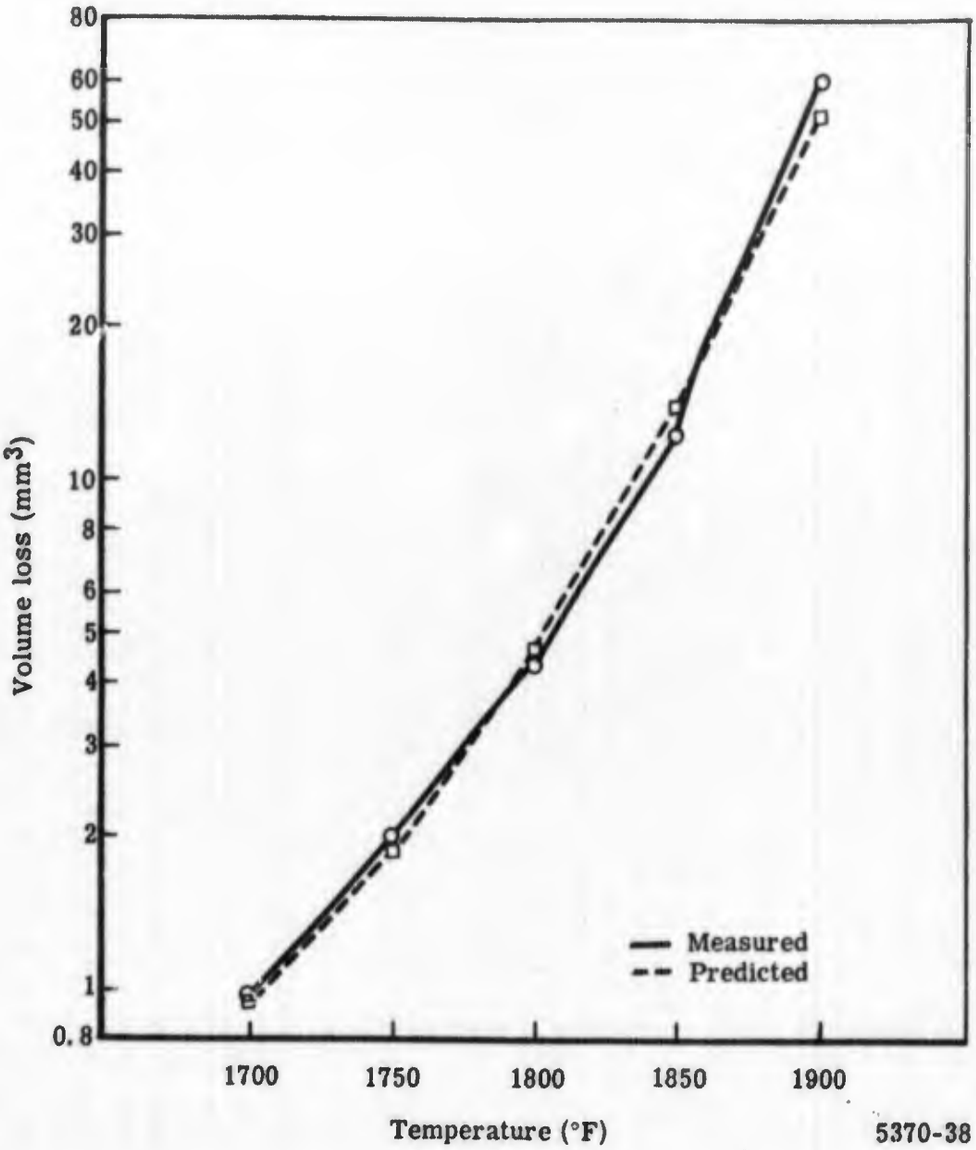

Figure 38. Comparison of the measured volume loss and the loss predicted by the regression equation for IN-728 NX.

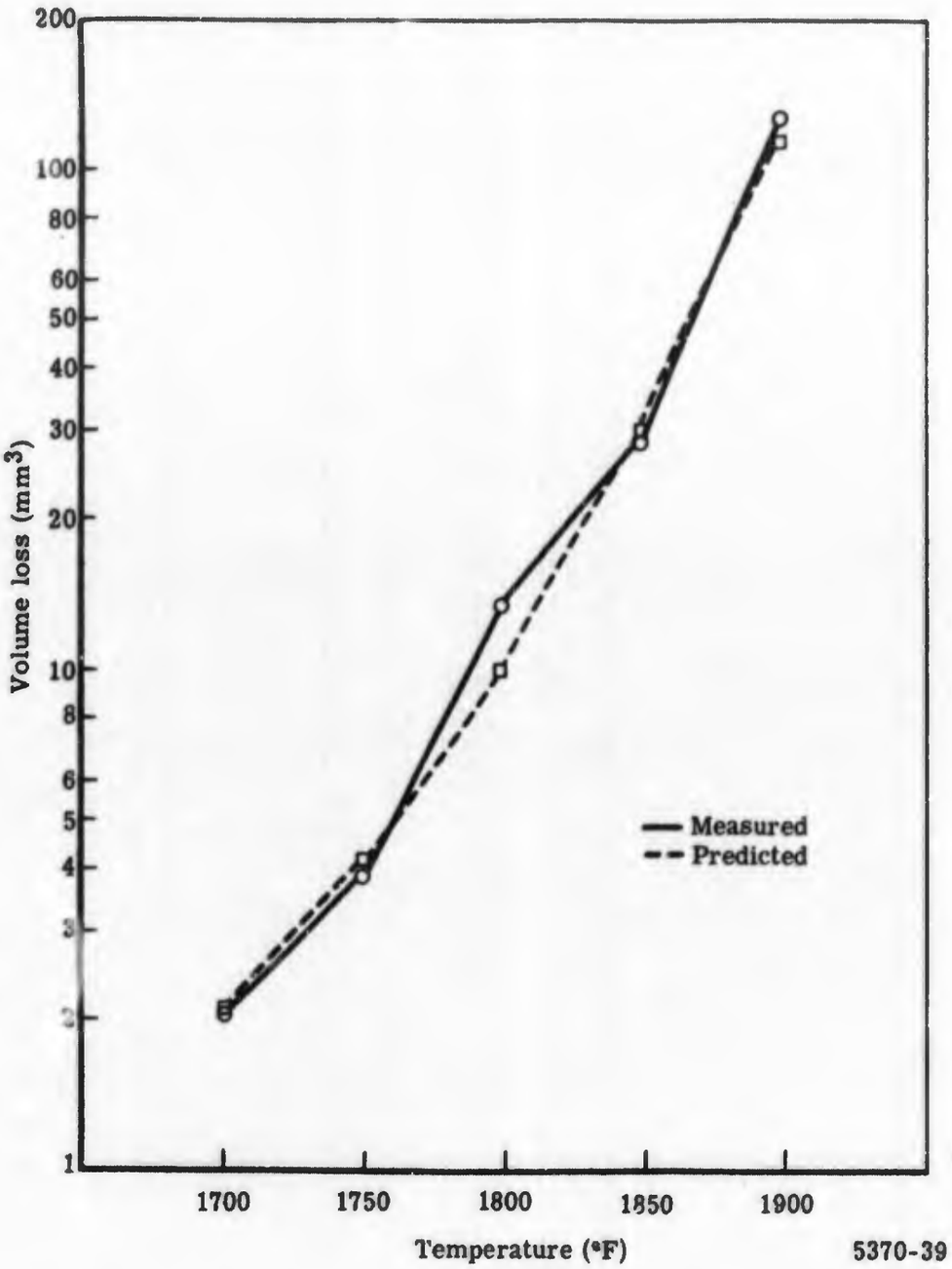

Figure 39. Comparison of the measured volume loss and the loss predicted by the regression equation for Mar-M421.

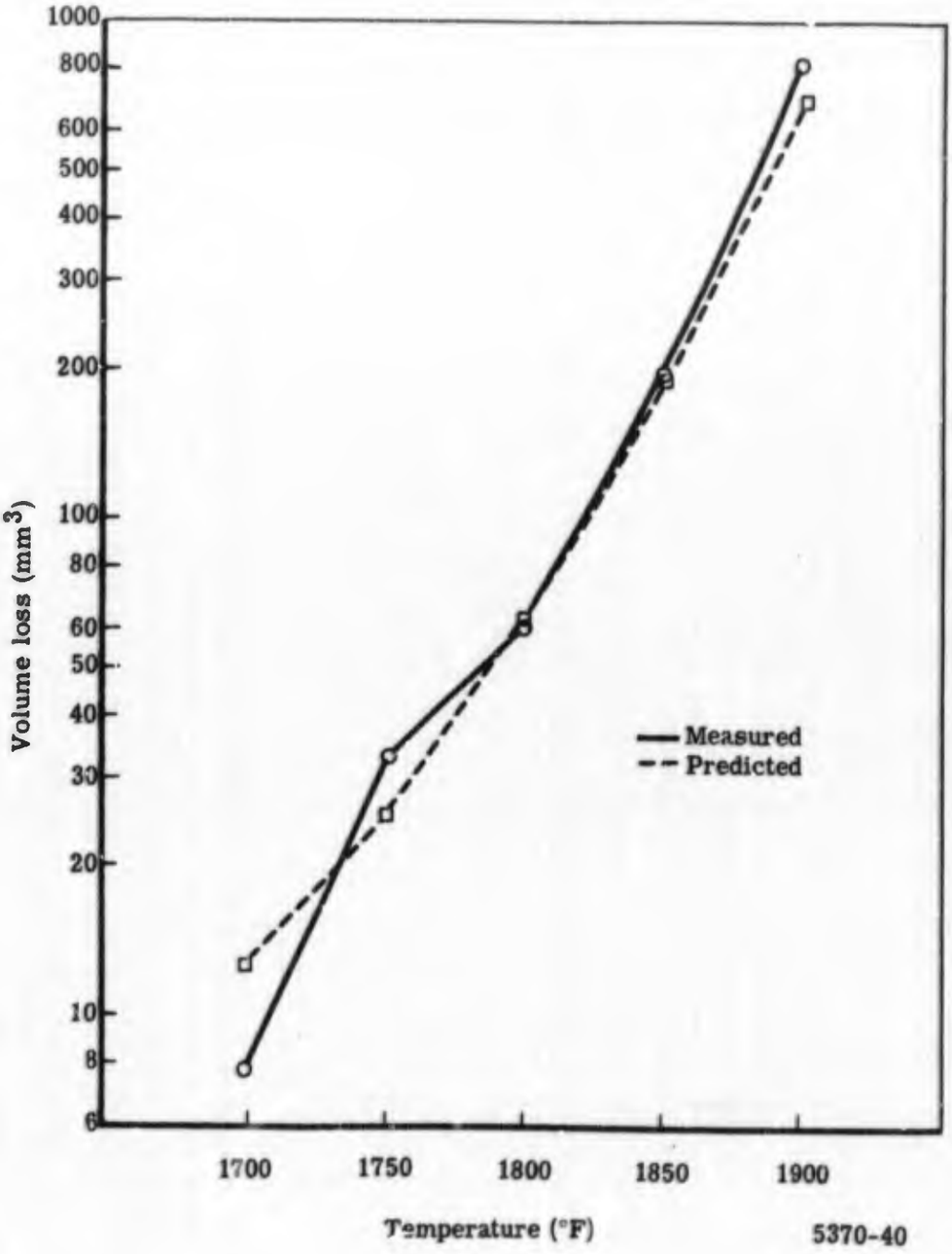

Figure 40. Comparison of the measured volume loss and the loss predicted by the regression equation for Mar-M246.

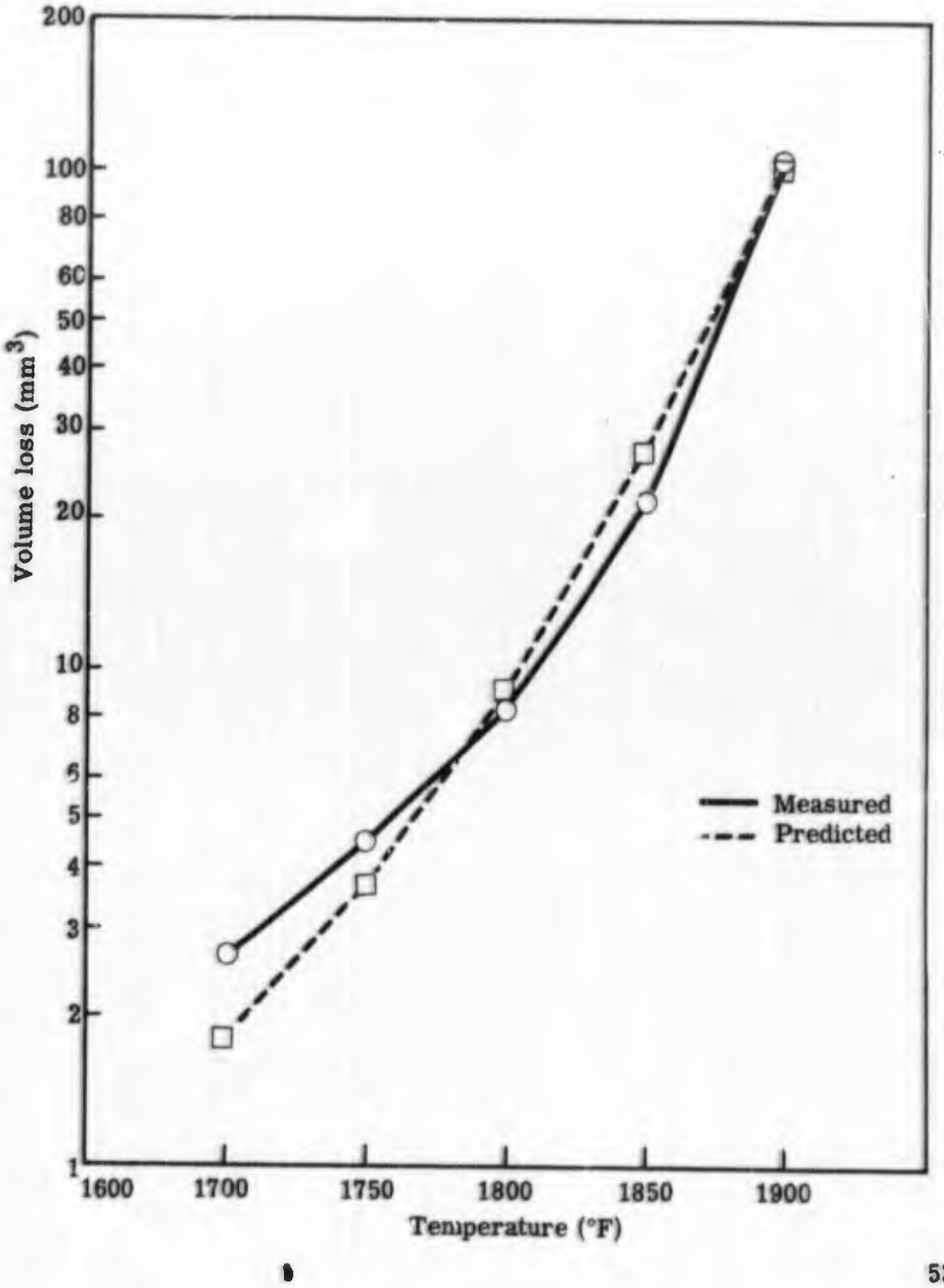

Figure 41. Comparison of the measured volume loss and the loss predicted by the regression equation for Inco 717.

BLANK PAGE

SECTION VI

MICROSTRUCTURAL EXAMINATION

D'-D' airfoil sections from the 1700, 1800, 1900, and 2000°F cyclic tests were examined with the light microscope. Selected samples were given electron microscope and electron microprobe examinations.

LIGHT AND ELECTRON MICROSCOPE EXAMINATION

The corrosion areas were divided into three general zones:

1. An outer layer of continuous oxide on the surface which gradually graded into an area of mixed metal and oxide

2. A layer of depleted metal

3. Globular sulfide particles. These generally formed a line between the depleted zone and matrix but occasionally a selective grain boundary attack preceded the frontal row of sulfides. In heavily corroded regions, sulfide particles extended throughout the depletion zone. The type of corrosion observed was the same whether the alloys were as cast or in the heat treated condition.

Figures 42 and 43 show typical corrosion zones on Alloy 713C after 1900 and 2000°F testing and Inco 717 after the 1900°F cyclic test.

ELECTRON MICROPROBE EXAMINATION

Electron microprobe traverses were run across typical corrosion areas on the following as-cast alloys.

Alloy	Cyclic test temperature (°F)
Alloy 713C	1800, 1900
Alloy 713C (modified Cr)	1800
Alloy 717	1800
GMR-235	1800

Two temperatures were selected for Alloy 713C to investigate the effect of higher test temperature on the type of corrosion. The modified chromium (16%) version of Alloy

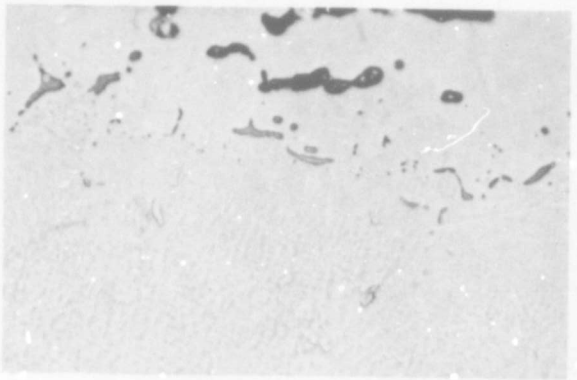

Cyclic Test Temperature = 1900°F

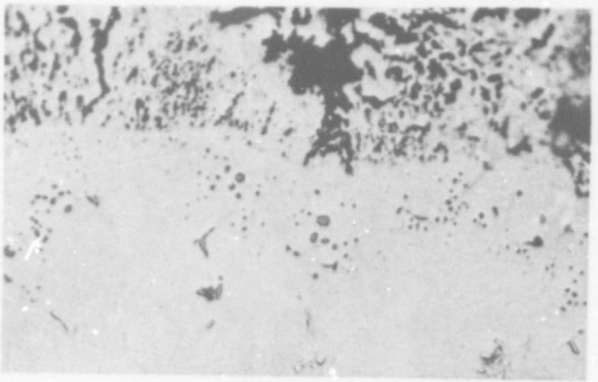

Cyclic Test Temperature = 2000°F

Magn 1000X

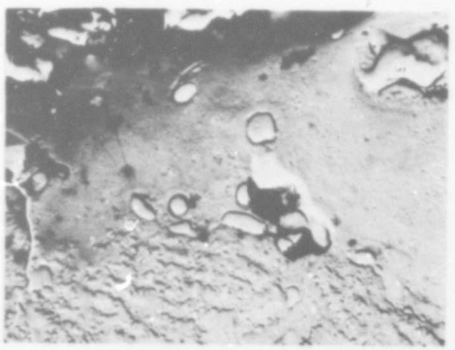

Cyclic Test Temperature = 1900°F

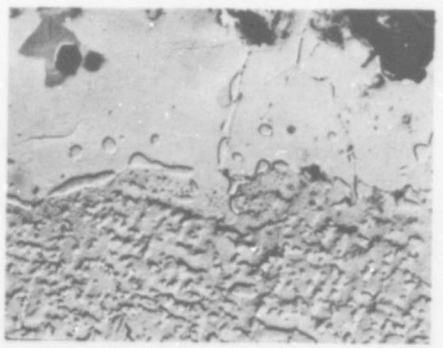

Cyclic Test Temperature = 1900°F

Magn 2500X

Figure 42. Light and electron micrographs of corrosion on Alloy 713C after 1900 and 2000°F cyclic tests.

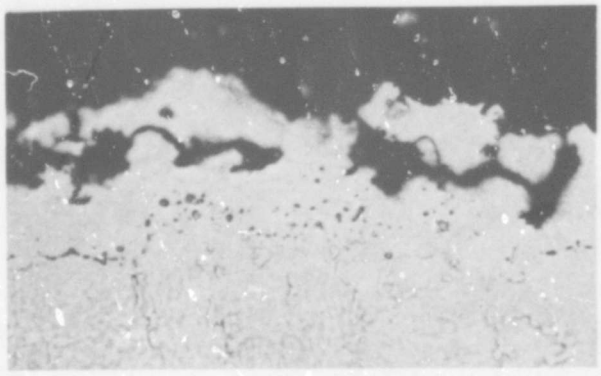

Magn 1000X

Magn 2500X

Figure 43. Light and electron micrograph of corrosion on Inco 717 after 1900°F cyclic test.

713C was chosen for comparison with standard 14% chromium Alloy 713C since it exhibited hot corrosion resistance superior to the base alloy. Alloy 717 (12% Cr) showed less susceptibility to hot corrosion than did GMR-235 (15.3% Cr). These alloys were selected to investigate which elements of composition modified the effects of their chromium contents in the manner observed experimentally. Figures 44 through 48 are light micrographs indicating the trace of the electron microprobe across the corrosion areas. Data listed with the photographs give the relative chemical compositions at or between points referenced on the photographs. The approximate weight percents are given for nickel, chromium, aluminum, and molybdenum. These were determined from the matrix composition. Relative X-ray intensity is given for titanium, niobium, and sulfur. The relative concentration or depletion of these elements can be determined by comparing the intensity at any location to the intensity in the matrix.

Oxide Zone

All elements present in the matrix were found in varying degrees in the oxide zone. As would be expected, nickel had the highest concentration, followed by aluminum and chromium with lesser amounts of the other elements. Sulfur was present in greater amounts than the traces present in the matrix compositions; however, no high concentrations of sulfur were observed.

Depletion Zone

The depletion zones of the alloys examined were depleted in chromium with a high percentage of nickel remaining. There were several variations in the chemistry of the depletion zones which could have influenced corrosion resistance. Alloy 713C at the two test temperatures and the modified version showed relatively low aluminum and high molybdenum. Regression analysis has indicated that aluminum was beneficial and molybdenum harmful to hot corrosion resistance. GMR-235 also showed very high molybdenum and low aluminum. The depletion zone of this alloy contained a high iron content which may have contributed to its relatively poor corrosion resistance. Inco 717 had relatively lower molybdenum and higher aluminum than the Alloy 713 versions or GMR-235. Inco 717 also had a high percentage of cobalt in its depletion zone. In general, for the four alloys, the percentage of nickel was increased; molybdenum, cobalt, and iron were present in the same percentages as in the matrix; aluminum, niobium, and titanium were partially depleted; and chromium was severely depleted. Sulfur was present in quantities only slightly greater than the trace amounts in the matrix. No differences in depletion zone chemistry were detected between the Alloy 713C and the modified version or between the Alloy 713C tested at two temperatures.

Magn. 500X Etchant: ferric chloride No. 2

Microprobe traverse on Alloy 713C—1800°F cyclic test.

Location on traverse	Relative composition					
	Oxide → α	Depletion zone α→β→γ	Sulfide γ	Depletion zone sulfides γ→θ	Matrix interface θ	Matrix
Element						
Nickel*	51-81	78-92	28	65-91	72	72
Chromium*	1-6	1	29	1-12	12	13.2
Sulfur**	2-5	1-4	93	2-23	1	1
Aluminum*	9-26	2 (β 14)	2	2-3	4.5	6.3
Molybdenum*	4 1/2-6	2 1/2-4	2 1/2	2 1/2-3	4	4.7
Niobium**	3-7	2-3	4	3	4	5
Titanium**	1-7	1	1 1/2	1/2	2	2 1/2

*Approximate weight percent

**X-ray intensity—compare with matrix

Figure 44. Microprobe traverse across corrosion area of Alloy 713C after 1800°F cyclic test.

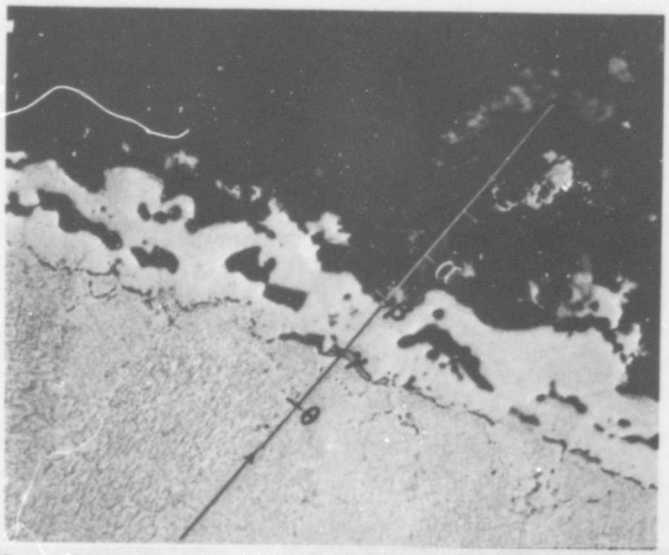

Magn 500X Etchant: ferric chloride No. 2

Microprobe traverse on Alloy 713C—1900°F cyclic test.

Location on traverse	Relative composition: Oxide α	Depletion zone β→γ	Sulfide γ	Interface γ→	Matrix
Element					
Nickel*	30-60	86-88	22	72	72
Chromium*	4-18	1-2	27	12	13.2
Sulfur**	2-15	2-3	77	1 1/2	1 1/2
Aluminum*	5-32	2-3	2	6	6.3
Molybdenum*	1 1/2	4-5	3 1/2	4 1/2	4.7
Niobium**	1-3	-	1 1/2	1 1/2	1 1/2
Titanium**	2-10	1-2	8	5	5

* Approximate weight percent

** X-ray intensity—compare with matrix

Figure 45. Microprobe traverse across corrosion area of Alloy 713C after 1900°F cyclic test.

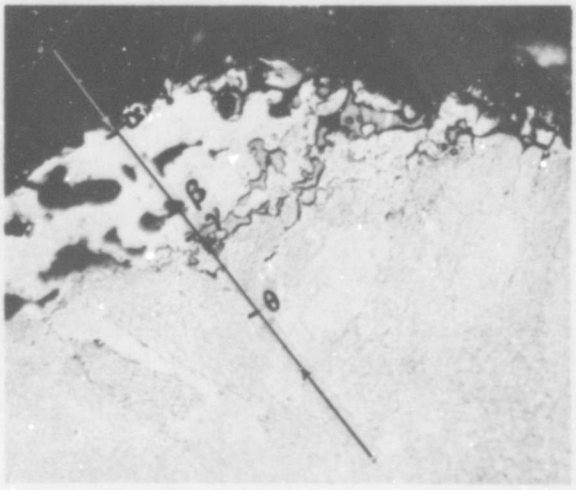

Magn. 500X Etchant: ferric chloride No. 2

Microprobe traverse on modified chromium alloy 713C.

Location on traverse	Oxide → α	Depletion zone α→β	Oxide β	Depletion zone β→	Sulfide γ	Matrix θ
Element	Relative Composition					
Nickel*	20-45	84-87	59	68-86	35	70
Sulfur**	2 1/2-4	2-4	2	2	80	2
Titanium**	20-40	3-4	3	2 1/2	10	12 1/2
Chromium*	7-16	1 1/2-2	1 1/2	1 1/2-2	23	15.7
Molybdenum*	2	4-7	4	3-4	4	4.7
Niobium**	2-11	2-2 1/2	2	2-3	3	4
Aluminum*	10-35	2	8	3	2 1/2	5.9

*Approximate weight percent

**X-ray intensity—compare with matrix

Figure 46. Microprobe traverse across corrosion area of Alloy 713C + 2% Cr after 1800°F cyclic test.

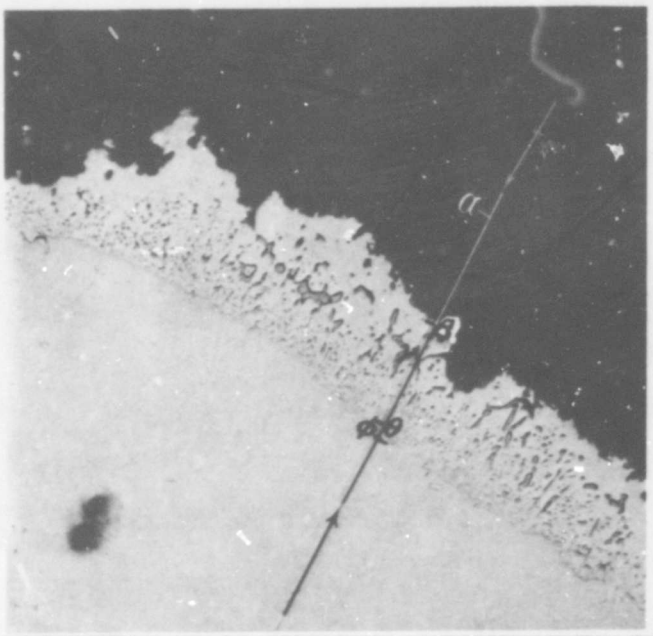

Magn 500X Etchant: ferric chloride No. 2

Microprobe traverse on Inco 717—1800°F cyclic test.

Location on traverse	Relative composition: Oxide scale $\alpha \rightarrow \beta$	Depletion zone $\beta \rightarrow \gamma$	Sulfide γ	Depletion zone sulfides, γ - θ	Matrix Interface θ	Matrix
Element						
Nickel*	25-48	76-87	71	73-84	66	66
Cobalt*	3-12	7-11	8	8-9	10 1/2	10.5
Aluminum*	7-16	4-5	4	4 1/2-5	6	7.1
Sulfur**	8-15	16-21	76	25-77	10	10
Chromium*	4-8	2	6	3-3 1/2	12	12.0
Titanium**	16-65	3-5	6	4-12	18	20
Molybdenum*	1-1 1/2	2-4	4	3 1/2-4	3 1/2	4.2
Niobium**	3-15	2-3	2 1/2	2 1/2-7	5	5

*Approximate weight percent

**X-ray intensity—compare with matrix

Figure 47. Microprobe traverse across corrosion area of Alloy 717 after 1800°F cyclic test.

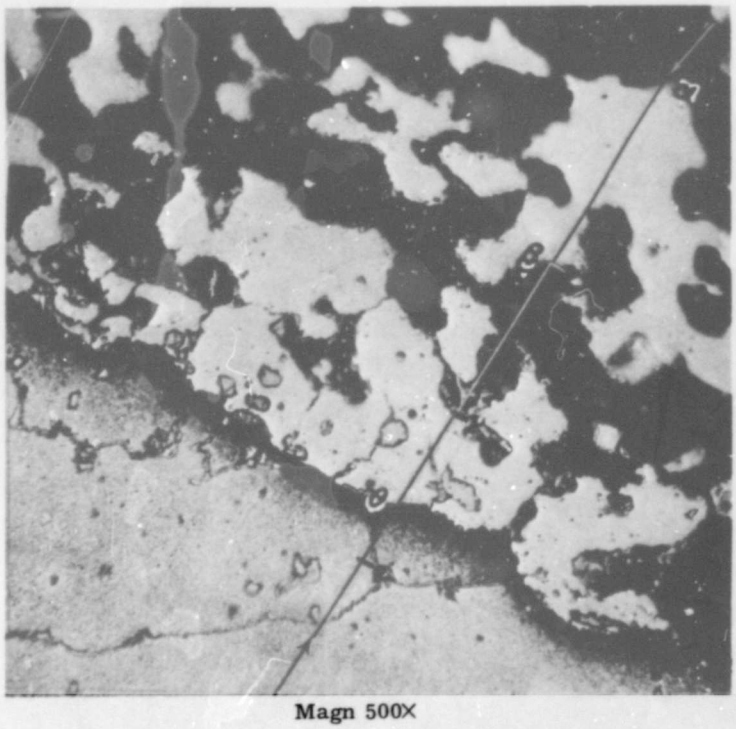

Magn 500X

Microprobe traverse on GMR-235—1800 °F cyclic test.

Location on traverse	Relative composition: Depletion zone $\alpha \rightarrow \beta$	Oxide, sulfides $\beta \rightarrow \gamma$	Sulfide γ	Depletion zone, γ - θ	Sulfide θ	Matrix
Element						
Iron*	10	3-11	3	8-10	8	10.4
Nickel	76-85	10-79	20	65-85	60	66
Sulfur**	2-3	3-59	45	1-2 (peak to 40)	62	1
Chromium*	1 1/2-2	3 1/2-18	10	1 1/2	15	15.3
Titanium	1-1 1/2	4-30	15	1/2	4	6
Aluminum*	2	2-17	17	2	2 1/2	2.6
Molybdenum*	6-8	3-14	33	6-8	8	6.2

*Approximate weight percent

**X-ray intensity—compare with matrix

Figure 48. Microprobe traverse across corrosion area of GMR-235 after 1800°F cyclic test.

Sulfide Particles

The globular particles were predominantly rich in chromium and sulfur. Nickel was apparently high in some particles; however, on the smaller sulfide particles, the electron beam was influenced by the adjacent nickel rich and chromium deficient alloy depletion zone. GMR-235 and Inco 717, in particular, showed this effect.

Matrix

The demarcation between the sulfide particles and the matrix and the depletion zone and the matrix was sharp. The matrix composition was relatively constant nearly to the edge of the corrosion interface.

SECTION VII

DISCUSSION OF RESULTS

The two principal methods of evaluation, volume loss (a measure of total corrosion) and corrosion area at airfoil section D'-D', were in substantial agreement. Hot corrosion severity increased at cyclic temperatures to 2000°F. On the 2000°F test, airfoil section D'-D' was above 1900°F for 61% of the heating time and experienced severe corrosion. The test rig creates a hot corrosion environment somewhat differently than the turbine engine since it does not employ all the engine operating parameters. Also, the sodium sulfate is sprayed on during the cooling cycle. The measure of the validity of the rig tests depends upon how well they simulate the hot corrosion behavior in the turbine engine. In this respect the rig has correlated well with Allison T56 engine tests with sea salt ingestion. These engine tests have shown severe hot corrosion attack at metal temperatures to 1850°F.

BLANK PAGE

SECTION VIII

CONCLUSIONS AND RECOMMENDATIONS

CONCLUSIONS

1. A regression equation was derived relating volume loss to alloy chemistry and showed chromium and aluminum to be beneficial to hot corrosion resistance, and tungsten and molybdenum to be detrimental to hot corrosion resistance.

2. Electron microprobe analysis indicated that hot corrosion resistance is related to the surface depletion zone chemistry of the corroded alloys. A high molybdenum content in this zone was detrimental and a high aluminum content beneficial to hot corrosion resistance.

3. Hot corrosion severity increased in approximately logarithmic fashion as the maximum cyclic temperature was increased from 1700 to 2000°F.

4. In order of decreasing hot corrosion resistance, the alloys ranked as follows: PDRL 163, IN728NX, Alloy 713C + 2% Cr + Y, Alloy 713C + 2% Cr, Inco 717, Alloy 713C, Mar-M421*, IN-100, GMR-235, and Mar-M246.

5. The two high chromium versions (+2% Cr) of Alloy 713C showed improvement over Alloy 713C at all test temperatures; however, the improvement was significant** only at 1800 and 1850°F.

6. Heat treatment had a detrimental effect on Mar-M246 and GMR-235 and no significant** effect on the other eight test alloys.

RECOMMENDATION FOR FUTURE WORK

Recent rig test programs have emphasized that when the turbine engine environment is to be directly simulated in a test rig, pressure should be included in the parameters. Tests

*The 14.6% chromium content for Mar-M421 was below the 15.0 to 16.0% chromium content recommended by Martin Metals Division of Martin Marietta Corporation.

**Statistically significant at $\alpha = 0.05$ (95% confidence level).

run at Lycoming[1] with an unpressurized hot corrosion rig indicated that hot corrosion decreased in severity above a certain temperature and terminated above 1700 to 1750°F. Phillips Petroleum[2], while rig testing at a combustor inlet pressure of 15 atmospheres, reported that in the high temperature range (1800 to 2200°F) increasing temperature always increased weight loss whenever the effect was significant. These tests also point out that high temperature (1700°F or greater) hot corrosion severity may vary from engine to engine depending on the operating parameters.

Rig and engine testing at Allison and elsewhere has shown that it is essential, when simulating hot corrosion behavior of turbine materials, that all major engine parameters be included in the test rig environment; consequently, it is recommended that programs conducted to study turbine alloy hot corrosion response include varying conditions of temperature and pressure as well as sea salt ingestion.

---

[1] Wheaton, H. L., Study of the Hot Corrosion of Superalloys, Quarterly Progress Report No. 2, Contract No. AF33(615)-5212. January 1967

[2] Schirmer, R. M. and Quigg, H. T., Effect of JP-5 Sulfur Content on Hot Corrosion of Superalloys in Marine Environment, Sixty-Ninth Annual Meeting of the American Society for Testing and Materials, Atlantic City, June 1966

APPENDIX

DISCUSSION OF THE REGRESSION ANALYSIS

MATHEMATICAL MODEL USED IN THE ANALYSIS

It was assumed that the following model characterized the hot corrosion test data:

$$Y = A_o + A_1X_1 + \ldots + A_{20}X_{20} + \epsilon$$

where

- The dependent variable, Y, is $\log_{10}$ volume loss. The mean of the four measured volume losses at a particular test condition was entered as the value for volume loss in the analysis. The mean volume losses are recorded in Table XXI.
- The independent variables, X_1, X_2, X_{19}, and X_{20} are expressions of temperature. See Table XXII. Temperature was included in the model since volume loss was significantly affected by changes in temperature.
- The independent variables, $X_3, \ldots, X_{18}$, are the weight percents of the 16 elements in the alloy compositions. These are identified, along with the percent of each in the individual alloys, in Table XXIII. The tabled value is the mean of the percents found by chemical analysis of the test specimens.
- The A_i's are constants calculated by the computer program. See Selection of the Independent Variables subsection which follows for the discussion of these constants.
- The presence of ϵ in the model indicates that the measurement of Y is not exactly repeatable even if the X_i's are constant. The variability of ϵ is called the "standard error of the estimate of Y" and is interpreted later.

A data point for the analysis, in accordance with the assumed model, is denoted by ($Y, X_1, \ldots, X_{20}$) where Y is $\log_{10}$ volume loss for a particular alloy, identified by $X_3, \ldots, X_{18}$ at some known temperature. All ten alloys were included in the analysis to obtain one regression equation applicable to all of the alloys. This also permits a wider range of weight percents for the elements to be considered.

SELECTION OF THE INDEPENDENT VARIABLES

Once the data are submitted, the program is written to select the smallest set of X_i's which will contribute significantly to the prediction of the response in Y. The confidence desired for a variable that is entered or removed from the model can be set at any level.

Table XXI.
Volume loss* (mm^3).

Condition	713C	713C + Cr	713C + Cr + Y	IN-100	GMR-235	PDRL 163	IN-728 NX	Mar-M421	Mar-M246	Inco 717
1700°F - AC**	2.07	1.89	1.83	2.32	3.04	0.34	0.95	2.07	7.67	2.68
1750°F - AC	3.62	3.33	2.91	4.60	10.19	1.74	1.92	3.94	32.46	4.46
1800°F - AC	7.92	7.08	5.69	11.84	19.93	4.07	4.37	13.96	61.63	8.25
1850°F - AC	24.73	18.45	18.48	37.69	58.58	11.46	12.19	29.57	198.9	21.53
1900°F - AC	105.2	68.46	66.01	135.0	209.9	53.5	60.08	131.0	843.4	106.3
1700°F - HT†	2.56	2.06	2.17	2.36	6.65	0.50	1.28	2.04	16.09	2.66
1750°F - HT	4.46	4.04	3.59	4.31	13.46	1.25	2.09	2.65	55.72	4.29
1800°F - HT	10.84	6.96	6.30	8.73	30.20	3.54	4.24	8.47	118.9	6.85
1850°F - HT	30.92	20.68	19.71	26.5	80.02	12.93	14.86	27.36	353.9	21.87
1900°F - HT	86.89	68.63	72.14	122.1	436.2	67.65	83.05	222.9	2120.0	87.89

*The table value is the average of the four adjusted measured volume losses recorded in the experiment.
**AC = as-cast.
†HT = heat treated.

Table XXII.
Expressions of temperature.

Variable						
X_1	= Log_{10} (temperature)	3.23045	3.24304	3.25527	3.26717	3.27875
X_2	= temperature, °F	1700	1750	1800	1850	1900
X_{19}	= (temperature)^2, °F	2.89×10^6	3.06×10^6	3.24×10^6	3.42×10^6	3.61×10^6
X_{20}	= (temperature)^3, °F	4.913×10^9	5.355×10^9	5.832×10^9	6.332×10^9	6.859×10^9

Table XXIII.

Alloy compositions—weight percent.*

Variable	713C	713C + Cr	713C + Cr + Y	IN-100	GMR-235	PDRL 163	IN-728 NX	Mar-M421	Mar-M246	Inco 717	Mean Value
X_3 = C	0.13	0.11	0.14	0.16	0.155	0.0675	0.0675	0.14	0.13	0.115	0.1215
X_4 = Cr	13.23	15.72	15.70	10.125	15.365	16.75	16.18	14.725	8.91	12.08	13.8785
X_5 = W						1.945	1.915	3.57	9.985		1.7415
X_6 = Co				14.93			9.557	10.28	10.55	10.60	
X_7 = Ni	72.3805	70.344	69.9435	59.3125	63.4354	69.8309	59.384	61.672	58.547	61.738	
X_8 = Ti	0.79	0.80	0.85	5.21	1.92		0.4975	1.605	1.32	1.065	
X_9 = Al	6.37	5.95	6.26	6.08	2.61	6.515	6.3275	4.45	5.61	7.12	5.7292
X_{10} = Cb	2.17	2.11	1.79			1.375	1.40	1.85		2.82	
X_{11} = Mo	4.70	4.62	4.62	3.11	6.13	1.45	1.92	1.66	2.66	4.295	3.5165
X_{12} = Fe	0.11	0.24	0.21		10.16						
X_{13} = Zr	0.105	0.096	0.097	0.04		0.130	0.20	0.04	0.038	0.15	
X_{14} = B	0.0145	0.01	0.0095	0.0125	0.0346	0.0166	0.019	0.008	0.015	0.017	
X_{15} = Y			0.38								
X_{16} = V				0.102							
X_{17} = Mn					0.19						
X_{18} = Ta						1.92	2.5325		2.235		

*Table values are the average of the weight percents determined by chemical analysis of the test specimens.

A high confidence level, say 99%, will minimize the risk of selecting a variable erroneously but will result in a higher probability of ignoring an important variable than if some lower level were chosen. The confidence level chosen for this analysis was such that there are three chances out of ten that a variable is entered or removed erroneously. This 70% confidence level reduces the probability of missing a significant variable by permitting the selection of a larger number of variables.

Each time a variable is entered or removed, the regression coefficients (A_i's), the standard error of the coefficients (σA_i's), the standard error of the estimate (σ_ϵ), and the multiple correlation coefficient (explained in the following subsection of this report) are computed for the variables in the regression equation. To determine which variables selected by the computer are important in predicting Y, the significance of each A_i is tested by use of the t-test. The test statistic $t = \frac{A_i - 0}{\sigma A_i}$ is calculated for every A_i and compared with the table value of t at some α. If the calculated statistic is greater than the table value, it is 100 $(1 - \alpha)$ percent certain that A_i is significantly different from zero. This is synonymous to saying it is 100 $(1 - \alpha)$ percent certain that X_i belongs in the regression equation. If the statistic is less than the table value, it is 100 $(1 - \alpha)$ percent confident that A_i is not significantly different from zero and that X_i was entered erroneously. This same technique is used to test the significance of a variable which is removed.

INTERPRETATION OF σ_ϵ (STANDARD ERROR OF ESTIMATE)

The standard error of the estimate, σ_ϵ, gives a measure of the variability of the response in Y about the estimate. Prior to the selection of any X_i's, Y is estimated by $\bar{Y}$ and σ_ϵ is simply $\sum_{i=1}^{h} (Y_i - \bar{Y})^2/df$ where the degrees of freedom (df) is n-1, n being the number of responses of Y.

When the X_i's are used to predict Y, the estimate becomes the regression equation $Y = A_0 + A_1X_1 + \ldots + A_pX_p$ where p is the number of X_i's in the regression. The degrees of freedom of σ_ϵ is now n-p-1. Each time a new variable is entered, σ_ϵ is generally reduced because the new variable helps predict the response in Y. The amount of the reduction is equal to the variation explained by the new variable.

MULTIPLE CORRELATION COEFFICIENT, R

The multiple correlation coefficient measures the overall extent of association between values of the independent variables and the corresponding dependent variable. The coefficient is defined as

$$R = 1 - \frac{SS_R}{SS_T}$$

where

SS_R is the residual sum of squares of the response in Y about the regression line.

$$SS_R = \sum_{i=1}^{n} (Y_i - \hat{Y})^2.$$

SS_T is the total sum of squares of the response in Y about the mean of Y. $SS_T = \sum_{i=1}^{n} (Y_i - \bar{Y})^2$.

If no association between the X_i's and Y is defined, then $\hat{Y}$ is just $\bar{Y}$ and SS_R is equal to SS_T. This would result in a multiple correlation coefficient of zero. This situation is illustrated graphically in Figure 49a for one X_i.

If $\hat{Y} = A_o + A_i X_i$ is then assumed to define an association between X_i and Y, then SS_R is reduced giving a value of R greater than zero. Assuming SS_R is 7/16 of SS_T, then R is equal to $\sqrt{9/16}$ or 0.75. See Figure 49b. Note that if X_i exactly predicts Y, then SS_R is equal to zero giving F as one.

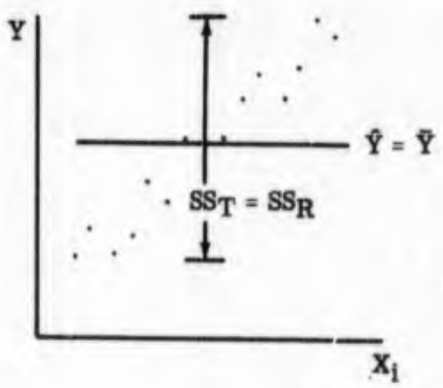

a

5370-49

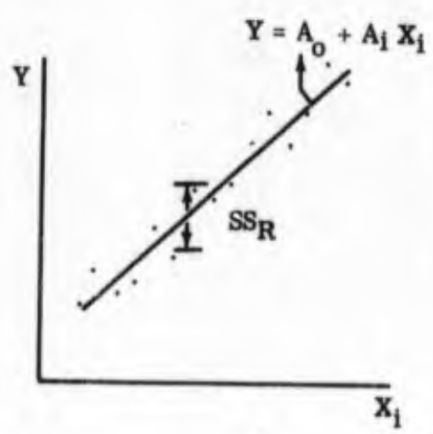

b

5370-50

Figure 49. Graphs illustrating multiple correlation coefficients of zero and approximately 0.75.

RESULTS

The independent variables in the regression were entered and removed from the model with only 70% confidence. It is necessary to test the significance of each variable by testing the significance of each A_i from zero. The α level used is 0.05. See Table XXIV.

Table XXIV.
Results of regression analysis.

Variable	Regression coefficient (A_i)	Standard error of coefficient (σA_i)	Computed t—value
X_4 = Cr	-0.0677702	0.0068359	9.914*
X_5 = W	0.0632837	0.0069669	9.083*
X_9 = Al	-0.0898200	0.0131055	6.854*
X_{11} = Mo	0.0863834	0.0126837	6.811*
X_{19} = (temperature)^2	-1.3386×10^{-5}	3.33847×10^{-6}	4.010*
X_{20} = (temperature)^3	5.85238×10^{-9}	1.23488×10^{-9}	4.739*
Constant	11.2807		

$$t_{computed} = \left| \frac{A_i}{\sigma A_i} \right|$$

$$t_{table} = \left| t_{0.05/2,\ 43} \right| = 2.017$$

*Denotes significance at $\alpha = 0.05$.

Thus, it is 95% certain that each of the independent variables are significant in predicting volume loss. The significance of the removed variables was tested in the same manner.

The standard error of the estimate of Y was reduced from 0.7172 (when $Y = \bar{Y}$) to 0.0964 when the independent variables were used to predict Y. This provided a multiple correlation coefficient of 0.9928. Of the four elements, Cr was most important in reducing the error.

Unclassified
Security Classification

DOCUMENT CONTROL DATA - R&D
(Security classification of title, body of abstract and indexing annotation must be entered when the overall report is classified)

1. ORIGINATING ACTIVITY (Corporate author)
Allison Division, General Motors Corporation
Indianapolis, Indiana

2a. REPORT SECURITY CLASSIFICATION
Unclassified

2b GROUP
N/A

3. REPORT TITLE
INVESTIGATION OF HOT CORROSION OF NICKEL BASE SUPERALLOYS USED IN GAS TURBINE ENGINES

4. DESCRIPTIVE NOTES (Type of report and inclusive dates)
Final Report 1 July 1966 through 31 August 1967

5. AUTHOR(S) (Last name, first name, initial)
Ryan, Kenneth H.
Hamilton, Paul E.
Kildsig, John R.

6. REPORT DATE
August 1967

7a. TOTAL NO. OF PAGES
105

7b. NO. OF REFS
2

8a. CONTRACT OR GRANT NO.
AF33(615)-5211

b. PROJECT NO.
7381

c.

d.

9a. ORIGINATOR'S REPORT NUMBER(S)
EDR 5370

9b. OTHER REPORT NO(S) (Any other numbers that may be assigned this report)
AFML-TR-67-306

10. AVAILABILITY/LIMITATION NOTICES This document is subject to special export controls and each transmittal to foreign governments or foreign nationals may be made only with prior approval of the Air Force Materials Laboratory (MAAS), Wright Patterson Air Force Base, Ohio 45433.

11. SUPPLEMENTARY NOTES
None

12. SPONSORING MILITARY ACTIVITY
Air Force Materials Laboratory (MAAE)
Research and Technology Division
AF Systems Command, WPAFB, Ohio

13. ABSTRACT A program was conducted to investigate the hot corrosion resistance of nickel base alloys and is described. The most significant result obtained from the program was the derivation of a regression equation relating base metal volume loss to alloy chemistry and showing that chromium and aluminum were beneficial to hot corrosion resistance, whereas tungsten and molybdenum were detrimental. It was also established by electron microprobe study that hot corrosion resistance was related to alloy depletion zone composition. A high molybdenum content in the zone was detrimental and a high aluminum content beneficial to hot corrosion resistance. Hot corrosion severity increased with temperature in the range of 1700 to 2000°F in an approximate logarithmic fashion. The order of decreasing hot corrosion resistance of the ten alloys investigated was: PDRL 163, IN-728 NX, Alloy 713C + 2% Cr + Y, Alloy 713C + 2% Cr, Inco 717, Alloy 713C, Mar-M421, IN-100, GMR-235, and Mar-M246. Heat treatment had a detrimental effect on the hot corrosion behavior of Mar-M246 and GMR-235 and no observed effect on the other eight alloys.

It is recommended that test rig programs to simulate hot corrosion behavior in advanced turbine engines be conducted on turbine alloys under varying conditions of high temperature and pressure.

DD FORM 1 JAN 64 1473

Unclassified
Security Classification

Unclassified

Security Classification

14 KEY WORDS	LINK A		LINK B		LINK C	
	ROLE	WT	ROLE	WT	ROLE	WT
Hot corrosion Sulfidation Nickel base alloys High temperature testing						

INSTRUCTIONS

1. ORIGINATING ACTIVITY: Enter the name and address of the contractor, subcontractor, grantee, Department of Defense activity or other organization *(corporate author)* issuing the report.

2a. REPORT SECURITY CLASSIFICATION: Enter the overall security classification of the report. Indicate whether "Restricted Data" is included. Marking is to be in accordance with appropriate security regulations.

2b. GROUP: Automatic downgrading is specified in DoD Directive 5200.10 and Armed Forces Industrial Manual. Enter the group number. Also, when applicable, show that optional markings have been used for Group 3 and Group 4 as authorized.

3. REPORT TITLE: Enter the complete report title in all capital letters. Titles in all cases should be unclassified. If a meaningful title cannot be selected without classification, show title classification in all capitals in parenthesis immediately following the title.

4. DESCRIPTIVE NOTES: If appropriate, enter the type of report, e.g., interim, progress, summary, annual, or final. Give the inclusive dates when a specific reporting period is covered.

5. AUTHOR(S): Enter the name(s) of author(s) as shown on or in the report. Enter last name, first name, middle initial. If military, show rank and branch of service. The name of the principal author is an absolute minimum requirement.

6. REPORT DATE: Enter the date of the report as day, month, year; or month, year. If more than one date appears on the report, use date of publication.

7a. TOTAL NUMBER OF PAGES: The total page count should follow normal pagination procedures, i.e., enter the number of pages containing information.

7b. NUMBER OF REFERENCES: Enter the total number of references cited in the report.

8a. CONTRACT OR GRANT NUMBER: If appropriate, enter the applicable number of the contract or grant under which the report was written.

8b, 8c, & 8d. PROJECT NUMBER: Enter the appropriate military department identification, such as project number, subproject number, system numbers, task number, etc.

9a. ORIGINATOR'S REPORT NUMBER(S): Enter the official report number by which the document will be identified and controlled by the originating activity. This number must be unique to this report.

9b. OTHER REPORT NUMBER(S): If the report has been assigned any other report numbers *(either by the originator or by the sponsor)*, also enter this number(s).

10. AVAILABILITY/LIMITATION NOTICES: Enter any limitations on further dissemination of the report, other than those imposed by security classification, using standard statements such as:

(1) "Qualified requesters may obtain copies of this report from DDC."

(2) "Foreign announcement and dissemination of this report by DDC is not authorized."

(3) "U. S. Government agencies may obtain copies of this report directly from DDC. Other qualified DDC users shall request through _____."

(4) "U. S. military agencies may obtain copies of this report directly from DDC. Other qualified users shall request through _____."

(5) "All distribution of this report is controlled. Qualified DDC users shall request through _____."

If the report has been furnished to the Office of Technical Services, Department of Commerce, for sale to the public, indicate this fact and enter the price, if known.

11. SUPPLEMENTARY NOTES: Use for additional explanatory notes.

12. SPONSORING MILITARY ACTIVITY: Enter the name of the departmental project office or laboratory sponsoring *(paying for)* the research and development. Include address.

13. ABSTRACT: Enter an abstract giving a brief and factual summary of the document indicative of the report, even though it may also appear elsewhere in the body of the technical report. If additional space is required, a continuation sheet shall be attached.

It is highly desirable that the abstract of classified reports be unclassified. Each paragraph of the abstract shall end with an indication of the military security classification of the information in the paragraph, represented as *(TS), (S), (C), or (U)*.

There is no limitation on the length of the abstract. However, the suggested length is from 150 to 225 words.

14. KEY WORDS: Key words are technically meaningful terms or short phrases that characterize a report and may be used as index entries for cataloging the report. Key words must be selected so that no security classification is required. Identifiers, such as equipment model designation, trade name, military project code name, geographic location, may be used as key words but will be followed by an indication of technical context. The assignment of links, rules, and weights is optional

Unclassified

Security Classification